

**INTERPRETATION OF GROUND-BASED MAGNETIC AND GRAVITY DATA FOR
THE DELINEATION OF POTENTIAL GOLD MINERALIZATION ZONES IN
SUBENSO, GHANA**

KNUST
by

RALPH TAGOE, BSc (Hons)

**A Thesis Submitted to the Department of Physics,
Kwame Nkrumah University of Science and Technology
in partial fulfillment of the requirements for the degree**

Of

MASTER OF PHILOSOPHY

College of Science

Supervisor: Dr. K. Preko

©Department of Physics

October 27, 2015

Abstract

Data from integrated ground gravity and magnetic surveys were used to interpret the geology by delineating lithological units, geological structures as well as the delineation of potential gold mineralization zones within the Subenso South concession of Newmont Ghana Gold Limited. The two datasets were acquired along 3.6 km by 2.1 km block with 100 m profile line spacing and data was collected at 100 m station along the profile lines using L&R Gravimeter and Topcon DGPS for the ground gravity survey. Geometrics G856 and G858 were used in a continuous mode for the ground magnetic survey. Geosoft Oasis Montaj version 7.1 was used to process the data. Image enhancement techniques such as reduction to the pole and first vertical derivative aided in the delineation of geological structures like faults which are potential gold mineralization zones. A residual gravity map was produced from the gravity data which helped in enhancing the lithological contacts. The area is made up of predominantly metasedimentary units, mafic volcanic units and volcanoclastic units. The metasediments showed generally low magnetic and gravity responses. The mafic volcanic units showed high gravity and magnetic responses. Relatively intermediate gravity and magnetic responses were mapped as the volcanoclastic units. The superimposition of the Subenso South gold deposit on the gravity and magnetic results helped to establish a relationship between the mineralization zones in the area. The Subenso gold deposit was located on and along the contacts of the high gravity and magnetic anomalies. This relationship led to the delineation of unexplored potential gold mineralization zones in the study area.

Contents

Declaration	i
Abstract	ii
List of Tables	ix
List of Figures	xi
List of Symbols and Acronyms	xiii
Acknowledgements	xiv
1 INTRODUCTION	1
1.1 Study Area.....	3
1.1.1 Location and Accessibility.....	3
1.1.2 Physiography and Climate.....	4
1.1.3 Vegetation and Occupation of Inhabitants.....	4

1.2	Research Problem Definition	5
1.3	Objectives of the Research	6
1.4	Justification of Objectives	6
1.5	Literature Review	8
1.6	Structure of the Thesis.....	10
2	GEOLOGICAL SETTING	11
2.1	Regional Geology.....	11
2.1.1	The Summary of Ghana Paleo-proterozoic Geology.....	13
2.1.2	The Birimian Rock System	14
2.1.3	Birimian-hosted deposits	15
2.1.4	Tarkwaian hosted deposit	17
2.1.5	The Sefwi Gold Belt.....	17
2.1.6	Structures.....	19
2.1.7	Topography & Regolith	19
2.2	Local Geology	20
2.2.1	Style of Gold Mineralization.....	21
3	THEORETICAL BACKGROUND	22
3.1	The Principle of Gravitation	22
3.1.1	Units and Measurements of Gravity.....	25
3.1.2	Gravity Survey.....	26

3.1.3	Data Reduction	27
3.1.3.1	Drift Correction	27
3.1.3.2	Latitude Correction.	28
3.1.3.3	Free Air Correction.	29
3.1.3.4	Bouger Correction.	29
3.2	Rock Densities.	31
3.3	Gravity Anomalies.	33
3.3.1	Bouguer anomaly (BA).	34
3.3.2	Free-Air anomaly (FAA).	34
3.4	Enhancement Techniques	35
3.4.1	Wavelength filtering	35
3.4.2	Directional filtering	35
3.4.3	Vertical derivative methods	35
3.4.3.1	The first and second vertical derivative	35
3.4.4	Upward and Downward continuation	36
3.5	Regional and Residual gravity anomalies	37
3.6	Interpretation and modeling of gravity anomaly	38
3.6.1	Direct methods, or "forward modelling"	39
3.6.2	Indirect interpretation (or inverse modelling).	40
3.7	Principles of Magnetism	41
3.7.1	Magnetism of the Earth	44

3.7.2	Nature of the Geomagnetic Field	44
3.7.3	The Earth's magnetic Field	45
3.8	Magnetism of Rocks and Minerals	47
3.8.1	Magnetic susceptibility	50
3.8.2	Remanent Magnetisation	51
3.8.3	Magnetization at Low Magnetic Latitudes.....	52
3.9	Lithology, Structure and Magnetism	53
3.10	Rock Alteration	54
3.11	Magnetic Anomalies	55
3.11.1	Forms of magnetic anomaly	55
3.11.2	Basic Interpretation of Magnetic Anomalies	56
3.12	Depth Estimation by 3D Euler Deconvolution	56
4	MATERIALS AND METHODS	58
4.1	Gravity Data Acquisition	58
4.2	Gravity Data Processing	62
4.2.1	Gravity data correction.....	63
4.2.2	Regional and Residual Gravity	65
4.2.3	Enhancement Techniques	64

4.2.3.1	Microlevelling	64
4.2.3.2	Filtering	65
4.2.3.3	Upward Continuation.....	65
4.3	Magnetic Data Acquisition and Processing	65
4.3.1	Magnetic Data Processing	69
4.3.1.1	Reduction to the Pole	70
4.3.1.2	First Vertical Derivative (1VD) and Horizontal Derivative (1HD)..	70
4.3.1.3	Upward Continuation	70
4.3.1.4	Analytical Signal Amplitude	71
5	RESULTS AND DISCUSSIONS	72
5.1	Results of Ground Geophysical Measurements	72
5.2	Digital Elevation Map	72
5.3	Results of Magnetic Measurements	74
5.3.1	Total Magnetic Intensity (TMI) Map	74
5.3.2	Reduced to the Pole (RTP) map	77
5.3.3	Analytic Signal Map	80
5.3.4	First Vertical Derivative (1VD) map	81
5.4	Results of Gravity Measurement	84

5.4.1	Complete Bouguer Anomaly (CBA) map	84
5.4.2	Residual Gravity Map	84
5.5	Summary	89
5.6	Proposed geological map from the Gravity and Magnetic data.....	90
5.7	Gold Mineralization in the Subenso South study area	92
6	CONCLUSION AND RECOMMENDATIONS	97
6.1	Conclusions	97
6.2	Recommendations	100
	References.....	101
	Appendices	109
A		109
A.1	Processed Subenso South Ground gravity data.....	109
A.2	Processed Subenso South Ground magnetic data.....	112
B		118
B.1	Used Software.....	118

List of Tables

Table 3.1 Approximate density ranges (Mgm^{-3}) of some common rock types and ores..... 32

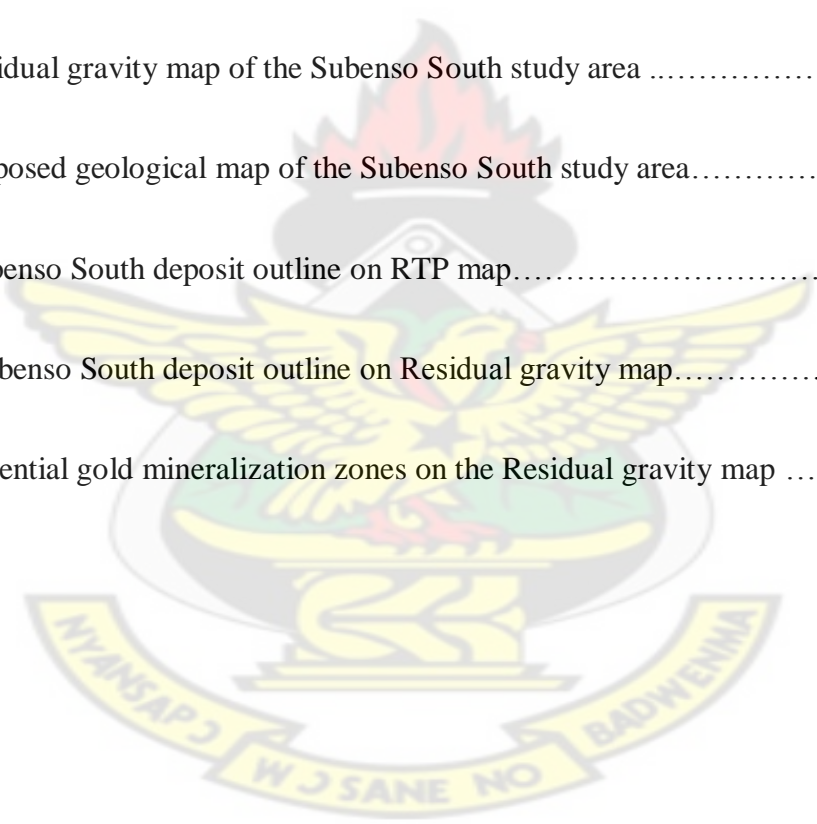
KNUST



List of Figures

Figure 1.1	Location map of the Subenso South concession.....	3
Figure 2.1	Geological map of South Western Ghana showing the various gold belt.....	18
Figure 2.2	Geological map of Subenso-South concession	20
Figure 3.1	Diagram showing Bouguer, Regional, and Residual anomaly.	38
Figure 3.2	Elements of the Earth's magnetic field	47
Figure 4.1	A picture of the Lacoste& Romberg gravimeter (A) used for the survey. . B is base plate and C is gravimeter case.....	60
Figure 4.2	Operator recording readings on the gravimeter on to a field sheet	61
Figure 4.3	Operator setting up and configuring base Differential GPS. A is GPS receiver, .. C is tribrach, and D is Tripod stand	61
Figure 4.4	Operator configuring field Differential GPS. A is controller, B is stand, . C is receiver, and D is antenna	62
Figure 4.5	Base Geometrics G856 Magnetometer (left) with its sensor (right) . used for the survey.....	67
Figure 4.6	Operator carrying and operating on the field Geometric magnetometer unit, .. A is the Console, B is Sensor and C is GPS tracker.....	68

Figure 5.1	Digital Elevation Map of the Subenso South study area.....	73
Figure 5.2	Total Magnetic Intensity map of the Subenso South area.....	75
Figure 5.3	Reduction to the pole (RTP) map of the Subenso South study area	78
Figure 5.4	Analytical signal map (from RTP map) of the Subenso South area	80
Figure 5.5	First Vertical Derivative map grey scale of the Subenso South Area.....	82
Figure 5.6	Complete Bouguer anomaly (CBA) map of the area.....	85
Figure 5.7	Residual gravity map of the Subenso South study area	87
Figure 5.8	Proposed geological map of the Subenso South study area.....	91
Figure 5.9a	Subenso South deposit outline on RTP map.....	93
Figure 5.9b	Subenso South deposit outline on Residual gravity map.....	93
Figure 5.10	Potential gold mineralization zones on the Residual gravity map	95



List of Symbols and Acronyms

k	Magnetic susceptibility	BA	Bouguer anomaly
F_e	The Earth's magnetic field	h	Elevation
Z_e	Vertical component of the Earth's magnetic field	r	distance
H_e	Horizontal component of the Earth's magnetic field	TC	Terrain Correction
I	Angle of inclination	BC	Bouguer correction
D	Angle of declination	CBA	Complete Bouguer A
M	Intensity of magnetization	FAC	Free Air Correction
H	Applied external field	FAA	Free Air Anomaly
1VD	First Vertical Derivative	π	Pi
<i>c.g.s</i>	centi gram second	RTP	Reduce to the Pole
J_r	Remanent magnetization	ρ	Density
J_i	Induced magnetization	g	Gravity
IP	Induced Polarization	m	Magnetic pole strength
F	Gravitational/Magnetic force	L	length
G	Gravitational constant	A	Cross-Sectional area
P	Gravitational Potential	M	Magnetic moments
ϕ	Angle of latitude	DEM	Digital Elevation Map
<i>g.u</i>	Gravity unit	TMI	Total Magnetic Intensity
μ_0	Magnetic permeability of vacuum	GPS	Global Positioning Systems
μ_R	Relative magnetic permeability	UTM	Universal Transverse Mercator

B Magnetic field

WGS World Geodetic System

DGRF Definitive Geomagnetic Reference Formula

FFT Fast Fourier Transform

∇ Spatial Vector Derivative

nT nanoTesla

CBA Complete Bouguer Anomaly

KNUST



Acknowledgments

First and foremost, glory be to God Almighty for His grace and provision for my life and how far He has brought me. I will like to thank my dear wife Dr. Mrs. Susan Tagoe for her support and encouragement through this project. I would like to show gratitude to the Regional and Project Geophysicists of Newmont Ghana Gold limited in the persons of Mr. Thomas Tsiboah and Mr. Kwaku Takyi -Kyeremeh for providing me equipment and data processing tools for this project. I thank them for their support, supervision and the knowledge they have imparted on me and the opportunities offered me throughout the time I have been with you. Also, a big thank you goes to Dr. Kwasi Preko my main supervisor for his guidance, tutelage, encouragement and patience. I want to thank Mr. David Wemegah my co-supervisor for his immense contribution towards this project. To my mum Lena Gespar and sister Abigail Tagoe, I say God richly bless you for all the support you have offered me throughout this period. My friends who in one way or the other helped me I say God bless you all especially Alfred Agyei Berko and his wife Akua Ayei Berko and Benjamin Kwasi Boadi, Ebenezer Krampa Aidoo and Jonas Sikah Narh.

CHAPTER 1

INTRODUCTION

Anomalous density contrasts within the Earth are defined by gravity measurements; most often, ground-based gravity meters are used to precisely measure variations in the gravity field at different points. Gravity anomalies are calculated by subtracting a regional field from the measured field, resulting in gravitational anomalies that have a correlation with the variations in density of the body causing the anomaly. Shallow and high density bodies give rise to high gravity anomalies whereas shallow and low density bodies produce lower gravity anomalies. Chromite, barite, and hematite because of their high density nature produce high gravity anomalies, unlike low-density deposits such as halite, weathered kimberlite, and diatomaceous earth which gives rise to negative anomalies. The guessing of the entire anomalous mass (ore tonnage) responsible for an anomaly is enabled by the gravity method. The gravity and magnetic methods can detect only lateral contrasts in density and magnetization respectively (Hoover et al., 1995).

Magnetic anomalies may be related to primary igneous or sedimentary processes that establish the magnetic mineralogy, or they may be related to secondary alteration that either introduces or eliminates magnetic minerals. In mineral prospecting and its geoenvironmental considerations, the secondary effects in rocks that host ore deposits associated with hydrothermal systems are important (Hanna, 1969; Criss and Champion, 1984).

Gravity and magnetic anomalies can sometimes coincide because rock alteration can effect a change in the bulk density as well as magnetization, magnetic anomalies when corrected for magnetization direction.

Banded iron formation or magnetite can be detected by magnetic prospecting and could also facilitate the deduction of subsurface lithology and structure that may indirectly assist the identification of mineralized rock, patterns of effluent flow, and extent of permissive terrains and (or) favorable tracts for deposits beneath surficial cover.

Newmont Ghana Gold Subenso South Concession is located within the Birimian Gold system of Ghana within the Sefwi belt. It is believed to be a type of hydrothermal deposit. The study area is made up of metavolcanics and metasedimentary rock units. These characteristics informed the decision to use the methods of gravity and magnetics to survey along profile lines within the Subenso South concession and over the Subenso South gold deposit. This is to improve the general geological and structural settings of the area by interpreting the magnetic and gravity anomalies in conjunction with known geological information of the area and also determine the suitability of the use of these methods as useful tools in the modern exploration for gold. This suitability will depend on how the gravity and magnetic anomalies relate to the known position of the Subenso South gold deposit. This information could lead to the delineation of other possible gold mineralization zones within the concession.

1.1 Study Area

1.1.1 Location and Accessibility

The Subenso South gold deposit is located between two main towns namely Teekyere and Adrobaa all in the Brong Ahafo region of Ghana. It is about 12 km East North East (ENE) of Sunyani which is the regional capital and about 300 km from Accra the National capital. The main Kumasi-Sunyani Highway traverses the southwestern portion of Subenso South deposit. The study area is accessed by a main feeder road connecting Terkyere and Adrobaa. There are also a couple of branch roads to the study area from the main feeder road.

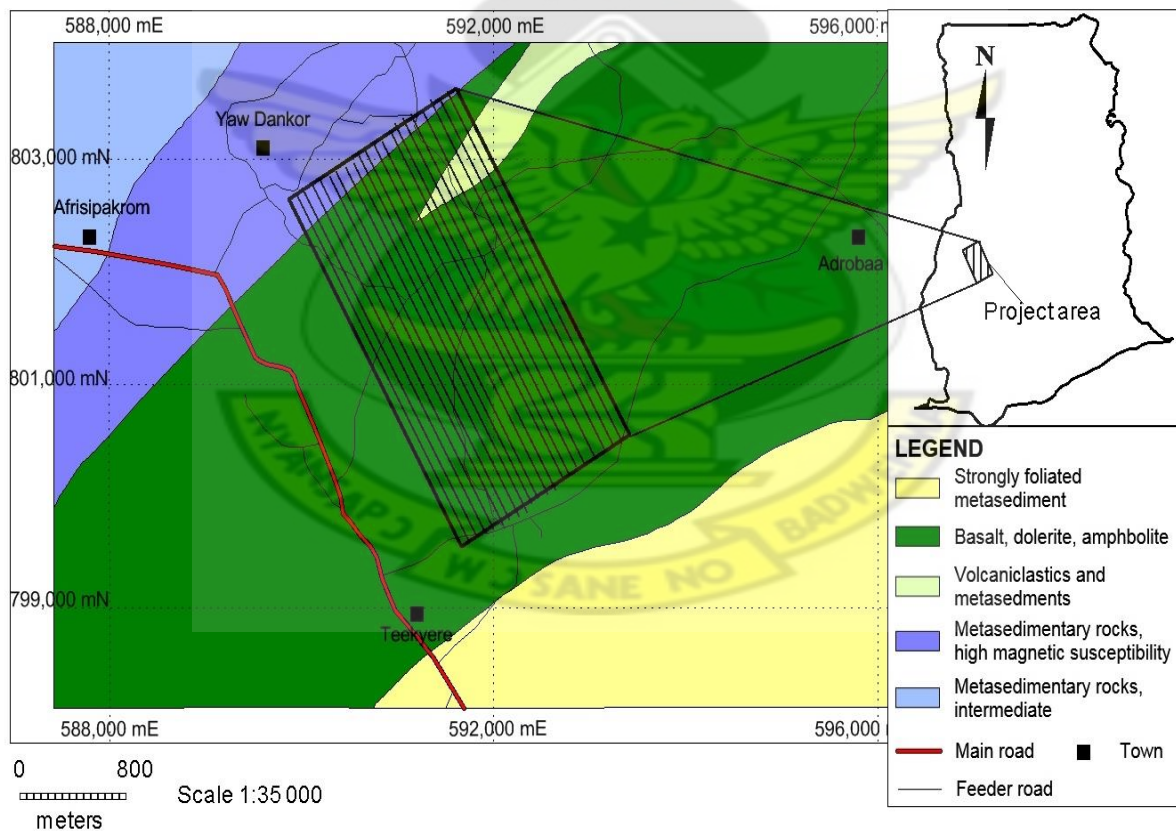


Figure 1.1: Location Map of Subenso South Concession

1.1.2 Physiography and Climate

Topographically the area consists of low, rounded hills rising to elevations of not more than 150 meters above the surrounding plains. The area is deforested and covered either by low, thick bushes or farm subsistence crops. There are no major streams running through this deposit.

The Ahafo Project Area falls within the wet semi-equatorial climatic zone of Ghana and is characterized by an annual maximum rainfall pattern occurring in the months of May to July and from September to October. The climate of the area is determined by movement of air masses which differ in air moisture and relative stability rather than temperature (Ahafo Mineral Resource and Reserve Report, 2006)

1.1.3 Vegetation and Occupation of Inhabitants

A mixture of natural plants communities in early stages of ecological succession, crops, and plantations, patches of second growth forest, and riparian communities along rivers and streams are the main vegetative cover in the project area. Agricultural activities, bushfire, and removal of timber has extensively depleted the natural vegetation of the project area consequently losing its resemblance to the native forest communities once typical of the region.

Following extensive nation-wide fires in 1983, The project area previously dominated by trees and shrubs have been taken over by dense stands of elephant grass following the extensive nation-wide fires in 1983 (Ahafo Mineral Resource and Ore Reserve, 2006).

The inhabitants within the study area are mainly into subsistence farming with a few small scale commercial farming. The major agricultural land is used to cultivate cocoa, crops, teak and rice.

1.2 Research Problem Definition

In recent times the gold exploration and mining companies have been faced with a lot of challenges including high operational costs and dwindling gold prices. Due to these challenges most of these companies have to re-strategize to reduce their operational cost and remain in business. Drilling is one activity that increases the cost of exploration and subsequent mining. Newmont Ghana Gold Ltd has also been hit by these challenges.

To reduce the cost of exploration, an integrated approach and cost effective geophysical methods such as gravity and magnetic methods should be employed in gold exploration. The integrated approach would give a better picture of the subsurface leading to more reliable exploratory drill targets thereby reducing wastage during drilling and also reduce the cost of exploration.

Additionally, the Geophysics section of Newmont Ghana Gold Limited have used different geophysical methods including IP/Resistivity (Gradient array and 3-D pole dipole), airborne magnetics, Transient Electromagnetics over the Subenso South concession but are yet to try an integrated approach involving detailed gravity and magnetic methods. Therefore this project seeks to undertake a detailed gravity and magnetic survey on the Subenso South concession to be able provide detailed and improved subsurface geological interpretation and possibly delineate other gold mineralization zones within the concession. This improved geological interpretation would help the company in its future exploratory work especially in generating drilling targets

which are more reliable and increasing the profitability and decreasing the wastage in exploratory works.

1.3 Objectives of Research

The area of study is characterized by gold deposit. Therefore the main objective of this project is to give a geological and structural interpretation of the ground gravity and magnetic data to aid in the delineation of potential gold mineralization zones. The specific objectives are

1. Map the various lithological units within the study area.
2. Delineate the geological structures and features in the study area.
3. Delineate potential gold mineralization zones.
4. Establish relationship between gravity and magnetic anomalies and zones of gold mineralization.

1.4 Justification of Objectives

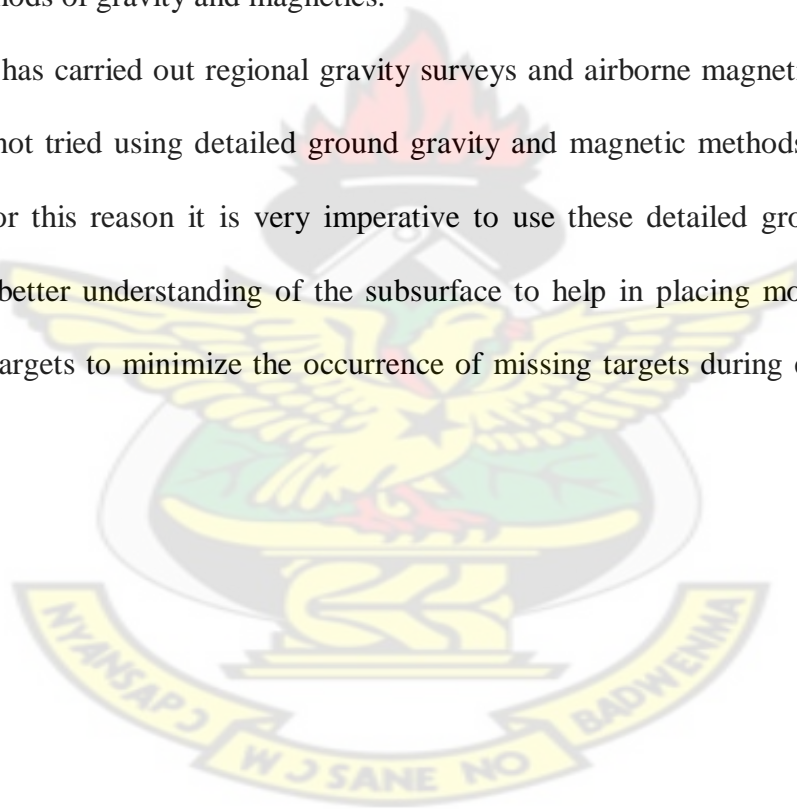
Geoscientists use the gravity and magnetic methods to indirectly look beneath the surface of the Earth by utilizing the density and magnetization of rocks.

Minerals, faults, and other economic resources can be detected by gravity and magnetic method. Because the potential fields are relatively cheaper, they can occupy large areas of ground. The main objective of studying potential fields is to provide an improved understanding of the

subsurface geological interpretation. They are relatively cheap, non-invasive and nondestructive to the environment. They are also passive and require portable small instruments which permit walking traverses.

The Subenso South deposit is believed to be a type of hydrothermal deposit typical of the Birimian style of mineralization with mafic, ultramafic and meta-sedimentary lithological units, which have been highly altered. These characteristic features make it conducive to be mapped out using the methods of gravity and magnetics.

Newmont Ghana has carried out regional gravity surveys and airborne magnetic surveys within the area but has not tried using detailed ground gravity and magnetic methods on the Subenso South deposit. For this reason it is very imperative to use these detailed ground geophysical surveys to get a better understanding of the subsurface to help in placing more confidence in subsequent drill targets to minimize the occurrence of missing targets during exploratory drills by the geologists.



1.5 Literature Review

Gravity and magnetic methods have been used as tools for the search for gold in many parts of the world. This section of the research will look at few of the works other investigators have done with these geophysical methods.

Roux, (1967) looked at the application of gravity and magnetic methods for gold exploration in South Africa. These two methods together with geological reasoning were able to locate three major extensions of the gold-bearing conglomerates of the Main Witwatersrand Basin under younger cover, and for the discovery of the outlier to the east of the main basin. The gravity and magnetic method was also responsible for discovery of four important fields namely West Wits Line, Free State Goldfields, the Klerksdorp Gold field and the Evander Goldfield.

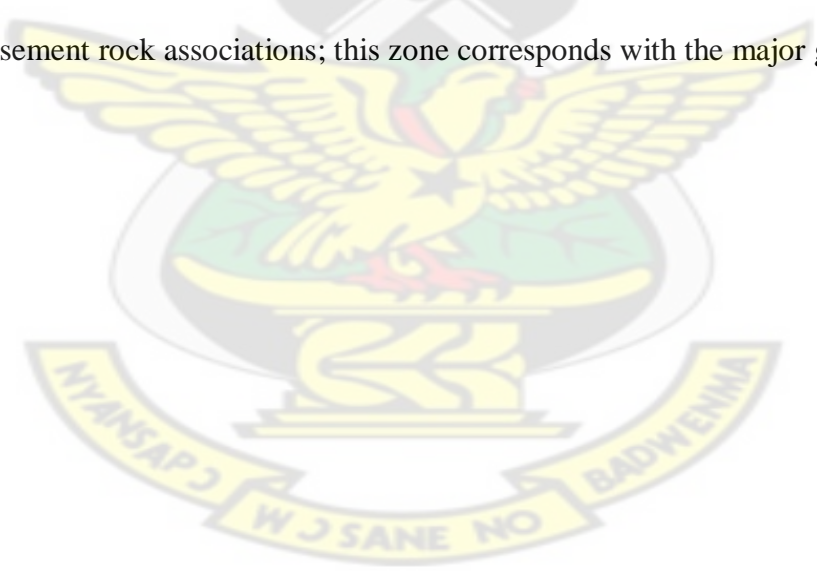
Floyd, (1993) integrated gravity and magnetic data in order to delineate and map concealed faults, to determine the horizontal extent and possible source of volcanic rocks and obtain a better understanding of range faulting within the Mosida Hills, Utah County, Utah in the United States.

Hash, (1995) carried out gravity and magnetic survey in the Mapleton Area of Northern Utah in the United States. The survey facilitated the location of buried faults within the area.

Leaman, (1987) used the gravity and magnetic method on the Boco Siding deposit of Western Tasmania to evaluate thickness of the glacial ice overlying the Boco siding deposit. The instruments used for the survey were the sodin gravimeter and the HcPhar proton magnetometer . The gravity data was fully corrected to yield a Bouguer anomaly. A Bouguer density of 2.67 t/m^3 was used. The magnetic data was corrected for diurnal variation by repeat reading at the base station.

Ghosh et al., (2010), used the gravity and magnetic method together with other geophysical techniques to map the deeper subsurface information and also to make out the potentially hydrocarbon prospect zone within the Assam-Arakan basin near the fore deep of Himalayan foot hills noted for geologically complex and logistically hostile terrain.

Whitaker et al., (1987) used detailed airborne and ground magnetic surveys, and a detailed gravity survey in mapping the geology of the Corsair area, about 10 km east of Kalgoorlie. The gravity and magnetic surveys interpreted together map out the distribution of mafics, ultramafics and sediments. The image of the gravity gradient provided the best representation of linears. Many of these linears are in part coincident with workings, so they are gold carriers. Known gold mineralization is preferentially developed along a sheared zone abutting the boundary between the two major basement rock associations; this zone corresponds with the major gravity gradient.



1.6 Structure of the Thesis

The thesis is made up of six chapters. Chapter 1 deals with the general introduction of the research topic including problem definition, brief description of the study area and discussion of similar works others have done on the research topic.

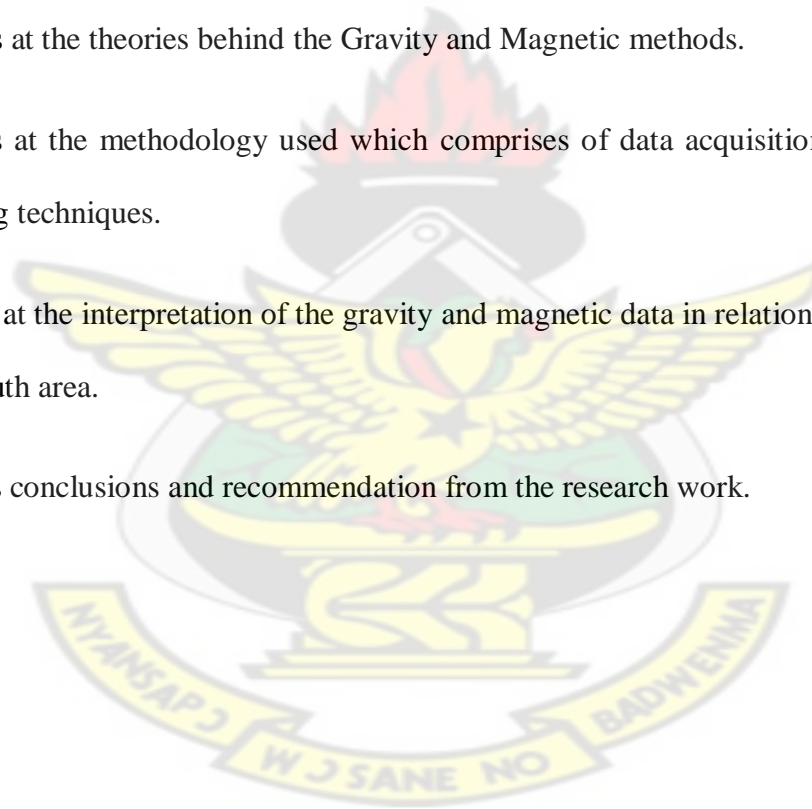
Chapter 2 deals mainly with the geological settings of the study area. The various lithological units and geological structures are extensively discussed.

Chapter 3 looks at the theories behind the Gravity and Magnetic methods.

Chapter 4 looks at the methodology used which comprises of data acquisition, processing and image enhancing techniques.

Chapter 5 looks at the interpretation of the gravity and magnetic data in relation to the geology of the Subenso South area.

Chapter 6 draws conclusions and recommendation from the research work.



CHAPTER 2

GEOLOGICAL SETTING

2.1 Regional Geology

Ghana is broadly divided into four (4) main geotectonic units. Each unit is associated with a particular mineral deposit. The West African Cratonic area which covers the western half of the country is made up of two (2) formations: the Birimian and the Tarkwaian (Kesse, 1985). On the regional structure elements only carry gold mineralization, if they are developed within the zone of the auriferous chemical sediments; those outside the zone tend to be barren. Gold mineralization in Ghana is reported to consists of three main types:

- Reef, vein or lode type
- Auriferous quartz pebble conglomerates and
- Recent alluvial and eluvial deposits associated with the rocks of these two systems.

The parallel nature of evenly spaced belts of folded Birimian metalavas makes it the most striking feature of the geology of Ghana. The belt is about 40 km to 50 km wide and the distance between individual belts is about 90 km and the belts generally trend in the Northeast direction. Lava flows separated by basins containing metasedimentary granitoids in different amount are the dominant lithologies.

Within the Tarkwa area, auriferous quartz-pebble conglomerates within the Tarkwaian system are exposed. The Tarkwaian is the second largest source of gold in Ghana and it is dominated by clastic sedimentary rock deposited in an elongated. The gold deposits are placer deposits the mineralization that remobilized may represent detrital gold weathered out of the mineralized Birimian rocks. The Tarkwaian rocks occur in two well defined and one smaller north easterly aligned belts. The main belt, lying immediately east of the main Prestea-Obuasi Birimian zone, extends from near the coast to the south of Tarkwa about 250 km to the northeast where it terminates at the edge of the Voltain basin. The main Tarkwaian belt is averagely about 16 km wide. It is believed that the Tarkwaian Banket series was deposited in a braided stream channel environment beyond from the primary vein and lode-type deposits in the underlying Birimian (Kesse, 1985). Another belt of similar rocks occurs in west central Ghana near Banda, and smaller occurrences exist to the north and south of Bibiani and Kibi.

The reef, vein or lode type of gold deposit is associated with the rocks of the Birimian system and has played a dominant role in the gold industry of Ghana. The auriferous quartz veins have been the most important source of gold in Ghana, and occur as intrusive veins in phyllites and greenstones within the Birimian system (Kesse, 1985). Gold may be free or contained within sulphide of pyrite and arsenopyrite. The quartz veins containing economic concentrations of gold are usually fractured and shattered and readily disintegrate on weathering. Sulphide ores within Birimian rocks usually consisting of tuffaceous argillites have also proven to be important sources of gold mineralization in Ghana. These are associated with dissemination and the stringers of pyrite and arsenopyrite.

The styles of gold mineralization differ among rock system. Birimian deposits are epigenetic gold quartz vein deposit-type associated with disseminated sulphides in fractured and sheared zones. Tarkwaian gold on the other hand is the Paleoplacer Banket conglomerates of the Witwatersrand-type (Dzigbodi-Adjima, 1992).

2.1.1 Summary of Ghana Paleo-Proterozoic Geology

Ghana lies within the eastern domain of the Man Shield which occupies the southeastern third of the West African Craton (Hirdes et al, 1993). The most extensive and important units of the Man Shield are generally referred to as the Birimian Super-Group that has an age of approximately 2.2 to 2.1Ga. It consists of Paleo-Proterozoic metasediments, metavolcanics and associated intrusive complexes.

In south-western Ghana, the Birimian Super-Group comprises several narrow north-east-trending belts of volcanic and volcanoclastic rocks of tholeiitic to acidic composition. These are separated by broad sedimentary basins dominated by turbidites.

Ghanaian gold deposits are categorized into three broad suites:

- Birimian-hosted,
- Tarkwaian-hosted and
- Modern alluvial deposits.

2.1.2 The Birimian Rock System

The rocks of the Birimian System deposited upon an unknown Archean (Liberian) basement underlie nearly one-sixth of the total area of Ghana. They crop out in areas to the north, west and southern parts of the country. The Birimian has been folded, metamorphosed and in places assimilated by granitoid bodies. The folding is intense with dips commonly on the order of 30° - 90° along a NE-SW axis and of 70° - 90° being more common than shallow dips (Kesse, 1985).

The metamorphism has generally been termed "low-grade" greenschist facies.

Kesse (1985) was of the view that metamorphism to amphibolites facies is common and grades, up to granulite facies, have been observed in several localities. Faulting tends to follow the strike of the folds and also trends perpendicular to the latter. Jointing in these rocks has many orientations, but most commonly is parallel to fold and fault directions and in north-south direction (Kesse, 1985).

The Birimian rocks have been intruded by granitoids during the later stages of the Eburnean orogeny at or after the end of the Birimian deposition. In terms of mineral deposits, the Birimian rocks are the most important in Ghana for minerals such as gold, diamond, bauxite, manganese and iron are all associated with this System. Just to mention a few, the following are some of the gold belts which are associated with the Birimian rocks:

1. Prestea belt
2. Akropong belt
3. Obuasi belt
4. Sefwi belt

5. Tokosea and Bibiani belts

Most Ghanaian Birimian gold occurrences and mines are concentrated in narrow 'corridors' of 10-15 km width in the transition zone between volcanic belts and sedimentary basins, as are the chemical facies and regionally extensive shear zones at the volcanics-sediment interface. There are two major type of Birimian gold presentation which are: (1) the disseminated sulphide type which is generally controlled by lithofacies, i.e. controlled by chemical sediments, and to a lesser extent by selvages of gold-quartz veins; and (2) the quartz vein type which is exclusively structure controlled (Leube et al., 1990).

2.1.3 Birimian-hosted deposits

The Birimian-hosted deposits are most important in terms of total gold production and are well represented on the western margin of the Ashanti belt. Examples are Obuasi, Bogosu, Prestea, Konongo, Bibiani and Chirano and also included the major new discoveries at Akyem and Ahafo. They usually feature complex quartz-vein systems and are commonly associated with extensive disseminated sulphides. They invariably appear to be related to regional NNE to NE-trending regional structures (tectonic corridors) which are typically concentrated along the margins of various Birimian volcanic belts and the adjacent sedimentary basins.

The most favoured host rocks are inter-bedded argillites, greywackes and volcanoclastic units that were frequently deposited in transitional zones between the volcanic belts and the sedimentary basins. In addition, intermediate and mafic intrusions (granitoids) that mainly occur within the volcanic belts, are also recognized as important host rocks.

A notable example of intrusive-hosted deposits is Ayanfuri, where intermediate granitoids host significant mineralised quartz stock-work systems. Other examples are Obotan, Chirano and Mpesetia. The Subika deposit at Ahafo also falls in this category, but Subika is associated with belt-type granitoids while the other deposits are hosted in basin-type granitoids.

Quartz vein systems are intimately related to wide zones of disseminated sulphides in the host rocks. The mineralized zones at Obuasi, Prestea and Bogosu feature extensive disseminated sulphides that commonly exceed 50 m in width.

Along the western margin of the Ashanti belt, arseno-pyrite is the major sulphide in the deposits. In the deposits along the eastern margin, for example at Wassa and Akyem, pyrite is dominant. Gold associated with arsenopyrite is often refractory in nature. Other new discoveries such as Chirano and Ahafo on the Sefwi volcanic belt also have pyrite as the main sulphide. To date, no significant arseno-pyrite has been observed in the Ahafo deposits and total rock analyses are commonly less than 50 ppm As. Alteration commonly consists of intense silicification, chlorite and carbonate alteration with sericite, albite and minor feldspar (Ahafo Mineral Resource/Reserve Report, 2006)

2.1.4 Tarkwaian-hosted deposits

Tarkwaian-hosted gold deposits consist primarily of auriferous, silicified quartz pebble conglomerates and examples are Tarkwa, Bogosu and Teberebie. However, sheeted quartz-vein stock-work hosted deposits in Tarkwaian sediments are exploited at Damang, north of Tarkwa. It is generally accepted that the Tarkwaian Banket conglomerates are paleo-placers following the general model proposed by Sestini (1973).

The major Tarkwaian-hosted deposits known to date are restricted largely to the Tarkwa District although other occurrences are known from the Ashanti (Ntronang), Bui and Nangode Belts. Exploration to date has not revealed any Tarkwaian units in the general Ahafo Project area and only small fault bounded enclaves of Tarkwaian exist in the Sefwi Belt.

2.1.5 The Sefwi Gold Belt

The Sefwi Belt is a width of about 40-60 km typical Birimian volcanic belt, striking 220 km in Ghana and extends Southwest to the coast in La Cote d'Ivoire. It is located north of, and parallel to, the prolific Ashanti Gold Belt, which hosts many of Ghana's active producing gold mines. Mafic volcanics, metasediments and intrusive granitoids are the dominant lithologies within the belt. The belt is also sandwiched between adjacent sedimentary basins (Sunyani Basin to the west and the Kumasi Basin to the east) and the shared margins are highly faulted and sheared. These northeast striking marginal faults can be traced along the full length of the belt. Additionally, within the interior of the belt, there are key prospective faults that splay off and link with the marginal fault structures which have association with mineralization of gold. Late

ENE trending crosscutting oblique lineaments are seen in regional data sets and are seen to be represented by similarly oriented structures at the deposit level which are also associated with gold mineralization. The overall structural fabric of the belt strike in NE- SW. Figure 2.1 shows the location of the Sefwi gold belt.

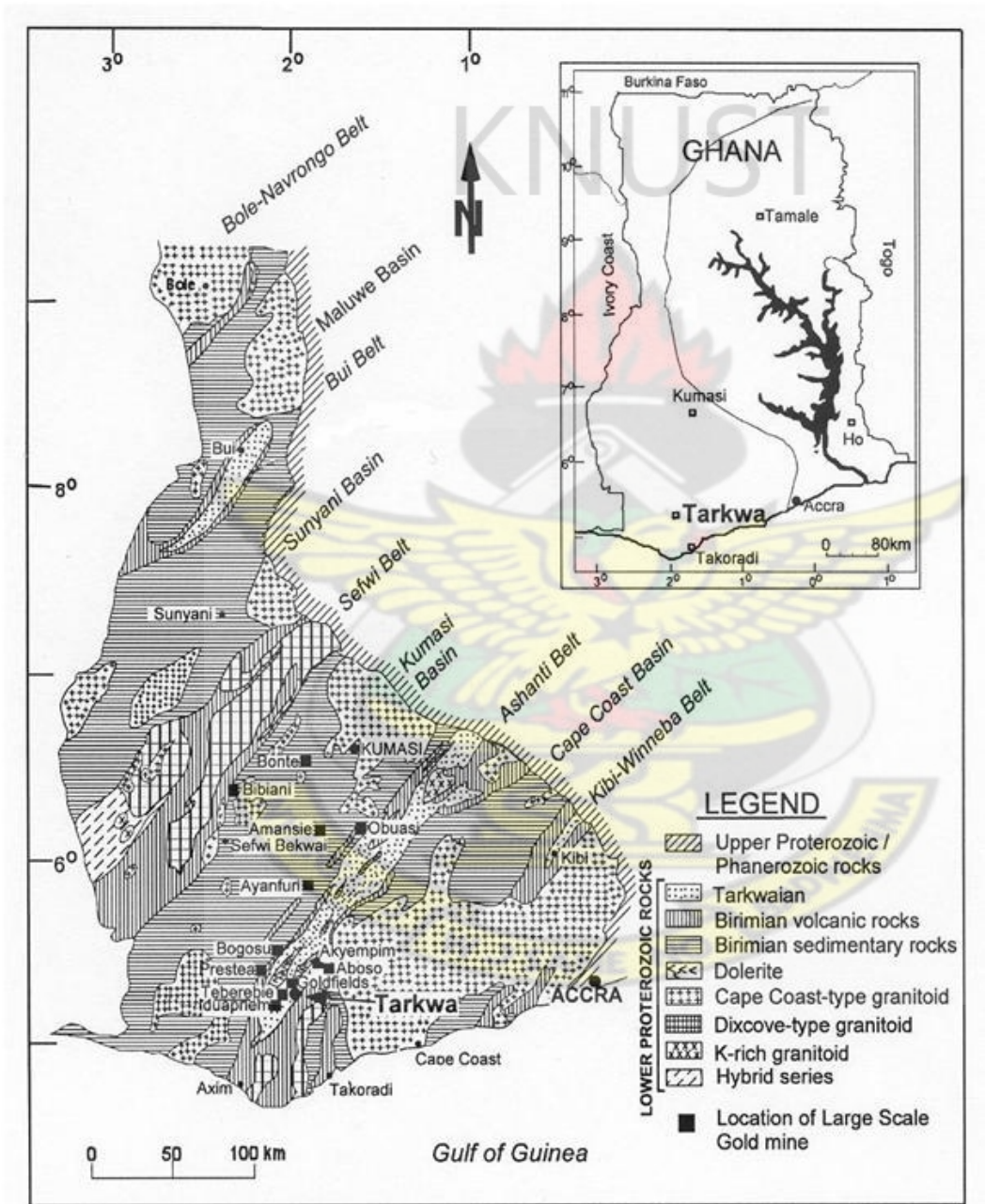


Figure 2.1 Geological map of South-Western Ghana showing the various gold belts (after Kesse (1985))

2.1.6 Structures

The main structural feature in the area is the north-east to south-west trending regional thrust that separates the Sefwi Belt from the Sunyani Basin. This structure is clearly outlined by the aeromagnetic interpretation and is locally referred to as the Kenyase Thrust. The structure spans the entire length of the Ahafo projects.

A number of splay of faults emanate from the Kenyase Thrust within the project area and several ENE-trending aeromagnetic structures are recognized. Notable among the latter is the Yamfo NE structure in the northern portion of the area. Significantly mineralized ENE-trending structures in the south include the Mehame and Mampehia trends.

NNW-trending structures are also evident from aeromagnetic data. Some of these structures in the region have been followed up by surface exploration and interpreted as cross-cutting mafic dykes (Ahafo Mineral Resource and Ore Reserve Report, 2006).

2.1.7 Topography & Regolith

The topography at Ahafo consists of a series of rolling hills and elevated pediments or plateaus covered with essentially residual to proximal lateritic weathering profiles. The terrain is interspersed by valleys, some of which are poorly developed with variable thickness of alluvial and distal colluvial cover.

2.2 Local Geology

Subenso South deposit is located in the contact zone of the predominantly metasediments of the Sunyani basin and the volcanics and granitoids of the Sefwi Belt.

Subenso South occurrence is located in the North Ahafo trend, between the Subenso North and the Teekyere West deposits. Regionally, Subenso South is found within the Paleoproterozoic basement of South Western Ghana (SW). It consists principally of rocks of the Birimian Supergroup (2.2-2.1Ga). The dominant lithologies at Subenso South are the metasedimentary - volcanic unit (MV) and the granitoid unit (GD). Subenso South is a different style of mineralization to the Kenyase Style (Kenyase Central and East and Bosumkase) and Area E Style (Ahafo Mineral Resource and Ore Reserve Report, 2006).

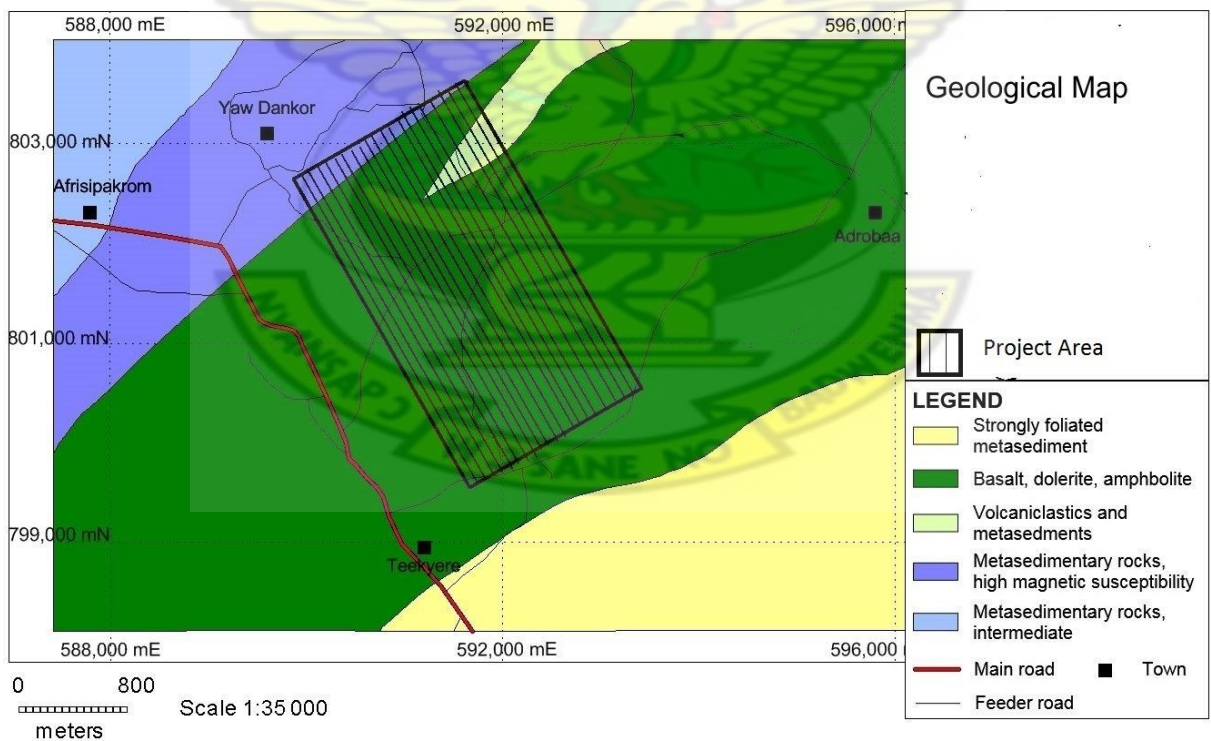


Figure 2.2: Geological map of Subenso-South concession (modified after Cees, 2006)

2.2.1 Style of Gold Mineralization

Subenso South is a shear hosted mesothermal deposit. The mineralization is focused in strongly altered tectonic and dilatent breccias, which typically contain more than 5 g/t gold grades over widths of 1 to 40m. The tectonic breccia provided plumbing to the systems and a permeable host rock. The dilatent breccias provided discontinuous permeable host rock, but are only mineralised if connected to a tectonic breccia feeder zone. The predominant host lithologies deform plastically (absorbing deformation with movement on the foliation planes). Very limited fracturing extends beyond the tectonic breccia zones. Therefore, lower grade between 0.5 g/t and 2 g/t halos are narrow (0 to 10m) and ore to waste contacts are very sharp compared to the Kenyase and Area E Style mineralization.

Like the Kenyase and Area E Style deposits, the Subenso Style includes higher-grade (>5 to >10 g/t) shoots in the plane of the brittle fault zones (tectonic breccias). The higher grade and generally thicker ore zones in Subenso Style deposits are controlled by a complex set of structural interactions. Some of the zones appear to be controlled by the intersection of the tectonic breccia zones with cross-cutting north-south trending structures. Other zones are clearly related to sharp changes in dip or strike associated with structures deflecting around granitoid bodies. Still others appear to be controlled by small left jogs in the brittle fault zones or by combinations of all factors (Ahafo Mineral Resource and Ore Reserve Report, 2006).

CHAPTER 3

THEORETICAL BACKGROUND OF GEOPHYSICAL METHODS USED

3.1 The Principle of Gravitation

Gravity surveying involves measuring variations in the Earth's gravitational field which are occur as a result differences in the sub-surface rock density. General search for oil and gas, particularly in the twentieth century was carried out using this method (Reynolds, 1977).

Isaac Newton in 1667 came out with the Universal Law of Gravitation. This law is a mathematical description of one of the most important phenomena of nature. The law states that each particle of matter in the universe attracts all others with a force directly proportional to its mass and inversely proportional to the square of its distance of separation (Telford, et al., 1976).

In cartesian coordinates, the mutual force between a particle of mass m centered at point $Q = (x', y, z')$ and a particle mass of m_o at $P = (x, y, z)$ is given by:

$$F = G \frac{m m_o}{r^2} \quad (3.1)$$

where, $r = [(x - x')^2 + (y - y')^2 + (z - z')^2]^{1/2} \quad (3.2)$

and where G is Newton's gravitational constant. Allowing the mass m_0 to be a test particle with unit magnitude, then dividing the force of gravity by m_0 results in the gravitational attraction produced by mass m at the location of the test particle:

$$\mathbf{g}(P) = -G \frac{m}{r^2} \mathbf{r} \quad (3.3)$$

where \mathbf{r} is a unit vector directed from the mass m to the observation point P . This value is negative because \mathbf{r} is directed from the source to the observation point, opposite in sense to the gravitational attraction.

So the gravitational acceleration \mathbf{g} can be described as the gradient of the scalar potential:

$$\mathbf{g}(P) = \nabla U(P) \quad (3.4)$$

where,

$$U(P) = G \frac{m}{r} \quad (3.5)$$

The convention used here defines the gravitational potential as the work done on a test particle and is the negative of the particle's potential energy, hence $U(P)$ is positive. Acceleration is seen to be a function only of the mass of the Earth and the distance from the center of it to the gravity station. The unit of gravitational acceleration is called the Gal and is equivalent to 1 cm/s^2 (Telford et al., 1976).

The principle of superposition is obeyed by the gravitational potential and so the net force on a test particle is the vector sum of the forces due to all of the masses in space. This principle is then applied to the gravitational attraction in the limit of a continuous distribution of matter whose mass can be thought of as an infinite number of very small masses $dm = \rho(x, y, z)dv$, where $\rho(x, y, z)$ is the density distribution. Applying the principle of superposition yields

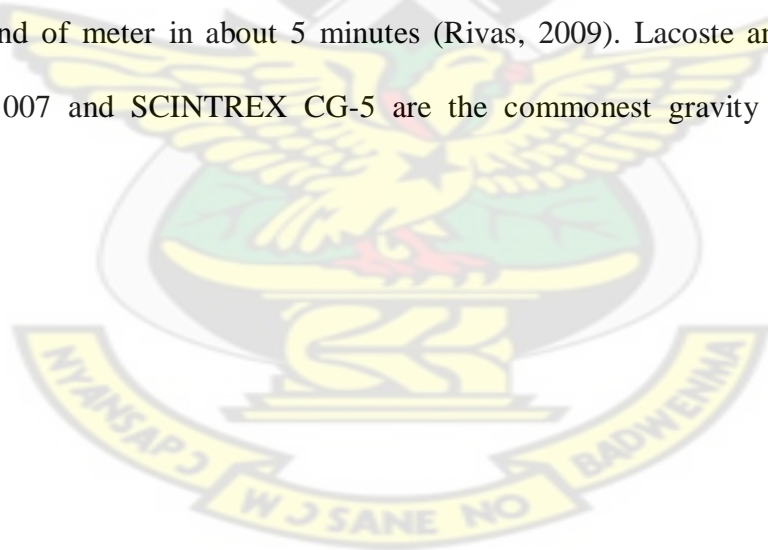
$$U(P) = \int G \frac{\rho(Q)}{r} dv \quad (3.6)$$

where integration is over V , the volume occupied by the mass. P is still the point of observation, Q is the point of integration, and r is distance separating P and Q . However, the gravity meter measures only the vertical component of the gravity.

3.1.1 Units and Measurements of Gravity

The normal value of g at the Earth's surface is 980 cm/s^2 . Extremely small variations in acceleration due to gravity, typically 1 part in 10⁹ can be measured by modern gravity meters. Modern instruments have sensitivity of about ten parts per million.

There are two kinds of gravity meters being used now. The actual value of g can be measured by an absolute gravity meter by measuring the speed of a falling mass using a laser beam. These meters are expensive, heavy, and bulky although they have precisions of 0.01 to 0.001 mGal (miliGals, or 1/1000 Gal). The other type of gravimeter measures relative changes in g between two points. This instrument uses a mass attached to the end of a spring that stretches where g is stronger. A precision of 0.01 mGal can be achieved by this kind of meter in about 5 minutes (Rivas, 2009). Lacoste and Romberg (L&R) model G1007 and SCINTREX CG-5 are the commonest gravity meters being used currently.



3.1.2 Gravity Survey

This is the measurement of the gravitational field at a series of different points over an area of interest. The aim in prospecting is to associate variations with differences in the density distributions and hence rock types (Sheriff, 1994).

In gravity surveys, the station spacing used may vary from a few metres in the case of detailed mineral or geotechnical surveys to several kilometres in regional reconnaissance surveys. Where the gravity field is changing most rapidly, the station density should be greatest as accurate measurement of gravity gradients is critical to later interpretation. At least one easily reachable base station should be available where the absolute value of gravity is known in situations where the absolute gravity values are needed in order to link the results with other gravity surveys. A gravity meter can be used to establish a local base by measuring the difference in gravity between the IGSN ((International Gravity Standardization Net) station and the local base if the location of the nearest IGSN station is inconvenient. Because of instrumental drift this cannot be accomplished directly and a procedure known as *looping* is adopted (Keary et al., 1991)

3.1.3 Data Reduction

Gravity reduction or reduction to the geoid is a process that involves the correction for all variations in the Earth's magnetic field which do not result from differences in the underlying rock densities before results of a gravity survey can be interpreted (LaFehr, 1991).

KNUST

3.1.3.1 Drift Correction

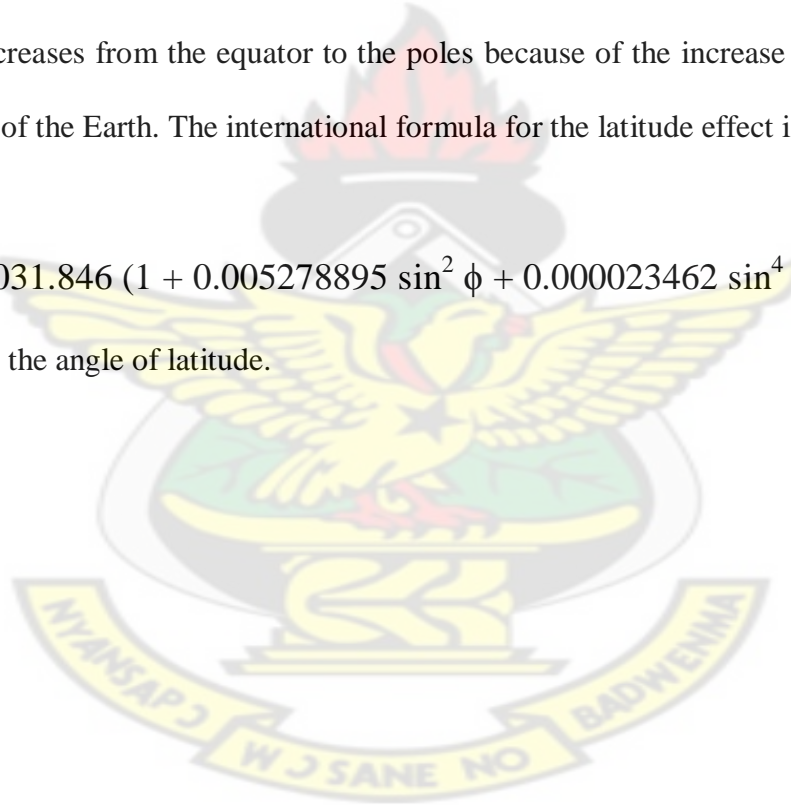
Drift is phenomenon which occurs in all gravity meters. It is the change in the elasticity of the springs over time and is different for every gravity meter. The base station must be occupied several times during the day of the survey to be able to correct the observed gravity readings for instrument drift. Because of the irregular nature of drift, it is necessary to take readings periodically. The meter reading is plotted against time and it is assumed that drift is linear between re-occupations. The drift correction is then subtracted for each station (Baldyga, 2001)

3.1.3.2 Latitude Correction

Two factors which contribute to the latitude correction are spinning of the Earth and its slight equatorial bulge. The centripetal acceleration of the Earth's rotation varies with latitude such that it is at a minimum near the poles and a maximum at the equator. Thus, the negative radial component generated by this rotation decreases the gravity from the poles to the equator. The radius of the Earth measured through the equator is approximately 21 km larger the radius of the Earth measured through the poles. So, gravity increases from the equator to the poles because of the increase in the distance to the center of the Earth. The international formula for the latitude effect is;

$$g = 978\ 031.846 (1 + 0.005278895 \sin^2 \phi + 0.000023462 \sin^4 \phi) \text{ mGals,}$$

where ϕ is the angle of latitude.



3.1.3.3 Free Air Correction

Free air effect which is the second correction to the Earth model accounts for the difference in elevation between the gravity point and the surface of the geoid. This correction is added to the measured gravity because the measured gravity would be smaller at an elevation higher than the geoid surface. The formula for the free air correction (FAC) is:

$$\text{FAC} = 0.3086 h \text{ mgal}$$

where h (in meters) is the elevation of the gravity station

3.1.3.4 Bouguer Correction

The Bouguer correction which is the third correction for gravity to the Earth model accounts for the material between the gravity station and the geoid surface. The correction is of three parts. The first part assumes an infinite horizontal slab of rock of uniform density whose thickness is the elevation difference between the gravity station and the geoid surface. The density is equivalent to the mean density of bedrock found in the region. Generally, a density of 2.67 gm/cm^3 is used to compare other surveys.

The rock mass between the station and the datum increases the measured gravity reading, therefore, the Bouguer correction is subtracted when the station is above the geoid surface.

The formula for Bouguer correction is:

$$BC = 0.012774 \rho h \text{ mGal}$$

where ρ is the density of the slab and h is the thickness of the slab.

The concept of a horizontal infinite slab existing between the station and the datum is not really valid due to local variations around the station in topography. Regions that exist above the Bouguer slab and therefore not accounted for in the Bouguer correction exert an upward pull at the station thus decreasing the observed gravity reading. It is necessary to add a positive terrain correction to make up for this upward attraction. Depressional features are accounted for in the Bouguer slab, however, they do not contain mass. The Bouguer correction therefore overcompensates for these regions and so a positive terrain correction is needed to restore the slab to a flat area. Therefore, the terrain correction is added back to the gravity readings for both hills and valleys.

Once corrections have been applied to the measured gravity values, the result would indicate the variations of geology within the Earth model. This is called the Complete Bouguer Gravity Anomaly (CBGA) and is represented below:

$$CBGA = g_{\text{measured}} - g_{\text{latitude}} + FAC - BC + TC$$

where TC is the value of the calculated terrain correction (Keary et al., 1991).

3.2 Rock Densities

The difference in density, or *density contrast*, between a body of rock and its surroundings produce gravity anomalies.

The sign of the gravity anomaly is determined by the sign of the density contrast.

Densities of rocks vary the least among all geophysical parameters. Most common rock types have densities in the range between 1.60 and 3.20 Mgm^{-3} . The mineral composition and porosity of rocks determine the density of the rocks. In sedimentary rocks, the main cause of density variation is due to variation in porosity. Thus, in sedimentary rock sequences, density increase with depth, as a result of compaction, and with age, due to progressive cementation. Most igneous and metamorphic rocks, composition is the main source of density variation because of their negligible porosity.

Density normally decreases as acidity increases; therefore there is a progression of density increase from felsic through mafic to ultramafic igneous rock types. Table 3.1 presents density ranges for common rock types and ores. A knowledge of rock density is important both for application of the Bouguer and terrain corrections and for the interpretation of gravity anomalies.

The most common way of determining density is by direct measurements on rock samples. A sample is weighed in air and in water. The volume of the sample is provided by the difference in weights and so the dry density can be obtained. The saturated density may be calculated if the rock is porous by following the above procedure after saturating

the rock with water. The density value employed in interpretation then depends upon the location of the rock above or below the water table.

Table 3.1 Approximate density ranges (Mgm^{-3}) of some common rock types and ores.

(Keary et al., 1991)

Rock Type	Density [Mgm^{-3}]
Alluvium	(wet) 1.96–2.00
Clay	1.63–2.60
Shale	2.06–2.66
Sandstone	
Cretaceous	2.05–2.35
Triassic	2.25–2.30
Carboniferous	2.35–2.55
Limestone	2.60–2.80
Chalk	1.94–2.23
Dolomite	2.28–2.90
Halite	2.10–2.40
Granite	2.52–2.75
Granodiorite	2.67–2.79
Anorthosite	2.61–2.75
Basalt	2.70–3.20
Gabbro	2.85–3.12

Gneiss	2.61–2.99
Quartzite	2.60–2.70
Amphibolite	2.79–3.14
Chromite	4.30–4.60
Pyrrhotite	4.50–4.80
Magnetite	4.90–5.20
Pyrite	4.90–5.20
Cassiterite	6.80–7.10
Galena	7.40–7.60

3.3 Gravity Anomalies

The average gravity on the Earth's surface is about $g=9.8 \text{ m/s}^2$, and varies by approximately 5300 mgal (about 0.5% of g) from pole to equator. ($1 \text{ mgal}=10^{-5} \text{ m/s}^2$) Gravity anomalies are local variations in gravity that result from topographic and subsurface density variations, and have amplitudes of several mgal and smaller (Conrad, 2011). There are two main anomalies associated with gravity. They are;

3.3.1 Bouguer anomaly (BA)

The equation for the Bouguer anomaly is:

$$BA = g_{\text{observed}} - g_{\text{latitude}} + FAC \pm BC + TC(\pm EC)$$

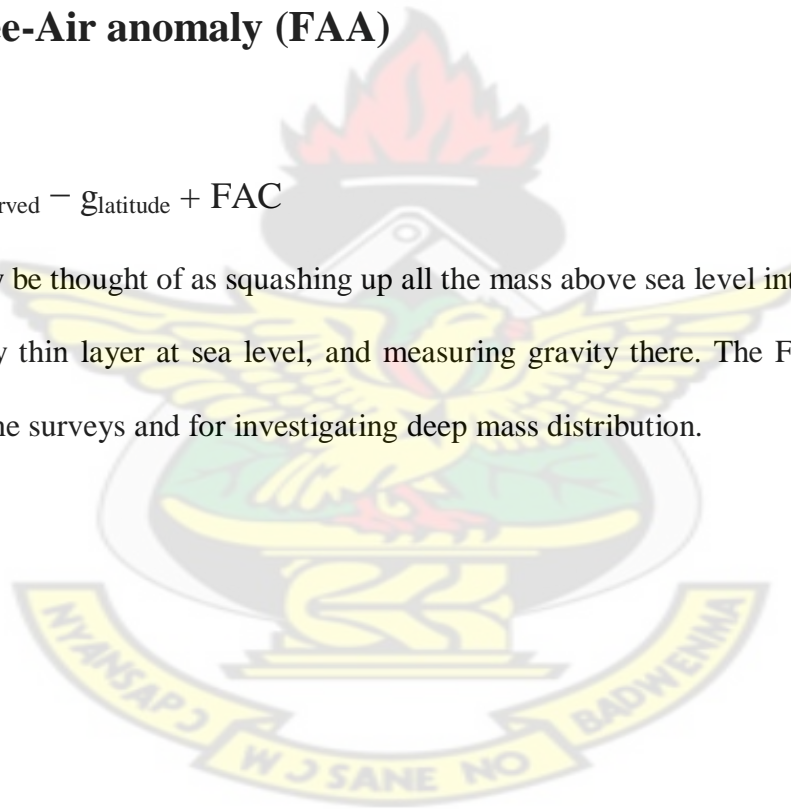
The BA is equivalent to stripping away everything above sea level. It is the anomaly most commonly used in prospecting.

KNUST

3.3.2 Free-Air anomaly (FAA)

$$FAA = g_{\text{observed}} - g_{\text{latitude}} + FAC$$

The FAA may be thought of as squashing up all the mass above sea level into an Infinitesimally thin layer at sea level, and measuring gravity there. The FAA is mostly used for marine surveys and for investigating deep mass distribution.



3.4 Enhancement Techniques

3.4.1 Wavelength filtering

This method may be helpful but artifacts can be created, and bodies of interest may have contributions from different wavelengths. Thus each survey must be looked at individually – there are no rules of thumb. Removing the regional is really a simple form of this process.

3.4.2 Directional filtering

This is useful for enhancing second-order effects if the dominant tectonic trend is in one direction, and cleaning up data with artificial trends in a preferred direction, *e.g.*, as a result of navigation of ship tracks having polarised errors.

3.4.3 Vertical derivative methods

3.4.3.1 The first and second vertical derivative

The first vertical derivative has a similar effect to the second vertical derivative in emphasizing features related to gradients in the field rather than the field itself. It suffers less from noise enhancement than the second vertical derivative and has an additional interesting use because it gives the magnetic field, if it is assumed that the strength and

direction of magnetisation is constant. “Pseudomagnetic anomalies” can be calculated in this way, and compared with real magnetic maps to see if bodies identified by gravity surveying are also magnetic or if magnetic material is present that is not related to density variations. For example, basic plutons have high density/high magnetisation and silicic plutons tend to have low density/low magnetisation (Foulger et al., 2003).

The second vertical derivative has certain properties because gravity falls off as r^{-2} , the 1st derivative falls off as r^{-3} and the second derivative as r^{-4} . Thus, the second vertical derivative:

- a) enhances shallower effects at the expense of deeper effects,
- b) can completely remove the regional,
- c) can determine the sense of contacts, and
- d) can be used to determine limiting depths (the “Smith rules”).

3.4.4 Upward and downward continuation

These are useful in gravity because upward continuation suppresses the signals due to small, shallow bodies, just as taking the second derivative enhances them. It is most useful when applied to magnetic data for:

- a) Upward continuing measurements made at ground level so they may be compared with aeromagnetic data, and
- b) Determining the depth to the basement.

Downward continuation is used to determine the values that a potential field (gravity and magnetics) would have at a lower surface. It is often used to resolve anomalies that overlap at the surface of measurement. It is problematic because noise will blow up exponentially, and if the data are continued down past some body, a meaningless answer will result. Thus, this process must be done carefully, using low-noise data, and in a known situation.

KNUST

3.5 Regional and Residual gravity anomalies

Bouguer anomaly maps are rather like topographic maps with highs and lows, linear features, and areas where the contours are closely packed and others where they are further apart. There may be a gentle trend in the gravity data, reflecting a long wavelength gravity anomaly attributable to deep seated crustal features; this is known as *regional anomaly*. Shorter wavelength anomalies arising from shallower geological features are superimposed on the regional anomaly and it is these anomalies that are often to be isolated for further analysis. The anomaly left after the separation of regional anomaly from the Bouguer anomaly is called *residual anomaly* (figure 3.1) (Reynolds, 1997).

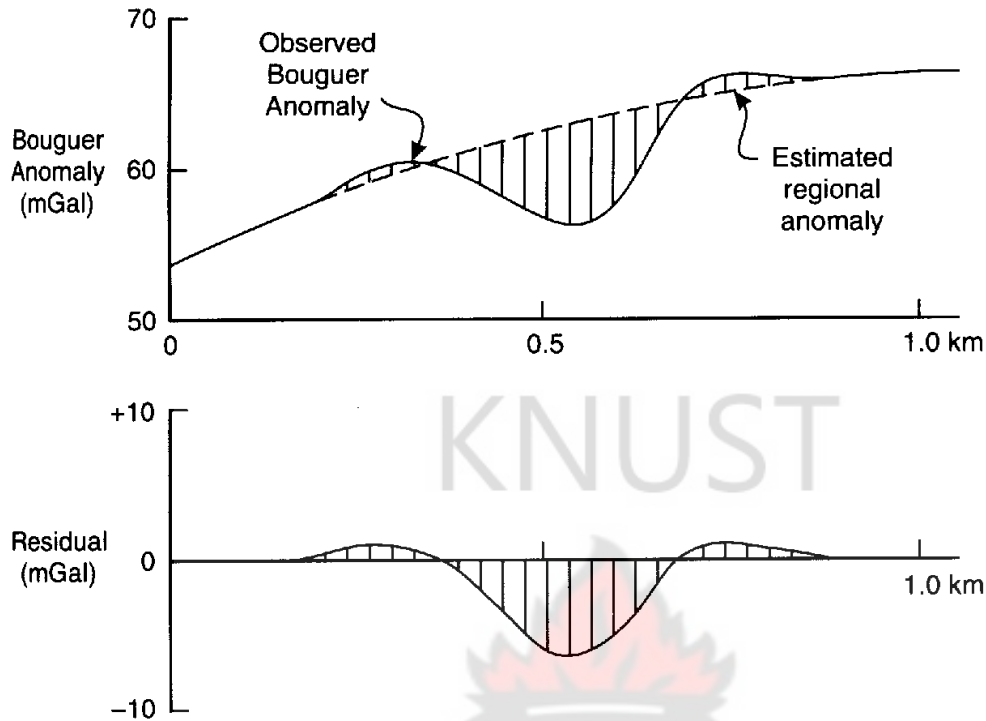


Figure 3.1 Diagram showing Bouguer, Regional, and Residual anomaly (Reynolds, 1997).

3.6 Interpretation and modeling of gravity anomaly

Formulae for simple geometric shapes are usually used to interpret gravity anomalies. There are two approaches to the interpretation namely Direct and Indirect methods.

1. Direct (forward) methods. Most interpretation is of this kind. It involves erecting a model based on geological knowledge, *e.g.*, drilling, or parametric results, calculating the predicted gravity field, and comparing it to the data. The body may then be changed until a perfect fit to the data is obtained.

2. Indirect methods. These involve using the data to draw conclusions about the causative body, *e.g.*, the excess mass, the maximum depth to the top. Some parameters may be calculated, but the full *inverse problem i.e.*, calculating the body from the anomaly, is inherently *non-unique*. (Foulger et al., 2003)

KNUST

3.6.1 Direct methods, or "forward modelling"

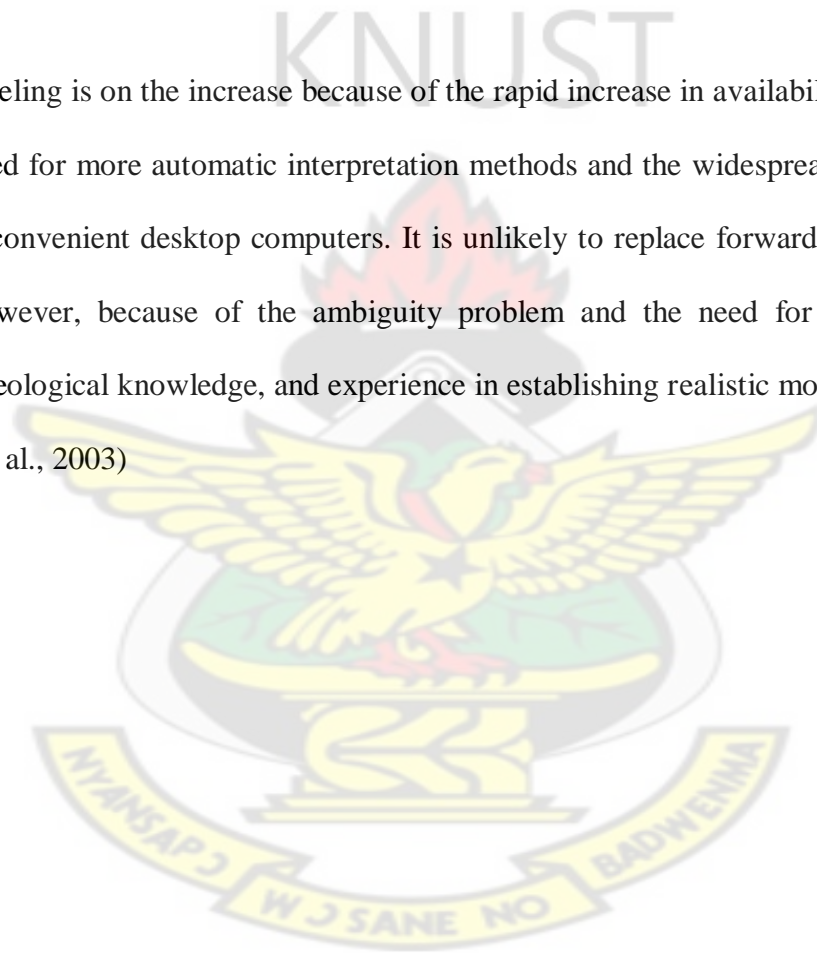
This involves setting up a model, calculating the gravity anomaly, comparing it with the observed data and adjusting the model until the data are fit well. The initial model may be obtained using parametric measurements and/or geological information. Simple shapes may be tried first, and analytical equations are available for these. These have been derived from Newton's Law. Formulae of this kind are useful because they approximate to many simple bodies, and irregular bodies can be approximated to the sum of many simple bodies (Foulger et al., 2003).

3.6.2 Indirect interpretation (or inverse modelling)

The nature of the body is calculated automatically by computer, from the data. Because of the ambiguity problem, this is only possible if limits are placed on variables (*e.g.*, density, the spatial nature of body) so the range of possible solutions is severely restricted.

Inverse modeling is on the increase because of the rapid increase in availability of gravity data, the need for more automatic interpretation methods and the widespread availability of fast and convenient desktop computers. It is unlikely to replace forward modeling by humans, however, because of the ambiguity problem and the need for using sound judgment, geological knowledge, and experience in establishing realistic models.

(Foulguer et al., 2003)



3.7 Principles of Magnetism

A magnetic flux is developed within the vicinity of a bar magnet which flows from one end of the magnet to the other. The directions assumed by a small compass needle suspended within this flux can be used to map it. Poles of the magnet are the points within the magnet where the flux converges. A freely-suspended bar magnet similarly aligns in the Earth's magnetic field flux.. The north-seeking or positive pole is the one which inclines to point in the direction of the Earth's north pole. This is equaled by a south-seeking or negative pole of equal strength at the opposite end of the magnet.

The force F between two magnetic poles of strengths m_1 and m_2 separated by a distance r is given by:

$$F = \mu_0 \frac{m_1 m_2}{4 \pi \mu_R r^2} \quad (3.7)$$

Where μ_0 and μ_R are constants which correspond to magnetic permeability of vacuum and the relative magnetic permeability of the medium separating the poles.

The force is attractive if the poles are of different sign and repulsive if they are of the same sign.

The *magnetic field* B due to a pole of strength m at a distance r from the pole is defined as the force exerted on a unit positive pole at that point.

$$B = \frac{\mu_0 m}{4 \pi \mu_R r^2} \quad (3.8)$$

Magnetic fields can be defined in terms of *magnetic potentials* in a similar manner to gravitational fields. For a single pole of strength m , the magnetic potential V at a distance r from the pole is given by;

$$V = \frac{\mu_0 m}{4 \pi \mu_R r} \quad (3.9)$$

The *magnetic moment* M of a dipole with poles of strength m a distance l apart is given by

$$M = m l \quad (3.10)$$

induced magnetization or magnetic polarization is a phenomenon which occurs when a material is positioned in a magnetic field and obtain a magnetization in the direction of the field which is lost when the material is taken away from the field.

The intensity of induced magnetization J_i of a material is defined as the dipole moment per unit volume of material:

$$J_i = \frac{M}{LA} \quad (3.11)$$

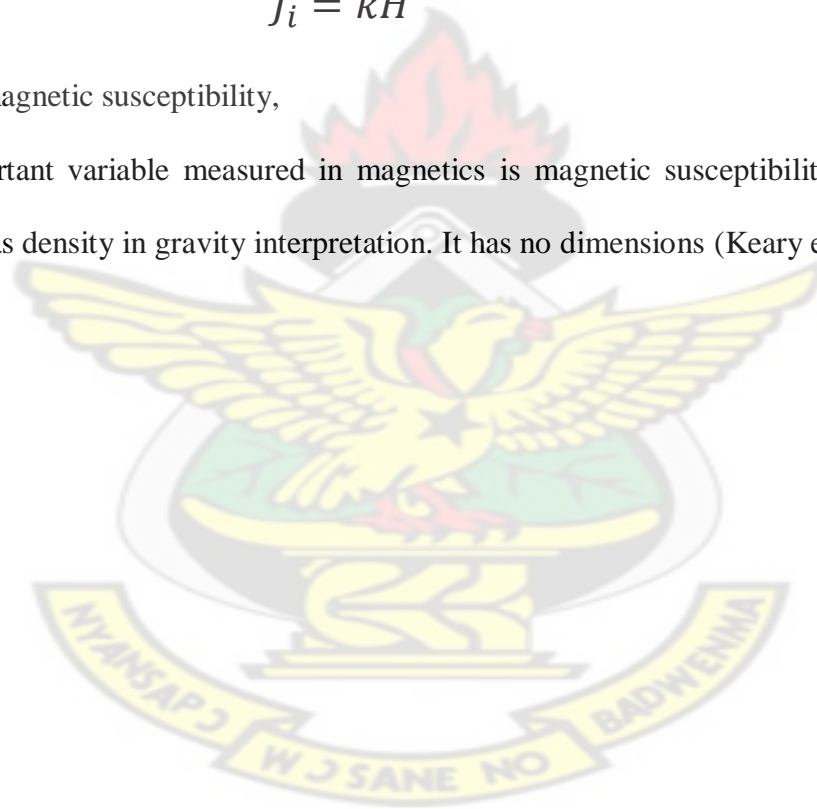
where M is the magnetic moment of a sample of length L and cross-sectional area A . J_i is consequently expressed in Am^{-1} . In the c.g.s. system intensity of magnetization is expressed in emu cm^{-3} (emu = electromagnetic unit), where $1 \text{ emu cm}^{-3} = 1000 \text{ Am}^{-1}$.

The induced intensity of magnetization is proportional to the strength of the magnetizing force H of the inducing field:

$$J_i = kH \quad (3.12)$$

where k is the magnetic susceptibility,

The most important variable measured in magnetics is magnetic susceptibility and serves the same purposes as density in gravity interpretation. It has no dimensions (Keary et al., 1991)



3.7.1 Magnetism of the Earth

Earth's magnetic field is produced in the fluid outer core by a self-exciting dynamo process. Electrical currents flowing in the slowly moving molten iron create the magnetic field. In addition to sources in Earth's core, the magnetic field observable at the planet's surface has sources in the crust and in the ionosphere and magnetosphere. The geomagnetic field varies on a range of scales, and a description of these variations is now made ordered from low- to high-frequency variations in both the space and time domains (Macmillan, 2004).

3.7.2 Nature of the Geomagnetic Field

The geomagnetic field of the Earth is made up of three parts when it comes to Exploration

Geophysics. They are;

- The main field, which varies relatively slowly and is of internal origin.
- A small field (compared to the main field), which varies rather rapidly and originates outside the Earth.
- Spatial variations of the main field which are typically smaller than the main field, are almost constant in time and place, and are caused by local magnetic anomalies in the near-surface crust of the Earth. These are the targets in magnetic prospecting.

The geomagnetic field looks like that of a dipole whose north and south magnetic poles are positioned approximately at 75°N, 101°W and 69°S, 145°E. The dipole is displaced about 300

km from the Earth's center toward Indonesia and is inclined some 11.5° to the Earth's axis (Telford et al., 1990).

3.7.3 The Earth's Magnetic Field

The Earth's magnetic field results from the superposition of fields of various origins that operate on a wide range of spatial and temporal scales. On the Earth, the magnetic field seem to be everywhere and it is no surprise that this physical quantity has been continuously observed for more than a century (Mandea and Purucker 2005). Geomagnetic field measurements are of extensive use for remote sensing, natural resource exploration, geophysical research, planetary science, and societal applications (Kono 2007). In particular, their interpretation was critical to the growth of a new paradigm of geosciences in the early 1960, that of Plate Tectonics (Vine and Matthew 1963).

If an unmagnetized steel needle could be hung at its center of gravity, so that it is free to orient itself in any direction, and if other magnetic fields were absent, it would assume the direction of the Earth's total magnetic field, a direction that is usually neither horizontal nor in-line with the geographic meridian (Telford et al., 1990). The magnitude of this field F_e , the inclination (or dip) of the needle from the horizontal I , and the angle it makes with geographic north (the declination) D , completely define the main magnetic field.

The magnetic elements (Whitham, 1960) are illustrated in Fig. 3.2. The field can also be described in terms of the vertical component, Z_e , reckoned positive downward, and the horizontal component H_e , which is always positive. X_e and Y_e are the components of H_e , which are considered positive to the north and east, respectively (Telford et al., 1990). Furthermore the

vertical component of the magnetic intensity of the Earth's magnetic field varies with latitude, from a minimum of around 30000 nT at the magnetic equator to 60000 nT at the magnetic poles.

These elements are related as follows:

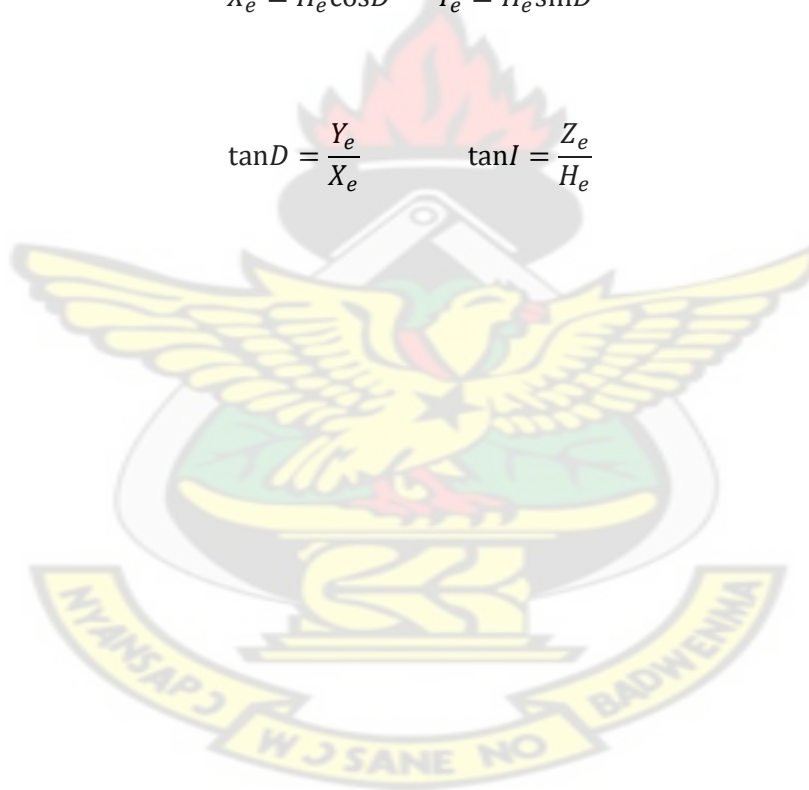
$$F_e^2 = H_e^2 + Z_e^2 = X_e^2 + Y_e^2 + Z_e^2$$

$$H_e = F_e \cos I \quad Z_e = F_e \sin I$$

$$X_e = H_e \cos D \quad Y_e = H_e \sin D$$

$$\tan D = \frac{Y_e}{X_e} \quad \tan I = \frac{Z_e}{H_e}$$

3.13



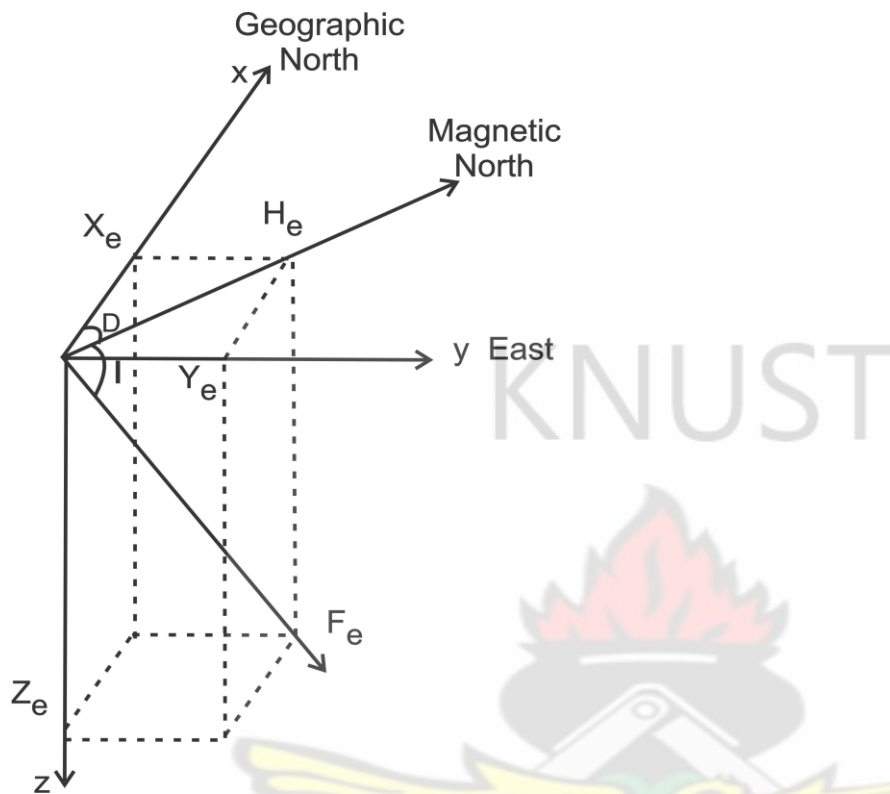


Figure 3.2: Elements of the Earth's magnetic field (Whitham, 1960)

3.8 Magnetism of Rocks and Minerals

Many rocks that contain iron-bearing minerals act as tiny magnets. As magma or lava cools, these minerals begin to form. At this point the molten rocks have not completely solidified, so the magnetic minerals moving in the molten mass become aligned to the magnetic field. When the rock finally hardens, these minerals 'lock in' the magnetic field. Sedimentary rocks also have a magnetic record. As iron bearing sedimentary minerals is deposited from the water column, they also become aligned with the existing magnetic field. The magnetism remains locked in the

rock unless the rock is subsequently heated above the Curie point, the temperature at which all magnets lose their magnetism. When the heated rock again cools below the Curie point, it will record the magnetic field at this later time, and the old magnetic field will be lost. It is imperative, therefore, to establish that a rock's magnetism is primary and has not been re-set at a later time (Reeves, 1989; Petersen, 1990).

(Telford et al., 1990) suggest that local changes in the main field result from variations in the magnetic mineral content of near surface rocks. The sources of local magnetic anomalies cannot be very deep, because temperatures below ~ 40 km should be above the Curie point, the temperature (~550°C) at which rocks lose their magnetic property.

Magnetic anomalies are caused by magnetic minerals (mainly magnetite and pyrrhotite) contained in the rocks. Substances can be separated on the basis of their behaviour when placed in an external field (Telford et al., 1990). The susceptibility in diamagnetic materials is low and negative, i.e., a magnetization develops in the direction which is opposite to the applied field. Paramagnetic materials are characterized by low and positive susceptibilities. Ferromagnetic materials can be subdivided into three categories. True ferromagnetism is a cooperative phenomenon observed in metals like iron, nickel and cobalt, in which the lattice geometry and spacing allows the exchange of electrons between neighbouring atoms (Lowrie, 2007).

This yields a *molecular field* by means of which the magnetic moments of adjacent atoms reinforce their mutual alignment parallel to a common direction. Ferromagnetic substances have high and positive susceptibilities coupled with strong magnetic properties. The crystal structures of certain minerals permit an indirect cooperative interaction between atomic magnetic moments. This *indirect exchange* confers magnetic properties that are similar to ferromagnetism. The mineral may display *antiferromagnetism* or *ferrimagnetism*. The small group of

ferromagnetic minerals is geophysically important, especially in connection with the analysis of the Earth's paleomagnetic field (Lowrie, 2007).

Ferromagnetism decreases with increasing temperature and disappears entirely at the Curie temperature. Truly ferromagnetic materials occur only rarely in nature but include substances such as cobalt, nickel and iron, all of which have parallel alignment of moments (Nagata, 1961). In anti-ferromagnetic materials, for example hematite, the moments are aligned in an anti-parallel manner (Nagata, 1961). Although the magnetic fields of the oppositely orientated dipoles cancel each other out, crystal lattice defects result in a net residual moment or parasitic (anti)-ferromagnetism (Reynolds, 1997).

In ferrimagnetic materials the magnetic sub domains align in opposition but their net moment is not zero either because one set of domains has a stronger magnetic alignment than the other or because there are more subdomains of one type than of the other. Examples of the first type are magnetite and titanomagnetite, oxides of iron and of iron and titanium. Pyrrhotite is a magnetic mineral of the second type. Practically all magnetic minerals are ferrimagnetic (Telford et al., 1990)

3.8.1 Magnetic susceptibility

Magnetic susceptibility is a measure of the ease with which particular sediments are magnetized when subjected to a magnetic field. The ease of magnetization is ultimately related to the concentration and composition (size, shape and mineralogy) of magnetizable material contained within the sample (Wemegah et al., 2009). Magnetizable minerals include the ferromagnetic minerals (strongly magnetizable) and any of the paramagnetic (moderately magnetizable) minerals and other substances (Telford et al., 1990; Wemegah et al., 2009; Reynolds, 1997).

A body positioned in a magnetic field obtains a magnetization which, if small, is proportional to the field:

$M = kH$ where M or J (also referred to as the intensity of magnetization) is the volume magnetization induced in a material of susceptibility k by the applied external field H (Milsom, 2003)

The *susceptibility*, k , is very small for most natural substances, and may be either negative (diamagnetism) or positive (paramagnetism). The fields produced by dia- and paramagnetic substances are generally considered to be too small to impact survey magnetometers, but modern high-sensitivity magnetometers are making exceptions to this rule. Most observed magnetic anomalies are due to the small number of *ferro-* or *ferri-magnetic* substances in which the molecular magnets are held parallel by intermolecular *exchange forces*. Below the *Curie temperature*, these forces are strong enough to overcome the effects of thermal agitation. Magnetite, pyrrhotite and maghemite, all of which have Curie temperatures of about 600 °C, are

the only significant naturally occurring magnetic minerals and, of the three, magnetite is by far the most common. Hematite, the most abundant iron mineral, has a very small susceptibility and many iron ore deposits do not produce significant magnetic anomalies (Milsom, 2003)

(Milsom, 2003) indicates that susceptibility of a rock usually depends on its magnetite content. Sediments and acid igneous rocks have small susceptibilities whereas basalts, dolerites, gabbros and serpentinites are usually strongly magnetic. Weathering generally reduces susceptibility because magnetite is oxidized to hematite, but some laterites are magnetic because of the presence of maghemite and remanently magnetized hematite. The susceptibilities, in rationalized SI units.

3.8.2 Remanent Magnetization

Permanent magnetization that was acquired during the formation the rock is called Remanent Magnetization. In igneous rocks, some of the dipoles within the magnetic minerals aligned with the existent Earth's magnetic field when solidified through the Curie temperature. If the field is strong enough then the dipoles would permanently position themselves across imperfections inside the grains of the mineral setting up a permanent magnetization that exists independently from an external field. Remanent and induced magnetizations can be acquired by any rock having magnetic minerals. The magnitude of the J defines amplitude of magnetic anomalies and the direction of J vector affects the shape of the anomaly (Telford et al, 1976).

3.8.3 Magnetization at Low Magnetic Latitudes

In low latitudes areas across the equator, the patterns of measured magnetic field are much complicated than that at high latitudes with same geological settings. At low latitudes, comparing with geological structures, the magnetic anomalies are very complex, with evident negative and increasing companion anomalies, and mostly strike in EW direction. At high latitudes, the features of magnetic anomalies are well correlated with geological structures, which even can be used to estimate the structural parameters, such as location and strike of faults, distribution of rocks, and rough scales of sedimentary basins. In current quantitative inversion interpretation, some successful methods, such as inversion calculation for magnetic interface, are based on the magnetic anomalies of vertical magnetization.

For both the qualitative and quantitative interpretations, people hope that the observed magnetic fields are influenced by magnetization direction as little as possible. It would be favorable to interpretation, if we can remove the complication caused by tilting magnetization (in particular, at low latitudes) through transformation calculation to the magnetization direction. The work of reduction to the pole (RTP) for magnetic anomalies is just to manage and remove such complications so that the interpretation of magnetic anomalies become a simple procedure (Changli et al., 2003)

(Rajagopalan, 2003) suggested that, at very low latitudes, typically between 10° inclination, the amplitude correction for north-south trending features unreasonably amplifies noise and several distorts magnetic anomalies from sources magnetized in directions different from the inducing

field. Due to the dipolar nature of the geomagnetic field, magnetic anomalies observed anywhere rather than magnetic poles are asymmetric even when the causative body distribution is symmetric. This property complicates the interpretation of magnetic data.

3.9 Lithology, Structure and Magnetism

Generally the magnetite content and, hence, the susceptibility of rocks is very variable and there can be substantial overlap between different rock types. Identifying with confidence the causative body of any anomaly from only magnetic information is not normally possible. Nevertheless, sedimentary rocks are effectively non-magnetic unless they possess a substantial magnetite content. Igneous and metamorphic basement and also intrusions may be the cause of a magnetic anomaly observed over a known sedimentary cover. The presence of dykes, faulted, folded or truncated sills and lava flows, massive basic intrusions, metamorphic basement rocks and magnetite ore bodies may be some of the common causes of magnetic anomalies. The amplitude of magnetic anomalies may reach several thousand nT over magnetite ores but generally magnetic anomalies range in amplitude from a few tens of nT (nanoteslas) over deep metamorphic basement to several hundred nT over basic intrusions.

(Keary et al, 2002)

Structures may be conveniently subdivided into two groups (Plummer et al., 2001):

- Brittle structures - recording the brittle-elastic failure of rocks in the past. Faults and joints fall in this broad category.

- Ductile structures - preserving the permanent viscoplastic deformation of rock throughout geologic time. Folds and metamorphic foliations are the expression of this type of structure.

Isolated magnetic anomalies, generally circular or oval in plan and several hundred meters across, and with amplitude of tens to hundreds of nanoteslas, may arise from accumulation of magnetite and pyrrhotite, which may be associated with economic grades of copper, lead, zinc, silver, gold such deposits (Plummer et al., 2001). For example, the Abra deposit in the Bagemall Basin of Australia, which precipitated from mineral bearing solutions are frequently located within the adjacent to major faults.

3.10 Rock Alteration

Rock alteration is the reaction of hydrothermal fluids with enclosing rocks, causing changes in mineralogy that are most marked adjacent to the vein and become less distinct further away (Appiah, 1991). Alteration of wall rock adjacent to hydrothermal veins by the fluid is responsible for formation of the mineral deposit. Wall rock alteration occurs in the form of pyritization, arsenopyritization, sericitization, chloritization, silicification, and carbonatization. The most abundant ore minerals are pyrite and arsenopyrite, each making up 20-30% of all ore minerals. Gold is commonly associated within bournonite and bonanza ores are associated with mariposite (Appiah, 1991). Rocks which should display large susceptibilities and greatest intensities of magnetization may exhibit much weaker magnetic properties owing to geochemical alteration of the magnetic minerals (Reynolds, 1997).

3.11 Magnetic Anomalies

Magnetic and gravity anomalies caused by rocks are superimposed the same way on the Earth's geomagnetic field and gravitational field respectively. Magnetic anomalies however are difficult to interpret because it varies not only in amplitude but also in direction whereas the gravitational field is everywhere and vertical (Keary et al., 1991).

3.11.1 Forms of magnetic anomaly

The shape of a magnetic anomaly varies dramatically with the dip of the Earth's field, as well as with variations in the shape of the source body and its direction of magnetization. Simple sketches can be used to obtain rough visual estimates of the anomaly produced by any magnetized body (Milsom, 2003).

3.11.2 Basic Interpretation of Magnetic Anomalies

Magnetic data can be interpreted in terms of specific geometric forms which approximate to the shapes of subsurface magnetized bodies. This tends to be true where profiles are to be interpreted only in terms of two dimensions. Three-dimensional models are far more complex and can be used to approximate to irregularly shaped bodies. The commonest shapes used are the sphere and the dipping sheet both of which are assumed to be uniformly magnetised and in the simplest cases have no remanence (Reynolds, 1997).

3.12 Depth Estimation by 3D Euler Deconvolution

The main focus of magnetic or gravity data interpretation is to determine the plan locations and depths of the causative subsurface sources. The popular methods such as the statistical method of Spector and Grant (1970), Werner deconvolution (Hartman et al., 1971), analytic signal (Nabighian, 1972), Euler deconvolution (Thompson, 1982), etc., were developed to enhance the estimations. Nabighian et al. (2005) gave a summary of their mode of applications which transformed from the earlier 2D in the 1970's and early 1980's to 3D in the 1990's and beyond (Reid et al., 1990; Roest et al., 1992; Hansen and Suci, 2002). Among these common methods, the Euler deconvolution method which can be used for rapid 3D interpretation of the potential field data is very popular and is particularly good at delineating contacts and depths of causative sources. It uses the magnetic residual field and its three orthogonal gradients (two horizontal and

one vertical) to compute spatial locations of the anomaly sources. Sometimes to apply the method, choices of the structural index (a function of the causative source geometry) and a square window within the grids of the gradient values and field values are made (Reid et al., 1990; Silva and Barbosa, 2003).

KNUST



CHAPTER 4

MATERIALS AND METHODS

4.0 Materials

All materials used for this thesis work were provided by Newmont Ghana right from the data collection through to data processing and interpretation with supervision from my supervisors from KNUST. The data collection was carried out with the help of the geophysics crew of the company. The main equipment used for this survey were Lacoste and Romberg gravity meter, Geometrics 856 magnetometer units, Topcon Differential Global Positioning System(GPS) and a Garmin Handheld GPS. The software included Geosoft Oasis Montaj version 7.1, ArcGIS 10, MapInfo 10.5 Discover.

4.1 Gravity Data Acquisition

A detailed ground gravity survey was carried out in the Subenso South area. The data was collected on a 3.6 km by 2 km block along profile lines spaced at 100 m. The length of each profile line was 3.6 km. There were 21 profile lines in all making a complete block. The profile lines were pegged at 50m interval along each profile but data was collected at 100 m interval along the profile. The profile lines were numbered from 10000E to 12000E. The block was further divided into 3 sub –blocks making the length of each profile within the sub block to be 1.2 km and the number of profile lines remained 21 in each sub-block. This was done to facilitate

the gravity survey activity. The whole block had 3 baselines, 1 in each sub-block. The baselines were numbered 10000N, 11200N and 12400N. A total of 9 gravity base stations were established along the baselines. There were 3 gravity base stations along each baseline. This was to reduce the time to return to base to repeat base readings therefore increasing data quality by reducing the amount of drift. There was an already established survey control pillar with known coordinates so the GPS base receiver was mounted on the control pillar so that the field GPS can be used to occupy the individual gravity stations to acquire their GPS coordinates. The gravity was collected by using Lacoste and Romberg (L&R) Gravimeter (G1007) model and a Topcon Differential Global Positioning System (GPS).

The data was collected using the method of looping. On a normal data collection day, the gravimeter is placed on the gravity base station and the gravity reading was taken and recorded in a field sheet. After occupying the gravity base station, the gravity meter was then carried to the first gravity point along the profile to take the reading. The readings were taken at 100 m interval. So after about 2-3 hours of measurements, the gravimeter was returned to the gravity base station to repeat the base reading. This was usually done to correct for drift. After repeating the base a series of measurements were taken for about 2-3 hours and then the meter was returned to the base station for measurement to be done to close the survey for the day. Also, before returning to the base station to tie in the field readings to it, it is advisable to repeat 1 or 2 already measured gravity points to check for repeatability. After each field reading, the GPS coordinates were also taken for the gravity points. These coordinates were used in the processing of the gravity data.

The procedure was repeated for all profile lines until all the gravity data were acquired. A total of 756 gravity stations were occupied together with their GPS coordinates. It took about 2 months to complete the data acquisition.



Figure 4.1 A picture of the Lacoste& Romberg gravimeter (A) used for the survey. B is base plate and C is gravimeter case



Figure 4.2 Operator recording readings on the gravimeter on to a field sheet



Figure 4.3 Operator setting up and configuring base Differential GPS. A is GPS receiver, B is antenna, C is tribrach, and D is Tripod stand



Figure 4.4 Operator configuring field Differential GPS. A is controller, B is stand, C is receiver, and D is antenna

4.2 Gravity Data Processing

The field readings were just the readings on the dial and not the actual gravity values. A calibration table was used to convert all the gravity meter readings to milliGal values using Microsoft Excel. Oasis montaj version 7.1 was used in processing the data. Three databases were constructed to process the data namely gravity base stations database, location databases, and the gravity stations data which had been merged. These three databases are needed in order to process the gravity data. The 1967 Gravity reference formula was used in latitude correction. The free-air correction formula used was 0.308596 mgal/m . These formulas are incorporated within the software. The Earth density used was 2.67 g/cc , the water and ice density used were 1.0 g/cc and 0.95 g/cc respectively.

The GPS coordinates were projected using a datum of WGS84 and a projection method UTM Zone 30 N. The geoid was used as reference level. After setting the processing parameters the the gravity survey data was imported into the created database. The data was then corrected for instrument drift to remove the effects of drift from the data in order to get the absolute gravity values. The repeated gravity stations are processed to get the average absolute gravity for those stations and also check the repeatability of the data to ensure maximum data quality.

Terrain Correction was applied to the data using an already created terrain grid using a regional and local DEM (Digital Elevation Model) grid in the software.

The following components of the gravity reduction were carried out on the data:

- (1) Latitude correction
- (2) Free Air Anomaly calculation
- (3) Bouguer anomaly calculation
- (4) Complete Bouguer anomaly (Bouguer anomaly + terrain correction)

4.2.1 Gravity data correction

The effect of latitude was corrected by subtracting the theoretical gravity (which are calculated from 1967 IGRF gravity formula) from the observed gravity.

The free air anomaly was calculated by subtracting the latitude correction (theoretical gravity) from the absolute gravity and adding a correction for the station elevation.

The Bouguer anomaly corrects the free air anomaly for the mass of rock that exists between station elevation and the spheroid. (Geosoft, 2009)

The Complete Bouguer anomaly corrects for the Bouguer anomaly for irregularities of the earth due to terrain in the vicinity of the observation point.

All the above reduction procedures are incorporated in the software and were applied to the data.

KNUST

4.2.2 Regional and Residual Gravity

The Bouguer anomaly is made up of broad and gently varying regional anomalies which may superimpose shorter wavelength local anomalies. In gravity surveying, the anomalies of interest are the local anomalies (Keary et al., 2002). Therefore in the data processing the regional field was removed from the observed gravity to isolate the residual field which is the one we are interested in. This was done by using command within the Geosoft Oasis Montaj software.

4.2.3 Enhancement Techniques

4.2.3.1 Microlevelling

This process was applied to the data to remove subtler inter and intra line errors that remain in the data after normal leveling corrections have been applied (Geosoft, 2009).

4.2.3.2 Filtering

The two-dimensional Fast Fourier transform (2D-FFT) filter was applied to the data to remove noise from the data therefore increasing the signal to noise ratio. This makes interpretation of gravity anomalies in relation to geological structures a lot easier.

4.2.3.3 Upward continuation

To be able to determine the form of the regional gravity variation over a survey area, this process is applied in the interpretation of gravity anomalies variation over a survey area, since the regional field is assumed to originate from relatively deep-seated sources. The upward continued field must result from relatively deep structures and consequently represents a valid regional field for the area. The field for the subenso south area was upward continued by 500 m.

4.3 Magnetic Data Acquisition and Processing

The Earth Total Magnetic Field data was acquired using the Geometrics G856 and 857 proton precision magnetometers. The system comprises of a magnetometer, the sensor, and staff and connector cable. Its magnetic field range of operation is 20,000 to 90,000 nT with a precision of 0.1 nT.

The magnetic data was carried out on the same profile lines used for the gravity survey. The only difference was the profile line spacing was reduced from 100 m to 50m. Therefore a total of 41 profile lines were surveyed but covering the same area size as the gravity survey.

Two Magnetometers were used in the survey, one for the base station and the other for the field measurements. A base station was located near the survey area and was placed away from power lines, buildings, and traffic for best result.

On a typical field day the base magnetometer was set up at the base station. The base station magnetometer was manually tuned to the approximate magnetic field strength within the survey area. In this a field strength of 32000 nT keyed into the magnetometer. It is then set up to read automatically at regular intervals. The base station and field magnetometers were synchronized each day so that they have exactly the same internal clock time. This is done for diurnal variation correction. After the base station was set up the field magnetometer is taken to the profile lines to begin the field survey. An external GPS was attached to the field magnetometer to collect the coordinates of the profile lines. The magnetometer was configured to collect data in a continuous mode.

Before start of survey the operator is cleared of any metallic object that may be carried on the body. The operator hangs the field magnetometer around the waist and the GPS and its battery pack at the back. To start measurements, the start key is pressed at the start point of the profile line and begins to move along the profile line until the full length of the profile line is covered then the stop key is pressed to end the measurement on that particular profile. The same procedure is repeated for the adjacent profile until all the profile lines were surveyed.



Figure 4.5 Base Geometrics G856 Magnetometer (left) with its sensor (right) used for the survey

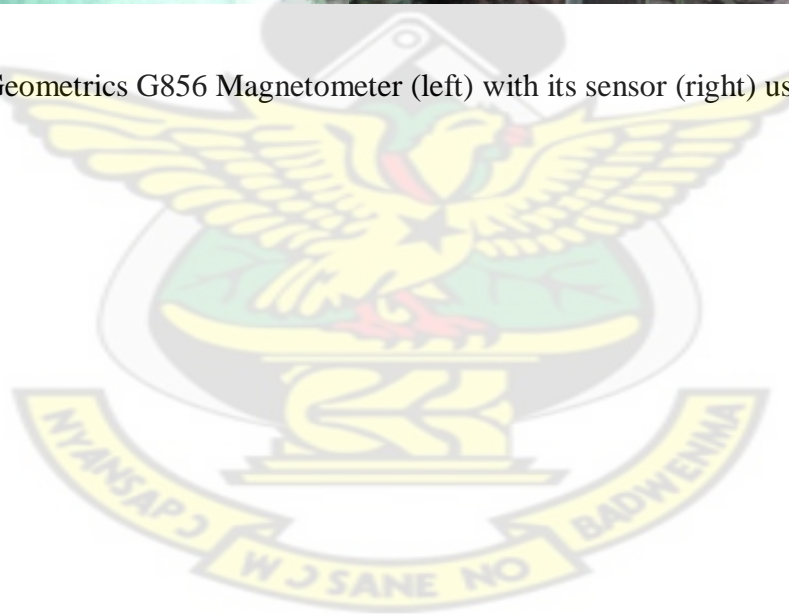




Figure 4.6 Operator carrying and operating on the field Geometric magnetometer unit. A is the Console, B is Sensor and C is GPS tracker.

4.3.1 Magnetic Data Processing

The data in the base station and field magnetometers were downloaded on to the computer with the help of software Magmap2000. The software was used for profile plotting, contouring, plotting and the diurnal correction of the survey measurements using the base station data.

The survey results were then exported to ASCII files and then used Geosoft to do the next stage of processing. The same coordinate system used for the gravity processing was also used for the magnetic data processing.

All the survey results were imported into Geosoft Oasis Montaj version 7.1 software as individual line data to undergo a sequence of editing. The individual line data were displayed and manually deleted and cleaned bad data to smoothen the magnetic profile of the individual lines.

The data was corrected for diurnal variation, heading errors, and instrument variations.

The next stage of data processing involved gridding, calculation of definitive geomagnetic reference field (DGRF), and the generation of the residual magnetic anomaly which was achieved by removing the DGRF from the observed magnetic data. The data was then microlevelled to remove apparent residual errors.

The MAGMAP tool which as an extension of Geosoft a number of utilities which were employed in the generation of magnetic anomaly grid. The GRID AND IMAGE tool was used in gridding the corrected mag channel of the data using the minimum curvature technique.

To aid interpretation, Two –Dimensional Fast Fourier Transformation (2D-FFT) filters were applied to further enhance the quality of the data. They included, Reduction to the pole, First vertical Derivative, Downward and Upward Continuation and Analytical Signal Amplitude.

4.3.1.1 Reduction to the Pole

A reduction to pole (RTP) filter for low geomagnetic latitudes was applied to the Residual Magnetic anomaly which is the Total Magnetic Intensity (TMI). Interpretation of magnetic data can further be helped by RTP in order to remove the influence of magnetic latitude on the anomalies, which is significant for anomalies caused by crust (Yao et al., 2010). The inclination and declination were computed using the central coordinates of the study area.

4.3.1.2 First Vertical Derivative (1VD) and Horizontal Derivative (1HD)

The resultant RTP grid was further subjected to a 1VD filter. This filter allowed both small and large amplitude responses to be evenly represented. Also, the 1VD in gray scale aided the enhancement of linear features within the study area. The RTP grid was also enhanced by applying the first horizontal gradient. The horizontal derivative helped in the identification of geologic boundaries within the study area.

4.3.1.3 Upward Continuation

This is useful in gravity because upward continuation suppresses the signals due to small, shallow bodies, just as taking the second derivative enhances them. The data was upward continued up to a height of 300 m above the plane of measurement.

4.3.1.4 Analytical Signal Amplitude

The analytical signal was calculated from the residual magnetic field. The analytical signal amplitude does not depend on the direction of magnetization. The most significant concentrations of mineral deposits in this area are correlated with high analytical signal amplitude (Silver et al 2003)



CHAPTER 5

RESULTS AND DISCUSSIONS

5.1 Results of Ground Geophysical Measurements

This session discusses the final results (in the form of maps) generated after the processing of the gravity and magnetic data. These maps include Total Magnetic Intensity (TMI), Reduction To Pole (RTP), Analytical signal, First Vertical Derivative, Complete Bouguer Anomaly, and the Residual Gravity. A geological interpretation was carried out using the gravity and magnetics data integrated with historic outcrop data. The residual gravity image and the TMI image were used in mapping the various lithological units while the 1VD image helped in structural mapping. The Digital Elevation Map (DEM) of the study area was also used to describe the general topography of the study area. These are the maps from which all discussions and interpretations were based on to meet the objectives.

5.2 Digital Elevation Map

Figure 5.1 shows the general topography of the project area. The study area is characterized by lowlands and highlands. The elevation ranges from about 150 m to above 330 m above mean sea level with relatively low lying areas between them. The highest elevations which are the red zones were found at the north eastern and north western part of the study area. The elevation decreases from the north to the south of the study area.

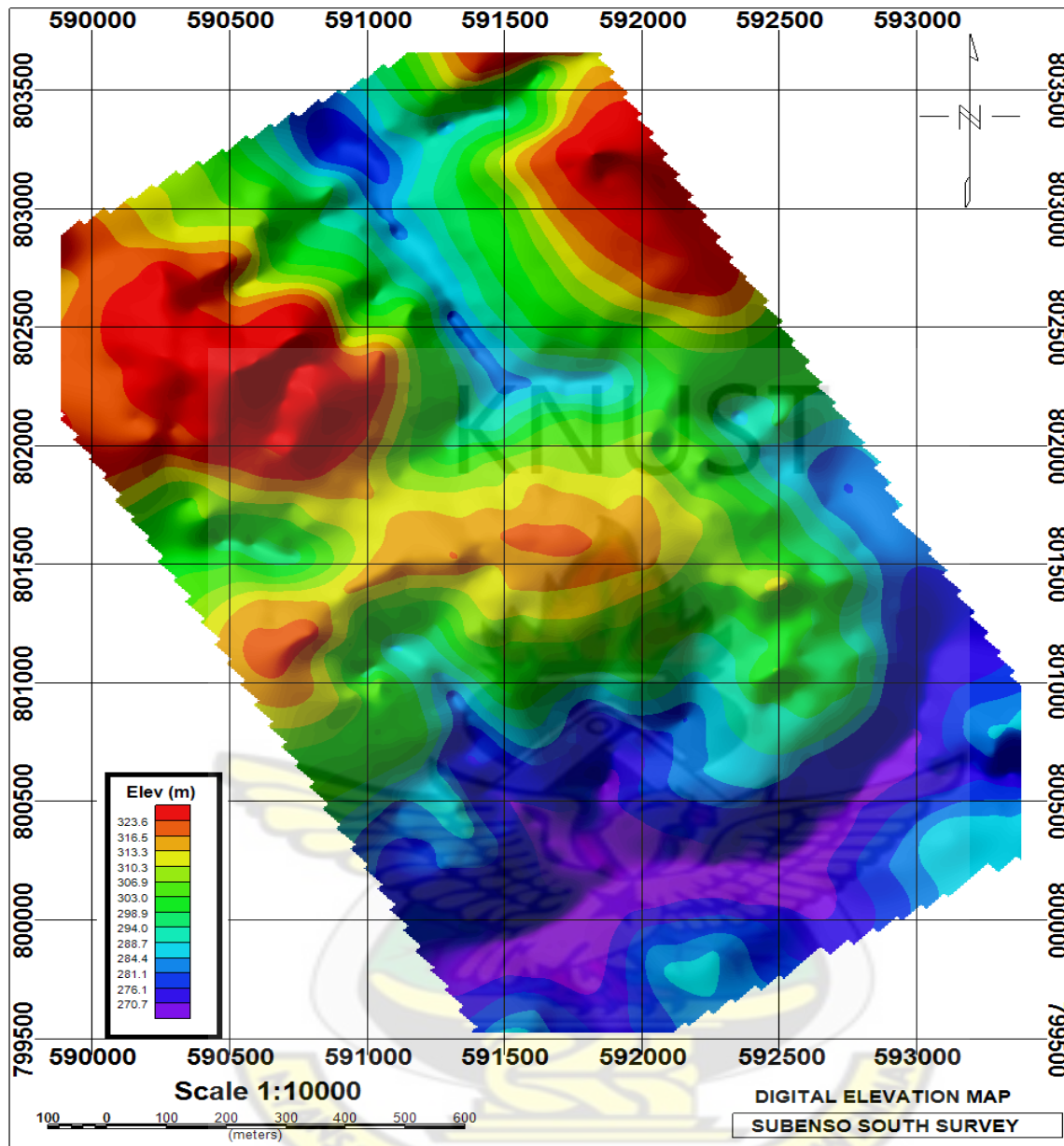


Figure 5.1: Digital Elevation Map of the Subenso South study area

5.3 Results of Magnetic Measurements

According to (Silva et al., 2003), Magnetic anomalies in the Earth's magnetic field are caused by magnetic minerals in the rocks, and images of these anomalies can be interpreted in terms of geology. The main objective for the use of the magnetic data is to delineate geology of an area and its associated geological structures. Geological structures normally serve as conduits for hydrothermal fluid deposition within the Birimian mobile belt and are important features in mineral exploration programmes (Amenyoh et al., 2009). This is seen in the case of Subenso South gold deposit where the mineralization is as a result of deposition of mineralizing fluid content within the conduits of the tectonic breccias leading to the gold mineralization. Faulting played a major role in the mineralization of the Subenso South deposit. The concentration of magnetic minerals or their excessive destruction by alteration especially along the tectonic structures allows the detection of geological structures (Plumlee et al., 1992).

5.3.1 Total Magnetic Intensity (TMI) Map

The total magnetic intensity is the magnetic field observed in a particular location and it is a combination of the Earth's magnetic field and the magnetic field generated by the subsurface structures. Minimum curvature method was used in gridding the TMI and displayed with pseudocolours. The map revealed different magnetic anomalies which correspond to the various lithologies found in the study area. Figure 5.2 below shows the Total Magnetic Intensity map.

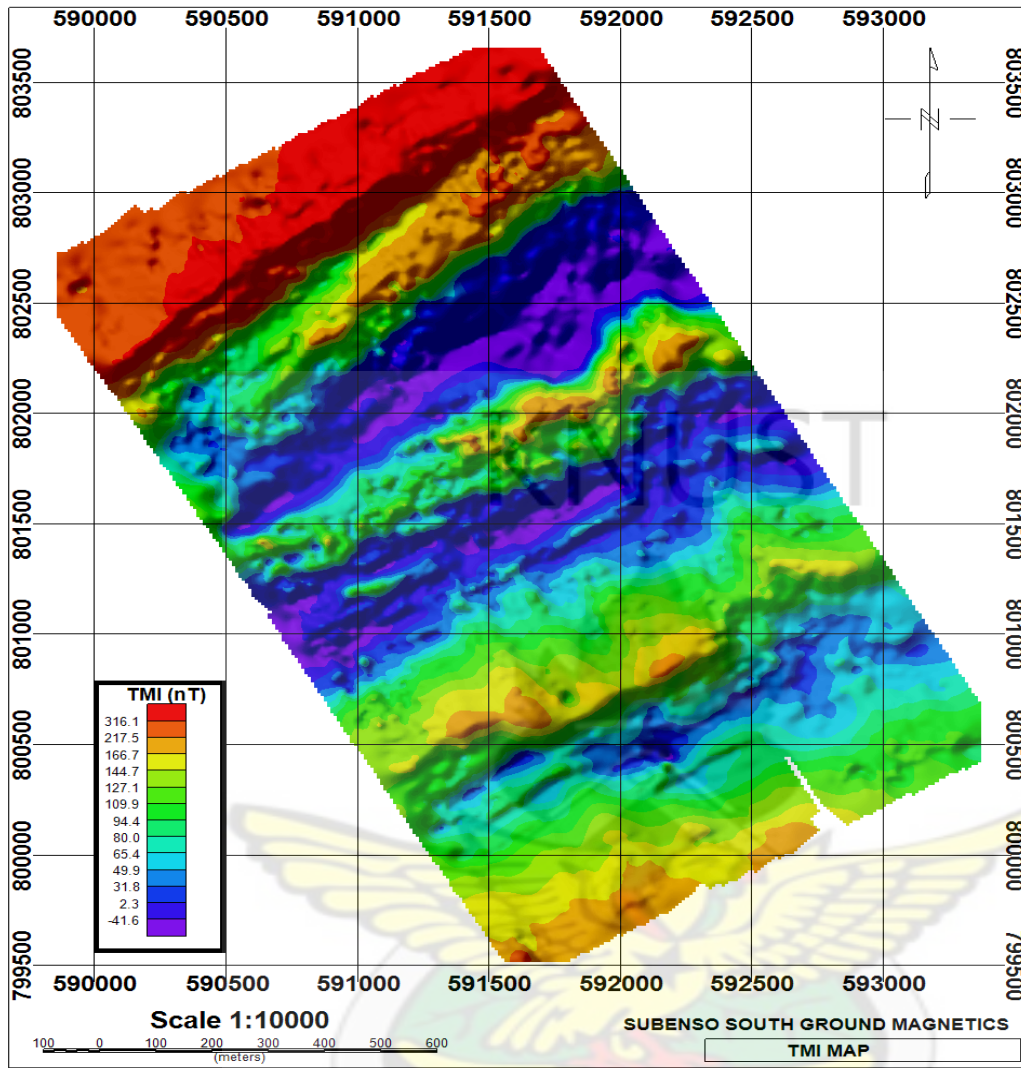


Figure 5.2: Total Magnetic Intensity map of the Subenso South area.

From the Total Magnetic Intensity (TMI) map of the study area in figure 5.2, three main anomalous zones are noticeable with different amplitudes of total field magnetization. The higher amplitudes range from 170 nT to over 316 nT. These are mostly the deep brown to red zones found on the northern part of the TMI map. The amplitude of the intermediate zones range from 80 nT to about 169 nT. These are the green to light yellow zones which are found at four different zones within the TMI map. The third zone is the one with the lowest amplitude of total

field intensity ranging from -40 nT to about 75 nT. These are the light purple to light blue regions.

There is a direct relationship between the amplitude of magnetic anomalies and the magnetization. The intensity of magnetization also depends on the magnetic susceptibility of the rock at certain geographical location.

The magnetic survey was carried out in an area of low magnetic latitude (close to the magnetic equator) so usually features of high magnetic susceptibility appear as low magnetic anomalies and those of low magnetic susceptibility assume high magnetic anomalies (Figure 5.2).

The low magnetic susceptibility regions depicted with anomalies located at the top of the TMI image (Figure 5.2) which strike in the northeastern direction correlate to the metasedimentary rocks of the Sunyani Basin. The high magnetic regions depicted with low anomaly zones which are located at the central part of the TMI image correlate to the mafic volcanic units presumably of the lower Birimian volcano sedimentary sequence.

The intermediate magnetic anomalies found in between the magnetic highs and lows correspond to the position of the volcanoclastic units in the area. These are a mixture of the metasedimentary rocks and the mafic volcanic units in the study area.

5.3.2 Reduced to the Pole (RTP) map

Asymmetric anomalies caused by the non-vertical inducing field are difficult to relate to the source bodies or geometry causing the anomalies in magnetic survey. Reduced-to-Pole converts the magnetic field developed by magnetic bodies from the magnetic latitude where the Earth's field is inclined, to the field at the Earth's magnetic pole, where the inducing field is vertical. (Murphy, 2007). Figure 5.3 below shows the Reduced to the pole (RTP) map of the study area



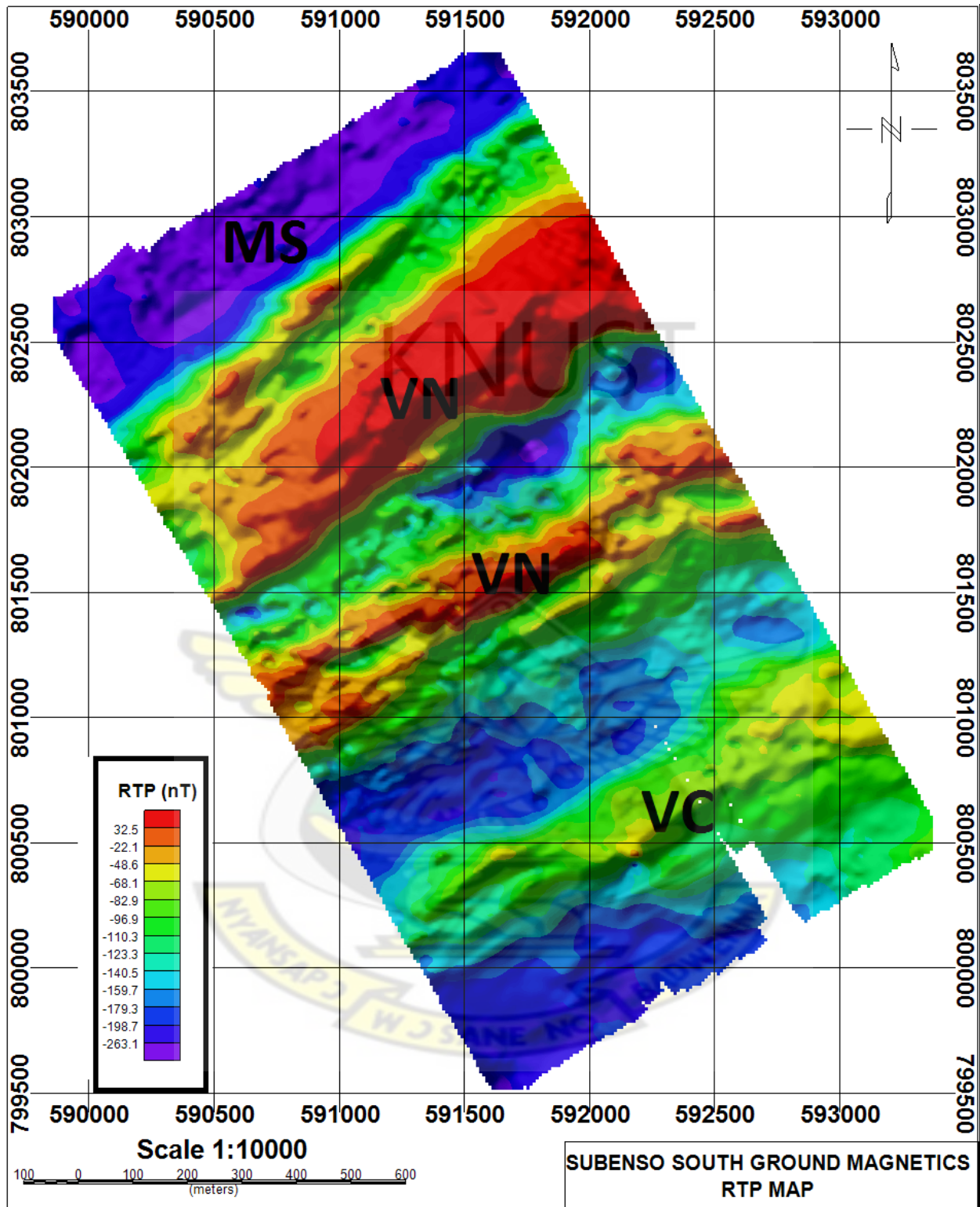


Figure 5.3: Reduction to the pole (RTP) map of the subenso south study area

Comparing the RTP map (Fig. 5.3) and the TMI map (Fig. 5.2) it can be deduced that the low magnetic anomaly features seen in the TMI map are now depicted as high magnetic anomaly features and vice-versa. In the RTP image the anomaly zones have assumed their correct physical property because the anomalies are now directly and vertically positioned on their corresponding causative bodies. It can also be deduced that the contacts between the magnetic anomaly features have been clearly defined and look sharper compared to their appearance in the TMI map.

According to the Ahafo Resource/Reserve Report, (2006), the low magnetic anomaly zone (MS) trending northeast at the top of the RTP map correlates to the metasediments of the Sunyani basin. The high magnetic anomalies (VN) which strike northeast near the central part of the map correlates to the mafic volcanic units presumably from the Birimian metavolcanics units. The intermediated anomalous zones (VC) can be interpreted as the volcanoclastics which resulted from the plastic deformation and intermixing of the metasedimentary and volcanic units. The very sharp contact with very low magnetic signature (light blue) between metasedimentary unit (blue) and the volcanoclastics (green) at the northern part of the map suggests the presence of a major fault zone. This feature will be clearly seen from the first vertical derivative map.

5.3.3 Analytic Signal Map

The analytic signal map is independent of the direction of the magnetisation of the source and is related to the amplitude of magnetisation and is a form of RTP (Nabighian, 1972; Roest and Pilkington, 1993). The analytic signal map also defines source positions regardless of any remanence in the sources (Macleod et al., 1993).

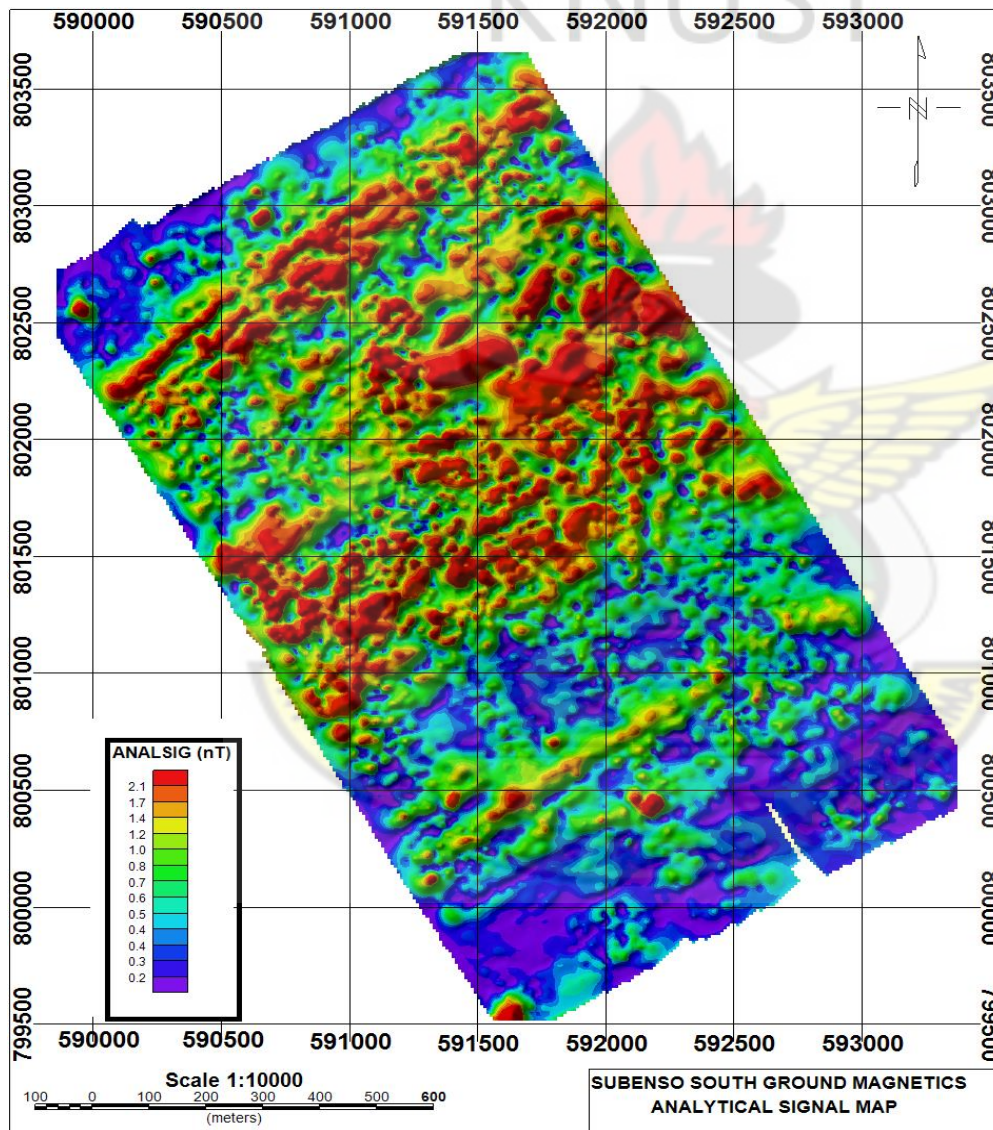


Figure 5.4: Analytical signal map (from RTP map) of the Subenso South area

The degree of magnetisation of the subsurface geological bodies is related to the amplitude of the analytical signal. Also, maximum magnetic anomaly is produced over the magnetic body irrespective of the direction of magnetization.

From figure 5.4 it can be seen that the high (red), low (blue), and the intermediate (green) magnetic features are well defined and located. This was not seen in the RTP and TMI maps. The analytic signal has placed the anomalies directly over their causative bodies because the source positions of the anomalies are defined vertically over the source irrespective of any remanence in magnetization.

The high magnetic anomalies found at the northern to central parts of the analytic signal map may be interpreted as magnetic responses from mafic units of the Birimian metavolcanics units. The low magnetic anomalies (blue) can be explained as magnetic responses coming from the metasedimentary unit of the Sunyani basin. The intermediate zones which are green in colour represents volcanoclastic unit.

5.3.4 First Vertical Derivative (1VD) map

The first vertical derivative (1VD) is a high pass filter that calculates the vertical gradient of the magnetic field. It enhances shallow features by suppressing deeper source features. The 1VD filter was applied to the Reduced to the pole (RTP) map to enhance the shallow geological features. Figure 5.5 shows the first vertical derivative map of the study area.

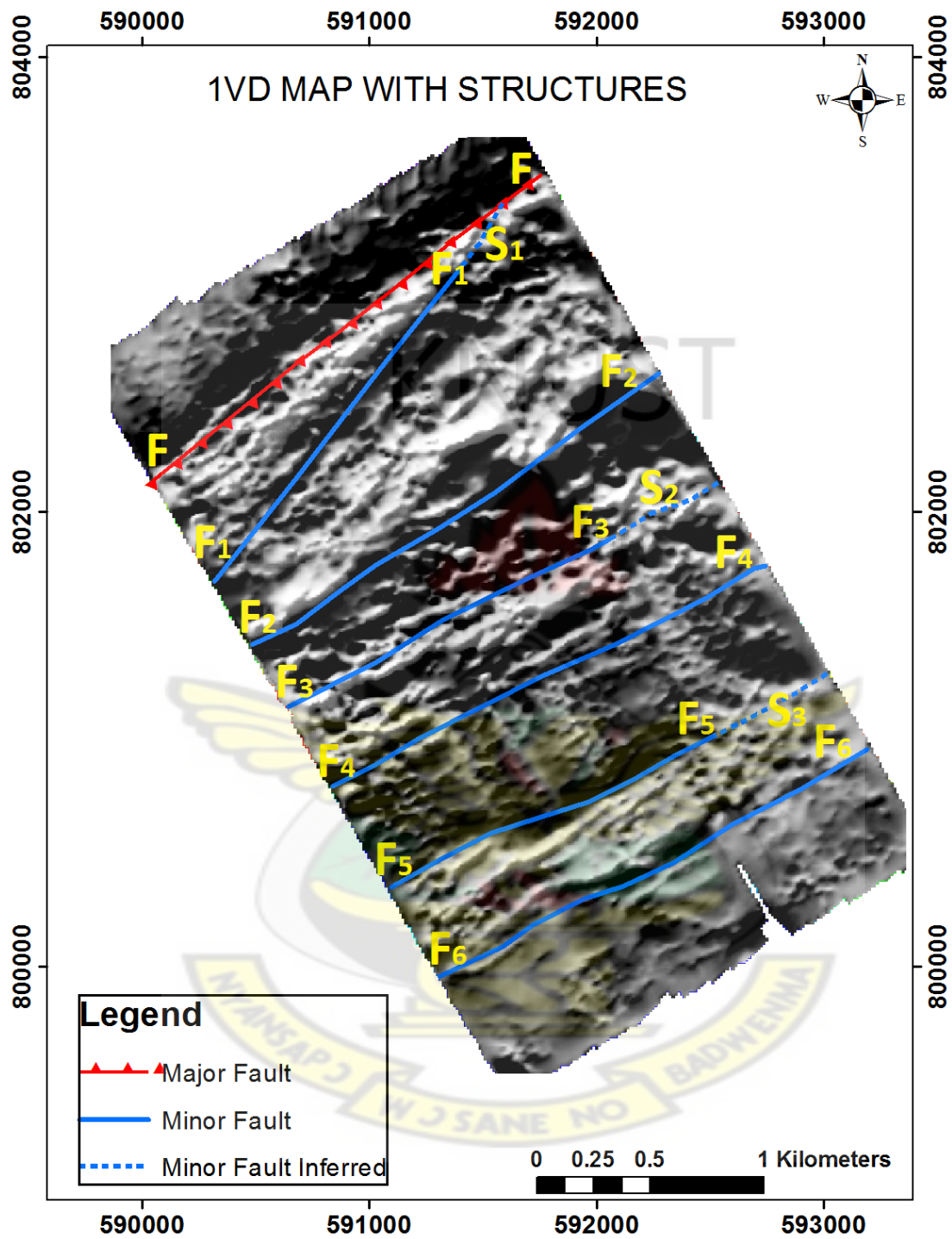


Figure 5.5: First Vertical Derivative map grey scale of the Subenso South Area

From Figure 5.5, the grey scale first vertical derivative reveals major lithological and structural features. The contacts between the magnetic anomaly zones has been well delineated. The solid blue lines represent minor linear structures mainly minor faults (F_1 --- F_1 , F_2 --- F_2 , F_3 --- F_3 , F_4 --- F_4 , F_5 --- F_5 , and F_6 --- F_6) and also represent lithological contact between the high magnetic features (white zones) and intermediate magnetic features (grey zones). The red line found on top of the map represents a major fault and also represents a major lithological contact between the high magnetic features and the low magnetic features (black zones). This major structure (F --- F in Figure 5.5) which strike in the North-East direction may be interpreted as the Subenso fault separating the low magnetic sedimentary rocks of the Sunyani basin and the high magnetic mafic volcanic units as suggested in the Ahafo Resource/Reserve report (2006). There are other inferred minor faults (S_1 , S_2 , S_3) depicted by the blue dotted lines between the metasedimentary (low magnetic zones) and volcanoclastics (relatively intermediate magnetic zones) units at the southern part of the map. There seems to be a discontinuation of the metasediments due to the truncation by the volcanoclastic unit. This can be noticed at the central and south eastern part of the map. They are not clearly defined though.

Comparing the features in the RTP map (Figure 5.3) to the 1VD map (Figure 5.5) it can clearly be seen that the 1VD operator has helped attenuate broad, more regional anomalies and enhanced local, more subtle magnetic responses because of their sensitivity to shallow magnetic source bodies and contacts. These features were not very obvious in the RTP map.

5.4 Results of Gravity Measurements

The gravity results are represented as maps showing the relationship between geological features using their rock density properties variations. The density contrast between geological bodies may produce a low or a higher density anomaly taking into consideration the average rock densities in the area under investigation. Gravity maps also highlight structures such as faults, folds, and lithological boundaries between different rock types as well as borders of intrusions.

The Bouguer anomaly map is used for the interpretation of the subsurface geology. A map of the Bouguer anomaly gives a good impression of the subsurface density. The low or negative values of the Bouguer anomaly indicate lower rock densities beneath the location of measurement. High or positive values of the Bouguer anomaly indicate high rock densities beneath the location of measurements.

5.4.1 Complete Bouguer Anomaly (CBA) map

Figure 5.6 represents the complete bouguer anomaly map of the Subenso South area. It is the representation of the gravity field for a given station, with corrections added in for instrumental drift, tidal variation caused by the sun and the Moon, latitude, (the Oblateness of the Earth's surface), and density of the rock lying between the station and sea level (Blakely 1995).

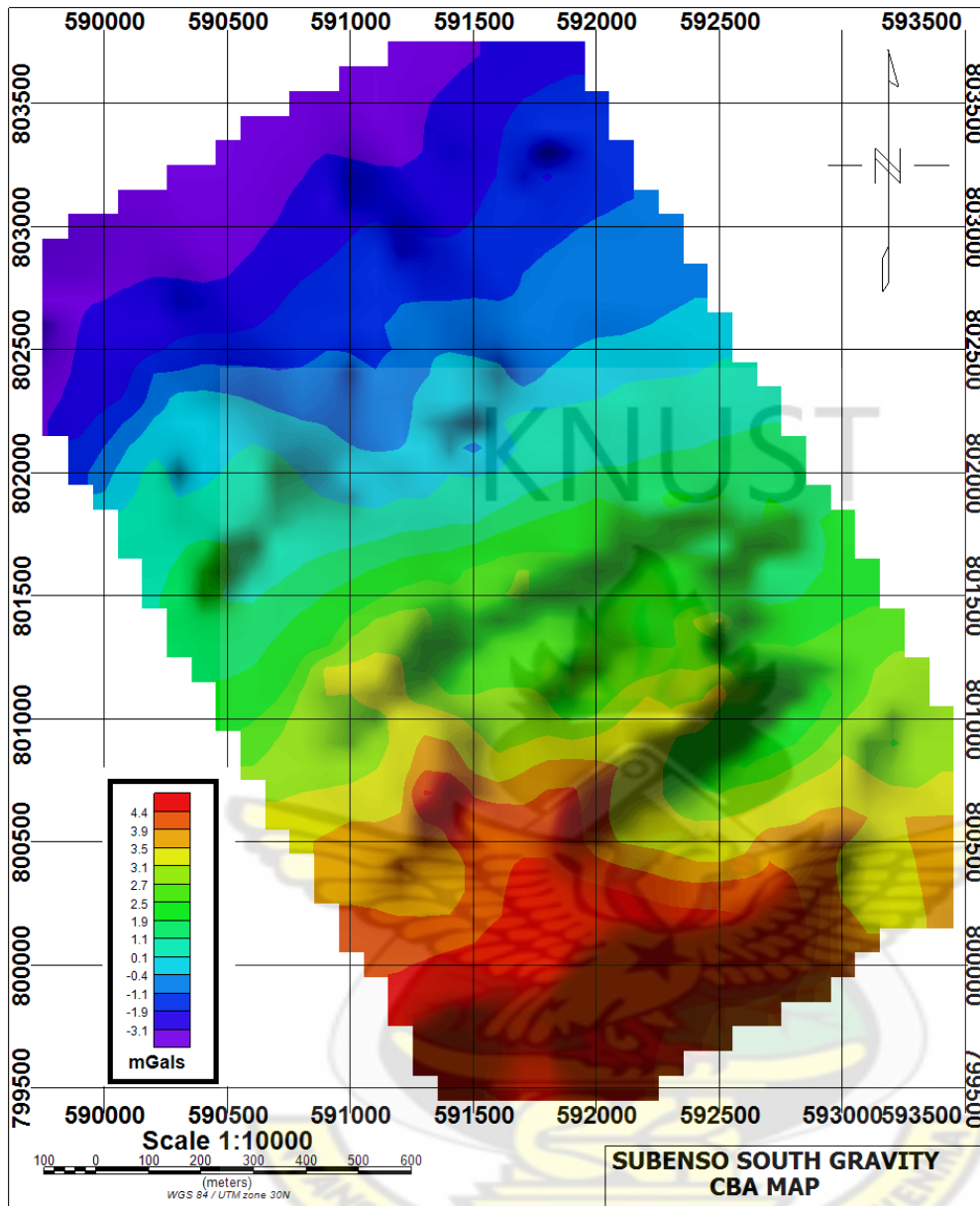


Figure 5.6: Complete Bouguer anomaly (CBA) map of the study area.

It can be seen from the Complete Bouguer Anomaly map that the study area is characterized by low gravity (blue region) anomalies at the northern part of the study area. The gravity values for this low gravity zones range from -3.1 mGals to 0.1 mGals. There is also a gravity high region (red regions) found on the south western corner of the study area with gravity values which range from 3.5 to above 4.4 mGals. Sandwiched between the low and the high anomalous zones is

another gravity anomaly which may relatively be intermediate between the low and high gravity features with gravity values which range from 1.1 mGals to below 3.5 mGals.. The low, high and intermediate gravity anomaly features are quite broad because of the effect of regional geologic bodies from deeper sources. The shallow, local, and short wavelength structures which are of interest have been enveloped by the effect of the regional bodies. The regional trend must therefore be removed to facilitate the identification the responses coming from the shallow, local structures to aid interpretation.

The low gravity anomaly can be interpreted as rocks of very low density probably from the metasedimentary units of the Sunyani basin. The relatively high gravity responses may be interpreted as the mafic volcanic units of the Birimian system. The intermediate gravity signatures may be correlated to the volcanoclastic units within the study area.

5.4.2. Residual Gravity Map

Figure 5.7 represents the residual gravity map of the Subenso South area. The density distribution in the residual gravity map of the study area is as a result of the responses coming from the local geological structures.

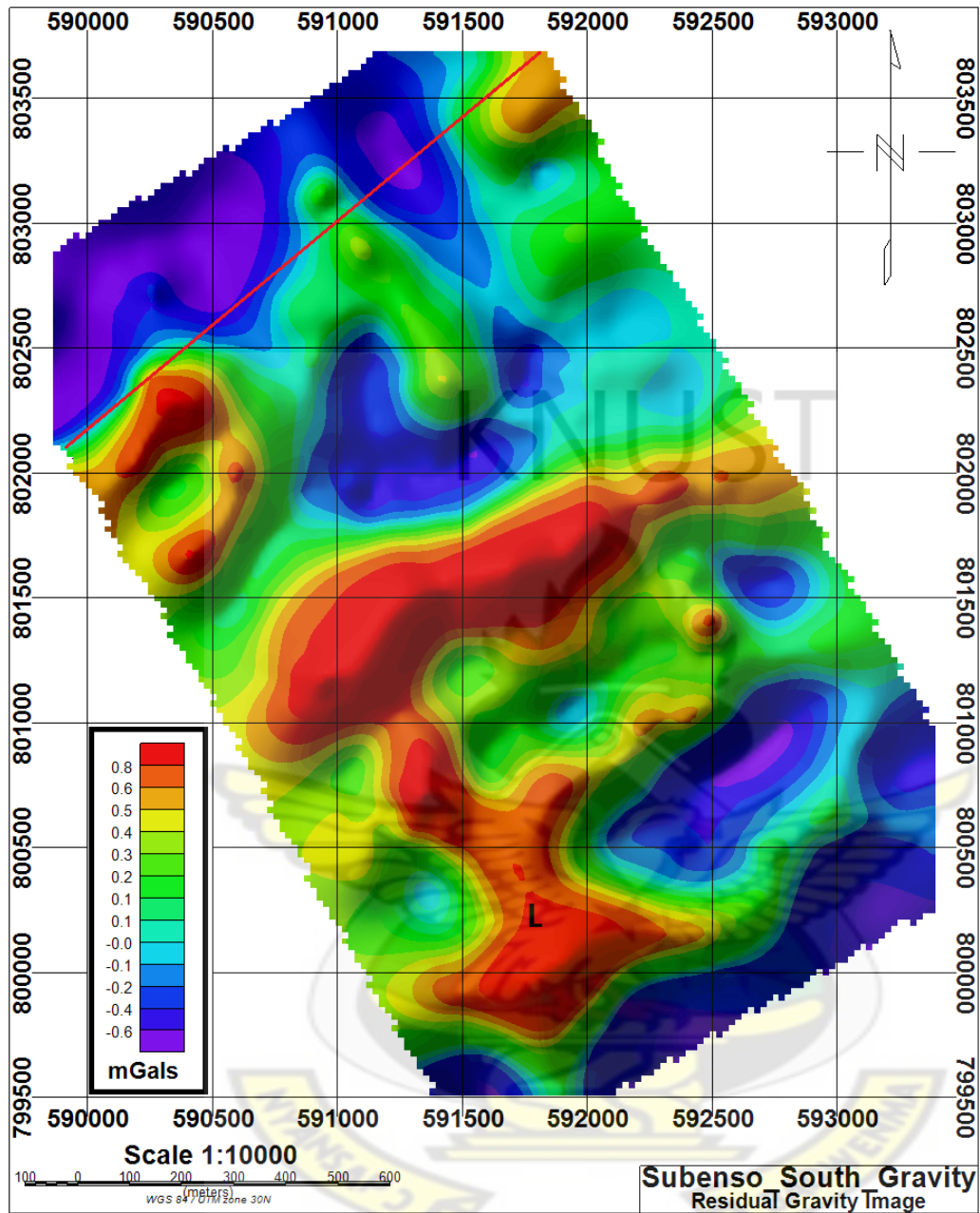


Figure 5.7: Residual gravity map of the Subenso South study area

It can be seen from the Residual gravity map (Figure 5.7) that the local features have been greatly emphasized compared to Figure 5.6 (Complete Bouguer anomaly map). The gravity anomalies have become sharper and their boundaries have been well defined. We still have the low, high and relatively intermediate gravity anomaly zones with clearly defined boundaries

showing the contact between the various lithological units within the area. The relatively high gravity anomalies (red) with gravity values ranging from 0.5 mGals to above 0.8 mGals found at the central and partly at the northern parts striking Northeast correlates to the very dense mafic volcanic units of the Lower Birimian system. Relatively low density response features (blue) with gravity values which range from -0.6 mGals to 0.1 mGals may be correlated to the metasedimentary rocks of the Sunyani basin. The relatively intermediate gravity anomalies (green) with gravity values ranging from 0.1 mGals to 0.5 mGals may be correlated to the plastically deformed intermixed volcanic and sedimentary units. There seems to be a truncation of the volcanic unit found on the northern part of the map by the low and intermediate gravity anomalies interpreted as the metasedimentary and volcanoclastics. This feature suggests a major fault and may be interpreted as the Subenso major fault located within the study area. The red line found at the upper part of the Residual gravity map represents the possible fault zone. The Residual map also revealed high gravity anomaly (marked as L in Fig 5.7) trending in the North-South direction cutting through the relatively lower density metasediments and the volcanoclastic units. This L structure was however not seen in the magnetic data.

5.5 Summary

Detailed ground geophysical was carried out along 3.6 km by 2 km grids across the strike direction of the subenso south deposit. In all 21 profile lines were surveyed. Gravity and magnetic data were collected, and processed using several filtering and enhancement techniques. Results in a form of maps were produced from the two geophysical data sets. Documentation on the geology of the study area was used in conjunction with integrated geophysics data to improve upon geology, delineate structures and also delineate probable places where gold mineralization may occur within the study area.

According to (Murphy, 2007), interpretation of gravity and magnetic (or any geophysical) data basically involves two exercises which are; firstly ascertaining the behaviour of the geophysical data and the physical nature of delineated anomalies and secondly, interpreting the geological significance of the geophysical indications.

Interpretation of the geology was done by carefully studying the patterns developed within the maps of the two geophysical datasets. Correlations were made between the developed patterns and their physical properties. The physical properties of the developed patterns in conjunction with the known geology helped in delineating lithological units and geological structures.

The density contrasts and the differences in magnetic susceptibility of the different rock types in the area helped in delineating and interpreting the gravity and magnetic signatures in their respective maps and hence facilitating the interpretation of the local geology and structures.

The boundaries (contacts) between the various lithological units appeared as a sharp changes in the intensity of the magnetics and the gravity responses.

5.6 Proposed geology map from the Gravity and Magnetic data

An improved geological map of the study area was produced from the information gathered from the integrated gravity and magnetic datasets in conjunction with outcrop mapped data. The Reduced to the pole (RTP) map, the first vertical derivative (1VD) map, together with residual gravity map facilitated the delineating of the different lithological units. The 1VD map together with the residual gravity map facilitated the interpretation of the geological structures like the faults, and lithological contacts. The proposed geological map of the Subenso South study area is presented in figure 5.8.

It can be observed from figure 5.8 that, three predominant lithological units are found within the study area. The lithology of the upper part of the study area (brown zones) correlates to the metasedimentary rock units of the Sunyani basin.

The yellow lithological units can be correlated to volcanoclastic units which are a mixture of the mafic volcanic units and polytropic to turbiditic sedimentary units regionally metamorphosed to greenschist or even lower amphibolite facies. These units belong to the Lower Birimian volcano-sedimentary sequence.

The green regions are the volcanic or granitoids units. This is a broad category including all upper Birimian Dixcove Granitoid units generally granodioritic to dioritic composition. These units occur as local, relatively narrow bodies striking northeast and dipping steeply southeast. They are moderately folded which suggest that they may have been thrust into the volcanoclastic units.

A major fault divides the metasediments and the volcanic and volcanoclastic units at the northern part of Subenso south. This can be interpreted as the Subenso fault which may have been formed by D3 brittle strike-slip event along multiple northeast-striking southeast structural zones. This led to the formation of tectonic and dilatant breccia zones, and other minor and inferred faults represented as solid black lines and dotted lines. The volcanic and volcanoclastic units are moderately folded as a result of regional D2 events (Ahafo Reserve/Resource report, 2006)

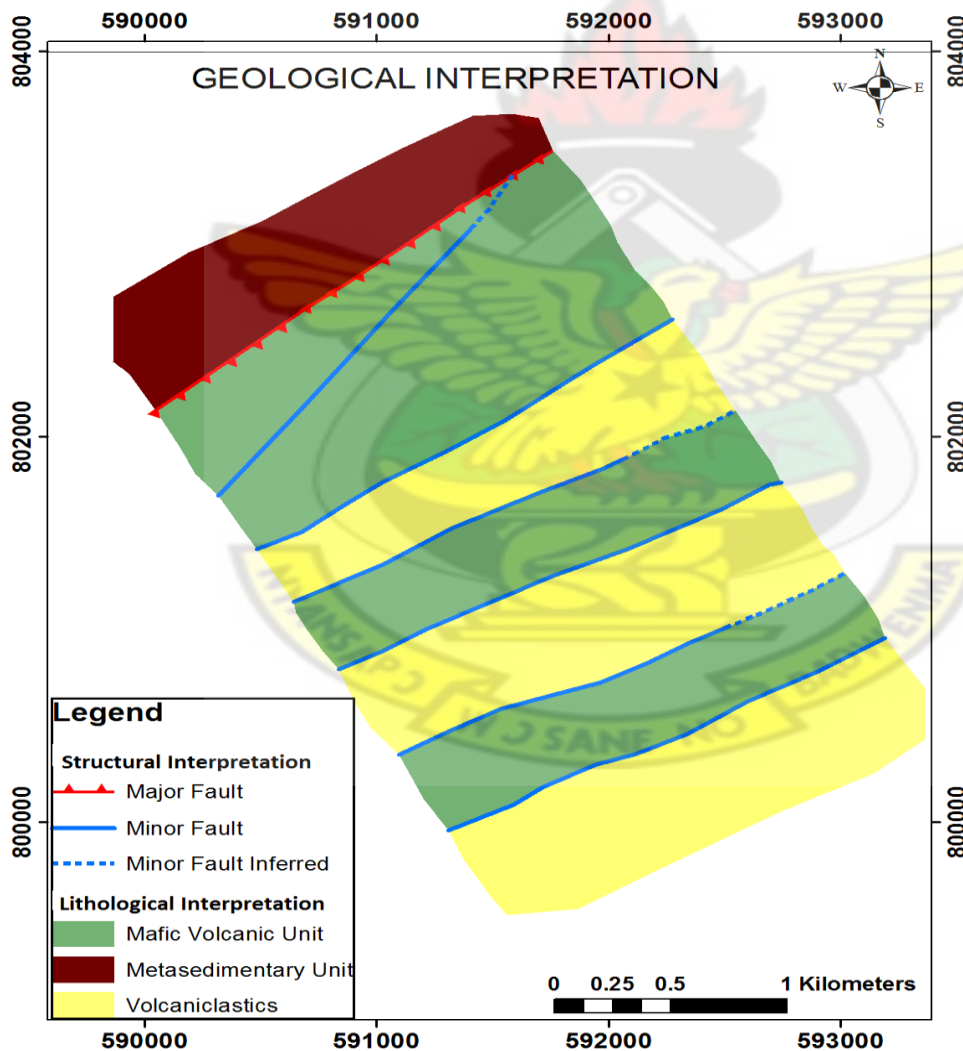


Figure 5.8: Proposed geological map of the Subenso South study area

5.7 Gold Mineralization in the Subenso South study area

According to the Ahafo Mineral Resource and Ore Reserve Report (2006), Subenso South is a shear hosted mesothermal deposit. The mineralization is focused on the strongly altered tectonic and dilatent breccias that resulted after brittle faulting along the volcanic bodies and the volcanoclastic units of the Subenso South. The breccias may have provided conduits for hydrothermal fluids to deposit their contents leading to mineralization. The breccias are the only permeable host lithologies in the Subenso South study area. The mineralizing fluids which went through the tectonic breccias altering the rock with different degrees of alteration reflecting differences in the degree of mineralization. Very intense alteration suggests high grade gold mineralization and vice-versa

The deposit is characterized by alteration of primary chlorite to sericite-silica and addition of silica, iron carbonate, pyrite and local albite to the host rock.

The results of the integrated ground gravity and magnetic measurements helped in identifying these major and minor structures and played important roles in subsequent mineralization in the Subenso South. Presented in figure 5.9a and 5.9b is the outline of the Subenso South deposit on the RTP image and the Residual gravity anomaly map.

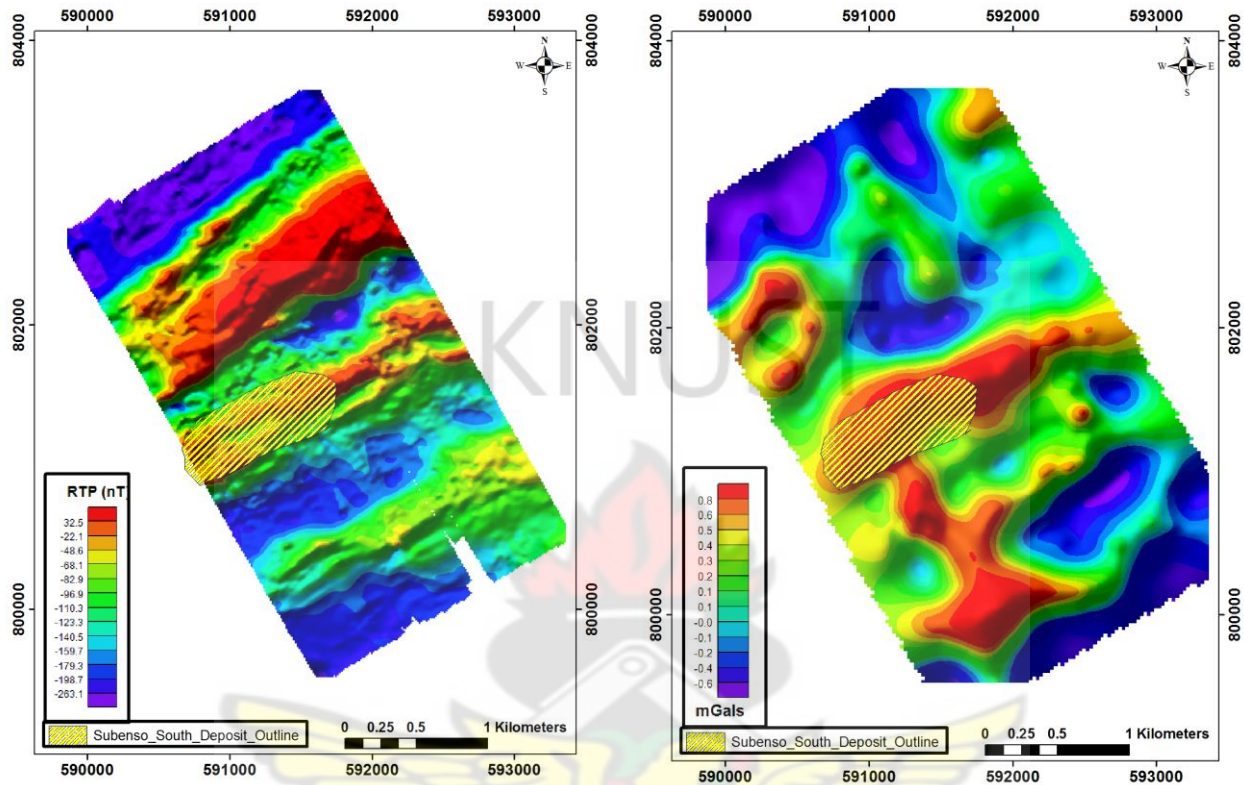
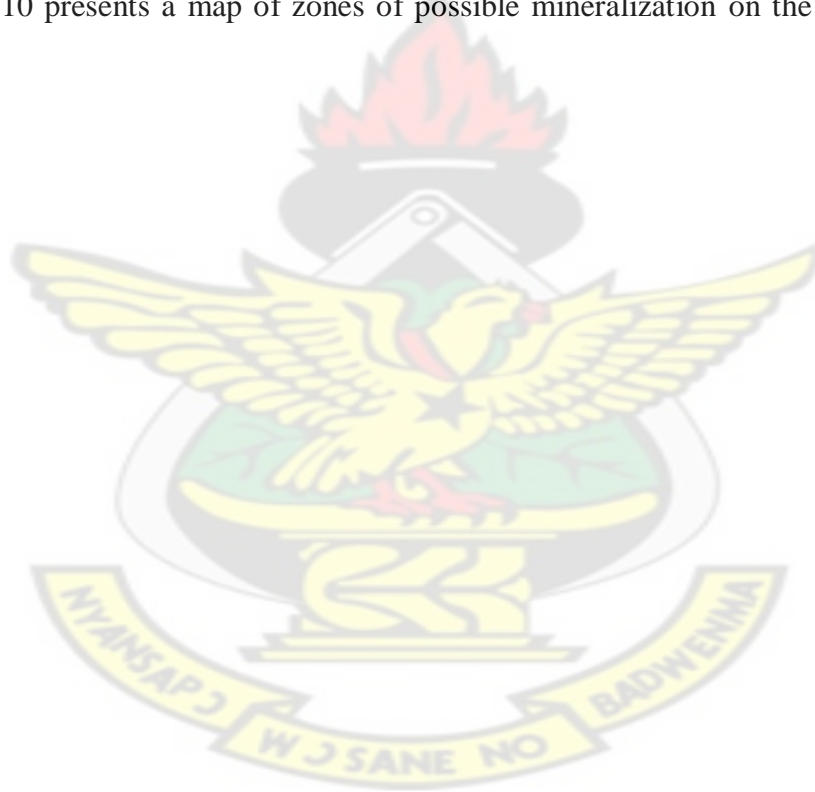


Figure 5.9a: Subenso South deposit outline on RTP map. Figure 5.9b is the subenso south deposit on the residual gravity map

It can be observed from the two maps that the location of the subenso south deposit (yellow stripped polygon feature) follows both delineated gravity structure and magnetic structure. The interesting phenomenon is that the Subenso South deposit is located largely on gravity high signature which was interpreted as the volcanic bodies and also around the contact between the volcanoclastic unit and the volcanic bodies. The same interesting pattern exists within the magnetic data where the subenso south deposit sits around the contact between magnetic high and intermediate magnetic zones and also largely on the magnetic high body striking northeast and found around the central part of the RTP map. It can be recalled from the geology of the area that the tectonic breccias that host the gold mineralization zones were formed as a result of the

brittle deformation of the volcanic bodies and the volcanoclastic lithological units. So it is possible to deduce that the tectonic breccias are largely located around the position of the subenso deposit as it appears on the gravity and magnetic data.

Similar zones within the gravity and magnetic images which exhibit the characteristics of the subenso south deposit in terms of its gravity and magnetic responses may be delineated as possible gold mineralization zones. The superimposition of the location of the subenso south deposit on the gravity and magnetic data serves as a lead to delineate possible mineralization zones. Figure 5.10 presents a map of zones of possible mineralization on the Residual gravity image.



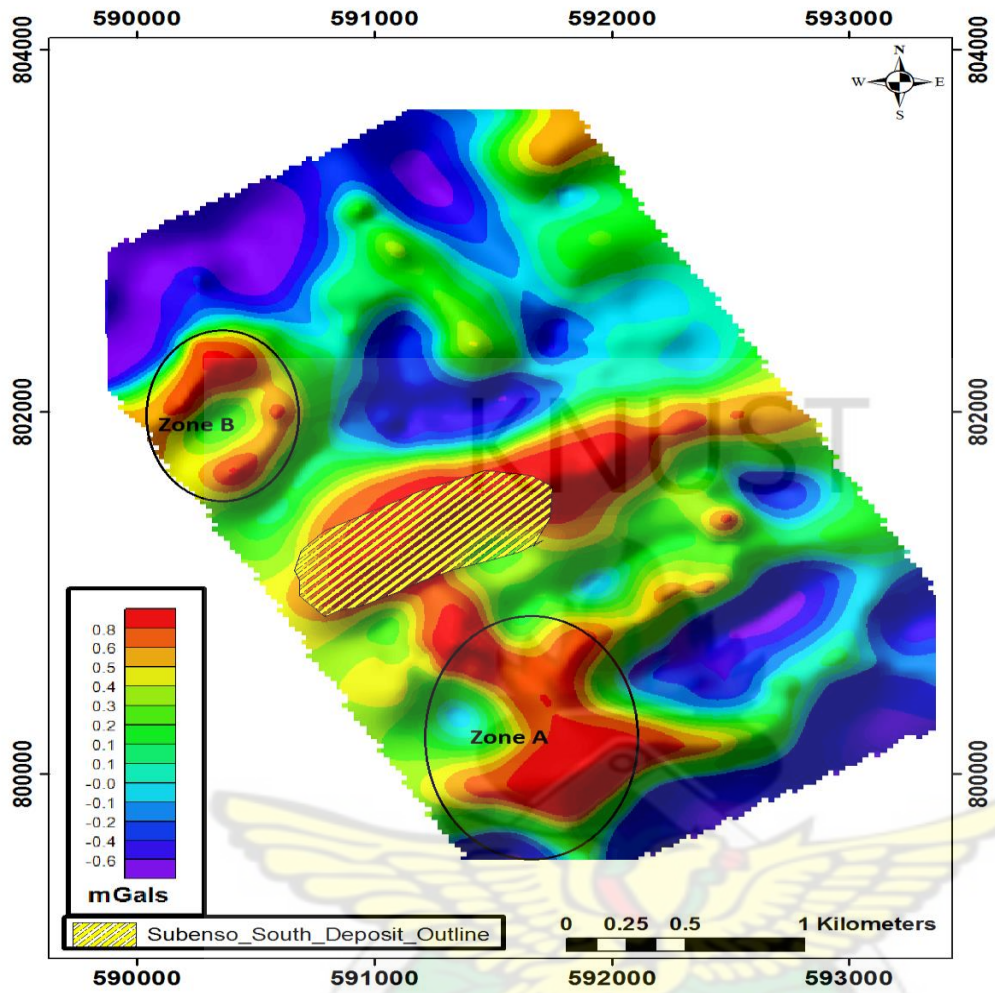
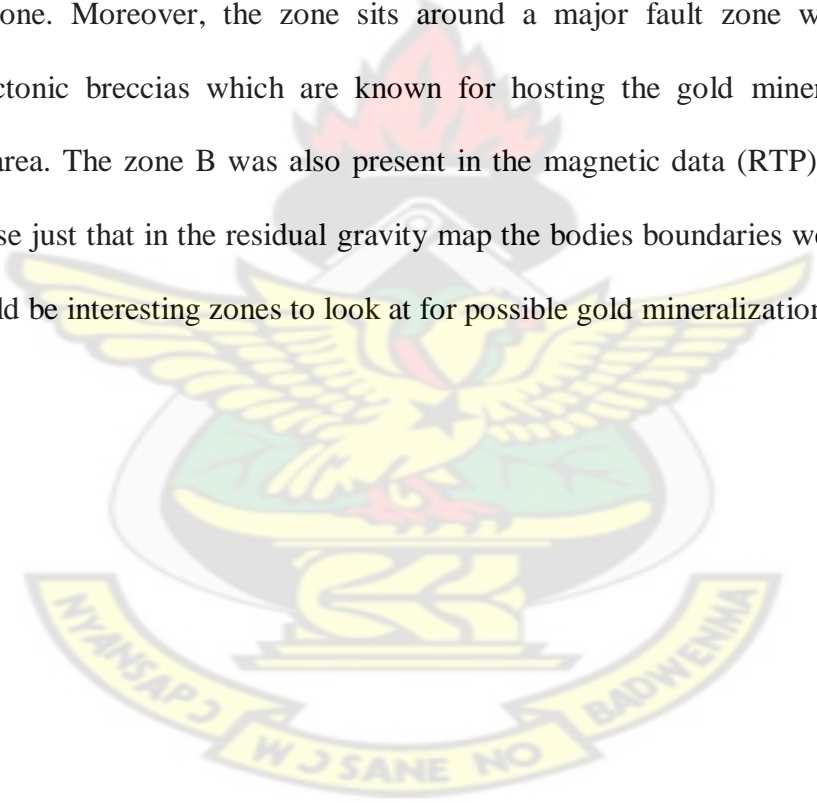


Figure 5.10: Potential gold mineralization zones (Zone A and B) on the Residual gravity map

From Figure 5.10 it can be seen that two zones have been delineated namely zone A and zone B in circular shape. In zone A, there is high gravity anomaly body striking in the north-south direction towards the southern part of the survey area. This body marked L in Figure 5.7, exhibits some characteristics with the central high gravity anomaly body trending north east found in the central part of the study map on and around which the Subenso South gold deposit is located. It is also in contact with the intermediate gravity signatures which were interpreted as volcanoclastic units. Due to these similarities in structure and lithological associations it could also host gold mineralization, hence its delineation as a possible gold mineralization zone.

Interestingly this volcanic body within the residual gravity map was however was not picked up by the magnetic data. It could be that it is at a deeper depth compared with other high density and magnetic susceptibility units in the area hence the relatively lower signature.

Within the zone B, are two relatively narrow high gravity anomalies found within the zone of the volcanoclastic units. These bodies are striking in the North-East direction. Since the Subenso South deposit was located on the dense volcanic bodies and around their contacts with the volcanoclastic units, zone B which shares similar characteristics could be a possible gold mineralization zone. Moreover, the zone sits around a major fault zone which led to the formation of tectonic breccias which are known for hosting the gold mineralization in the Subenso South area. The zone B was also present in the magnetic data (RTP) showing a high magnetic response just that in the residual gravity map the bodies boundaries were well defined. These zones could be interesting zones to look at for possible gold mineralization.



CHAPTER 6

CONCLUSIONS AND RECOMMENDATIONS

6.1 Conclusions

The gravity and magnetic data were able to delineate the various lithological units and geological structures in the study area. According to the Ahafo report (2006), the Subenso South study area is made of predominantly metasedimentary rock units from the sunyani basin, the volcanoclastic units from the lower Birimian system and the volcanic units which come from the Upper Birimian. The metasedimentary lithology was delineated by the magnetic data especially in the RTP image where the metasedimentary zones appeared at the upper most parts of the study area characterized by low magnetic regions. Residual gravity map also delineated this zone as zone of low density rocks and recorded the zone as low gravity zone.

The volcanic bodies were also mapped by the RTP and 1VD maps of the magnetic data. They depicted zones of high magnetic intensity. This signature was similar to the responses from the residual gravity map where they appeared as gravity high bodies.

The volcanoclastic units which were formed as a result of deformation of intermixed volcanic units and metasedimentary units were mapped by the RTP and 1VD by appearing as relatively intermediate magnetic intensity signatures. The residual gravity map also picked up this lithological unit as a zone of intermediate gravity signature hence intermediate density rocks.

Geological structures like major, minor, and inferred faults were mapped out by both the gravity and magnetic data. The Subenso fault was located at the upper part of the Subenso South area. It strikes north-east and divides the metasedimentary rock units and the mafic volcanic units.

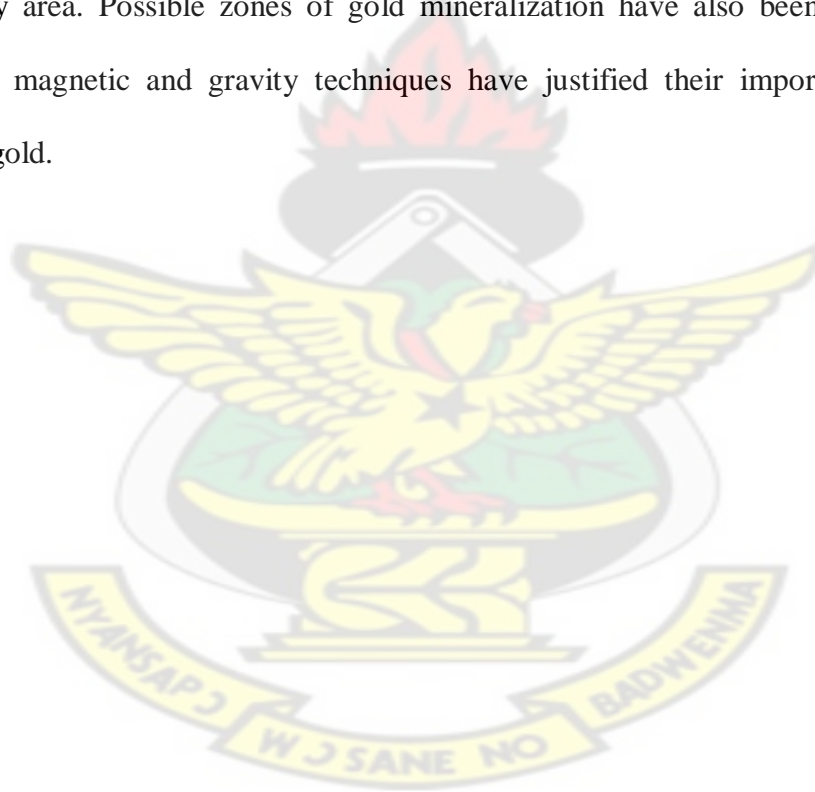
Minor structures interpreted as minor faults which strike north-east found on the central part and southern parts of the Subenso South area were mapped and served as lithological contacts between the Volcaniclastic units and the mafic volcanic units. There were other structures which were not too obvious so were interpreted as minor faults inferred. These were located at the central and south eastern part of the Subenso south area along the contacts between the volcaniclastic units and the mafic volcanic units.

Zones A and B were mapped in figure 5.10 as zones of possible gold mineralization. Zone A is located on the Southwestern part of the Subenso South area and the gravity anomaly in within the zone strikes in north-south direction The zone B is located at the Northwestern part of the subenso area and the anomalies strike in the NE-SW direction.. According to the Ahafo Resource report (2006) the Subenso South deposit is located at the contact between the volcaniclastic unit and mafic volcanic units. This is evident in figure 5.9a and 5.9b where the outline of the Subenso South deposit lies around the contact between the mafic volcanic unit (zone of high magnetic and gravity responses) and the volcaniclastic units (zone of intermediate magnetic and gravity responses). Similar gravity and magnetic signatures were evident in zones A and B hence considered as possible gold mineralization zones in the area.

The ground geophysical data has greatly enhanced the resolution of the subsurface geology. The lithological boundaries have been well defined. Comparing the proposed geological map (Figure 5.8) to the previous geological map (Figure 2.1 in chapter 2) of the Subenso South area

considerable amount of information has been added. Previously more than two thirds of the area was delineated as volcanic units but upon detailed geophysical survey it has been revealed that those areas were rather a combination of different lithologies namely volcanic units and volcanoclastic units.

The integrated ground magnetic and gravity survey has facilitated the interpretation of the lithological units and geological structures. It has helped improve the geology setup of the area and established a relationship between the gravity, magnetic anomalies and gold mineralization within the study area. Possible zones of gold mineralization have also been delineated. The detailed ground magnetic and gravity techniques have justified their importance in modern exploration for gold.



6.2 Recommendations

To validate the findings of the project it would be good to run an electrical Resistivity/IP survey preferably 3D IP pole-dipole along the block used for the gravity and magnetic survey. This will greatly enhance the resolution in terms of depth and give an improved geology and mineralization.

Secondly a 3D modelling can be run on the gravity and magnetic data to give the geometrical associations between the lithological units in terms of depth, shape, magnetic susceptibility and densities. A geophysical model should be developed from this to serve as guide for geologist to use in conjunction with their geologic model during exploratory drilling programmes. This will help in placing more confidence in drill targets therefore increasing productivity and minimizing loss.

Soil geochemistry programme should be conducted around the proposed zones of possible mineralization zones A and B to check whether indeed there is evidence of gold mineralization. Exploratory test drills should be run on the gravity and magnetic anomaly zones.

The study area should be extended to the west because the structures in zone B in figure 5.10 seem to be truncated so this may give the full extent of the structures and give a better picture of the subsurface geology.

Last but not least, a detailed gravity and magnetic survey along grids should be employed more in the exploration for gold and as a targeting tool.

References

- Ahafo Mineral Resource and Ore Reserve Report (2006). Newmont Ghana Gold Limited, Ahafo Project.
- Amenyoh, T., Wemegah, D. D., Menyeh, A., and Danuor, S.K. (2009). The use of landsat and aeromagnetic data in the interpretation of geological structures in the Nangodi Belt. Proc of the 26th Biennial Conference of the Ghana Science Association, University of Capecoast, 4th-9th July, 2009.
- Appiah, H. (1991). Geology and mine exploration trends of Prestea Goldfields, Ghana. *Journal of African Earth Sciences and the Middle East*, 13(2): 235-241.
- Baldyga, C. (2001). Relationship of faults in the basin sediment to the gravity and magnetic expression of their underlying fault Systems. *Open Report file*, United States Geological Survey, 20-45.
- Blakely, R.J. (1995). *Potential Theory in Gravity & Magnetic Applications*. Cambridge, New York, Port Chester, Melbourne, Sydney: Cambridge University Press. 441 pages
- Cees, S. (2006). South West Interpretation Geology of Ghana. consulting structural Geologist, . Greenfields Exploration.

- Changli, Y., Zhining, G., Dezhang, G., Xilin, Z., and Yuwen, Z. (2003). Reduction to the pole of magnetic anomalies at low latitudes by using suppression filter. *Chinese Journal of Geophysics*, 46 (5): 988-997.
- Conrad, C. (2011). Gravity Anomalies and Isostasy. Lecture notes, University of Hawaii.
- Criss, R.E., and Champion, D.E. (1984). Magnetic properties of granitic rocks from the southern half of the Idaho batholith-Influences of the hydrothermal alteration and Implications for aeromagnetic Interpretation. *Journal of Geophysical Research*, 89(8): 7061-7076.
- Dzigbodi-Adjimah, K. (1992). Geology and Geochemical patterns of the Birimian Gold deposits, Ghana. West Africa. *J. Geochem.* 47: 305-320.
- Floyd, A.R. (1993). An Integrated Gravity and Magnetic Analysis of the Mosida Hills Utah. Master's Thesis, University of Brigham Young, 78.
- Foulger, G.R., Du, Z., and Julian, B.R. (2003). Icelandic Type Crust. *Geophysical Journal International*, 155: 567-590.
- Geosoft (2009). Oasis Montaj User Manual, 24-71.
- Ghosh, G.K., Basha, S.K. Salim, M. and Kulshreshth, V.K. (2010). Integrated Intepretation of Seismic gravity and magnetic and magnetotelluric data in geologically complex thrust belt areas of Manabum, Arundachal Prodesh. *J. Ind. Geophysics Union*, 14: 1-14.
- Hanna, W.F. (1969). Negative aeromagnetic anomalies over mineralized areas of the Boulder batholith, Montana. United States Geological Survey Professional paper 650: 159-167.

- Hansen, R.O. and Suci, L. (2002). Multiple Source Euler deconvolution. *Geophysics*, 67: 525-535.
- Hartman, R.R., Teskey, D. and Friedberg J. (1971). A system for rapid digital aeromagnetic interpretation. *Geophysics*, 36: 891-918.
- Hash, S.T. (1995). An Integrated Gravity and Magnetic Analysis of Subsurface faults near Mapleton, Utah county, Utah. Brigham Young University.
- Hirdes, W., Senger, R., Adjei, J., Efa, E., Loh, G. and Tettey, A. (1993). Explanatory notes for the geological map of southwestern Ghana 1:100,000, sheet Wiawso (0603d), Asafo (0603c), Kukuom (0603b), Goaso (0603a), Sunyani (0703d) and Berekum (0703c). page 139. *Geologisches Jahrbuch, Reihe B, Heft 83*, Hannover, Germany.
- Hoover, D.B., Klein, D.P. and Campbell, C.C. (1995). Geophysical Methods in Exploration and Mineral Environmental Investigation. US Geological Survey, *Open File Report 95*, 19
- Keary, P. and Brooks, M. (1991). *An Introduction to Geophysical Exploration*. Blackwell Scientific Publications, second edition, 254.
- Keary, P. Brooks, M and Hill, I. (2002). *An Introduction to Geophysical Exploration*. Blackwell Scientific Publications, third edition, 265.
- Kesse, G. (1985). The Mineral and Rock Resources of Ghana. A.A.Balkema, Rotterdam.

Kono, M.(2007). *Treatise of Geophysics*, volume 5, Elsevier, New York.

LaFehr, T.R. (1991). Standardization in gravity reduction. *Geophysics*, 56: 1170-1178.

Leaman, D.E. (1987). *Mineralization Signature Study: Geophysics Gravity and Magnetic Report, Mineral Resources Tasmania, Leaman Geophysics. 77.*

Leube, A., Hirdes, W., Mauer, R., and Kesse, G. (1990). The early Proterozoic Birimian supergroup of Ghana and some aspects of its associated gold mineralization. *Precambrian Research*, 46:139-165.

Lowrie, W. (2007). *Fundamentals of Geophysics*, 2nd Edition, Cambridge University Press.

Macleod, I.N., Jones, K. and Ting, F.D. (1993). 3-D Analytical signal in the interpretation of Total Magnetic Field Data at low magnetic latitudes. *Exploration Geophysics*, 24: 679-688.

Macmillan, S. (2004). Earth's Magnetic Field. *Geophysics and Geochemistry in: Encyclopedia. Life Support Systems (EOLSS)*. EOLSS Publishers, Oxford, UK.

Mandea, M., and Purucker, M. (2005). *Observing, Modeling and Interpreting magnetic field of the solid Earth*. Kuwer Academic Publishers, Netherlands, 52.

Milsom, J. (2003). *Field Geophysics, the geological guide series*. John Wiley and Sons Ltd, The Atrium, Southern Gate, West Sussex PO198SQ, England, third edition.

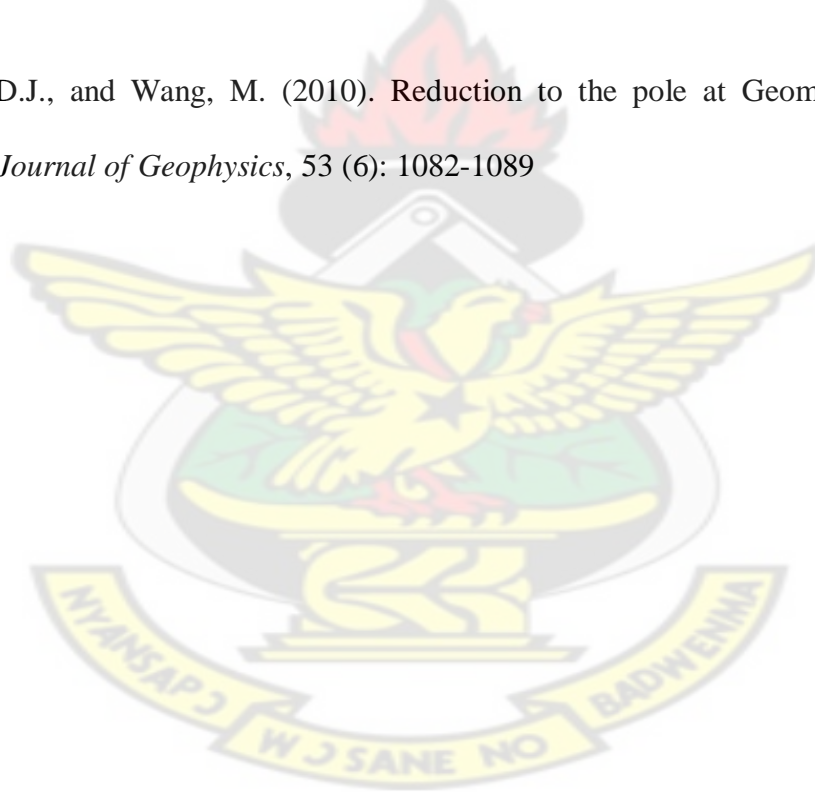
Murphy, B.S.R. (2007). Airborne geophysics and the Indian scenario, *J. Ind. Geophysics Union*, 11(1): 1-28.

- Nabighian, M.N. (1972). The analytical signal of two-dimensional magnetic bodies with polygonal cross-section: its properties and use for automated anomaly interpretation. *Geophysics*, 37(3): 507-517.
- Nabighian, M. N., Ander, M.R., Grauch, V.J.S., Hansen, R.O., LaFehr, T. R., Li Y., Pearson, W. C., Peirce, J.W., Phillips, J.D. and Ruder, M. E. (2005). Historical development of the gravity method in exploration. *Geophysics*, 70(6): 63-89.
- Nagata, T. (1961). *Rock Magnetism*. Tokyo: Maruzen, 2nd edition.
- Petersen, N. (1990). Curie temperature. In James, D. E. (ed.), *The Encyclopedia of solid Earth Geophysics*, New York: Van Nostrand Reinhold, 166-173
- Plumlee, G.S., Smith, K.S., Ficklin, W.H. and Briggs, P.H. (1992). Geological and geochemical controls on the composition of mine drainages and natural drainages in mineralized areas. Proceedings, 7th international Water-Rock Interaction Conference, Park City, Utah, 419-422
- Plummer, C. C., McGeary, D. and Carlson, D. H. (2001). *Physical Geology*. New York: McGraw Hill, 8th edition.
- Rajagopalan, S. (2003). *Exploration Geophysics*, 34(4): 257–262.
- Reeves, C.V. (1989). Aeromagnetic interpretation and rock magnetism. *First Break*, 7: 275-286.

- Reid, A. B., Allsop, J. M., Granser, H., Millet, A. J. and Somerton, I. (1990). Magnetic interpretation in three dimensions using Euler deconvolution. *Geophysics* 55: 80-91.
- Reynolds, J.M. (1997). *An Introduction to Applied and Environmental geophysics*. John Wiley and Sons Ltd, Baffins Lane, Chichester, West Sussex PO19 1UD, England.
- Rivas, J. (2009). Gravity and Magnetic Methods. Short course on Surface Exploration for Geothermal Resources. United Nations University, LaGeo, El Salvador, 1-13.
- Roest, W.R., Verhoef, J. and Pilkington, M. (1992). Magnetic Interpretation using the 3-D analytical signal. *Geophysics*, 57:116-125.
- Roest, W.R. and Pilkington, M. (1993). Identifying remanent magnetization effects in magnetic data. *Geophysics*, 58:653-659.
- Roux, A.T. (1967). The application of geophysics to gold exploration. *Mining and ground water geophysics*, 425-437.
- Sestini, J. (1973). Sedimentology of a Paleoplacer: The Gold-bearing Tarkwaian of Ghana. In Amstutz, G.C and Bernard, J.A. (Ed), *Ores in Sediments*, Springer Verlag Berlin, 275-305.
- Sheriff, R.E. (1994). *Encyclopedic dictionary of exploration geophysics*, 3rd Edition. SEG-Society of Exploration Geophysicists.

- Silva, A.M., Pires, A.C.B., McCafferty, A., Moraes, R.A.V., and Xia, H. (2003). Application of airborne geophysical data to mineral exploration in the uneven exposed terrains of the Rio Das Velhas greenstone belt. *Revista Brasileira de Geociencias*, 33(2): 17-28.
- Silva, J.B.C. and Barbosa, V.C.F. (2003). 3-D Euler deconvolution. Theoretical basis for automatically selecting good solutions. *Geophysics*, 68: 1962-1968.
- Spector, A. and Grant, F.S. (1970). Statistical models for interpretation of aeromagnetic data. *Geophysics*, 35: 293-302.
- Telford, W.M., Geldart, L.P., Sheriff, R.E., and Keys, D.A. (1976). *Applied Geophysics*: Cambridge University Press, 860.
- Telford, W.M., Geldart, L.P., and Sheriff, R.E. (1990). *Applied Geophysics*. Cambridge University Press. second edition, Cambridge, 870.
- Thompson, D.T. (1982). EULDPH: A new technique for making computer assisted depth estimates from magnetic data, *Geophysics*, 47: 31-37.
- Vine, F.J. and Matthews, D.H. (1963). Magnetic anomalies over Oceanic ridges. *Nature*, 199: 947-949
- Wemegah, D.D., Menyeh, B.A., and Danuor, S.K. (2009). Magnetic susceptibility Characterization of mineralized and mineralized rocks of the Subenso Concession of Newmont Ghana Gold Limited. Proc. of the 26th Biennial Conference of the Ghana Science Association, University of Cape Coast, 4th – 9th July, 2009.

- Whitaker, A., Wellman, P., Reith, H., and Cuneen, P. (1987). The use of gravity and magnetic surveys in mapping greenstone terrane near Kalgoorlie, Western Australia. *Exploration Geophysics*, 18 (4): 371-380.
- Whitham, K. (1960). Measurement of geomagnetic elements. In *Methods and Techniques in Geophysics*, 1: 134-48.
- Wright, P.M. (1981). Gravity and Magnetic Methods in mineral exploration. In Skinner, B.J.,(Ed), *Economic Geology*, 75th anniversary volume: 829-839.
- Yao, L., Xue, D.J., and Wang, M. (2010). Reduction to the pole at Geomagnetic Equator. *Chinese Journal of Geophysics*, 53 (6): 1082-1089



Appendices

Appendix A

A.1 Processed Subenso South Ground Gravity Data

Station ID	Reading	Elevation [m]	Longitude	Latitude	Gravity_Avg [ms ⁻²]	Free Air Anomaly [mGal]	Bouguer Anomaly [mGal]	Complete Bouguer Anomaly [mGal]	Bouguer_filter [mGal]
50500	1688.71	281.342	-2.17	7.23249	978062.7	35.8354	4.354185	4.385683	0.072175
50507	1689.45	276.634	-2.173	7.23789	978063.4	34.9924	4.038007	4.0729991	0.008752
50512	1688.05	288.845	-2.175	7.24181	978060.5	35.7172	3.396478	3.4478714	-0.002933
50525	1690.01	276.939	-2.169	7.2329	978063.9	35.641	4.652467	4.6721736	-0.053148
50526	1691.34	272.791	-2.168	7.23336	978065.1	35.6112	5.086802	5.1069907	0.1053
50532	1690.32	273.597	-2.171	7.23806	978064.1	34.725	4.110435	4.1451389	-0.162702
50542	1690.83	274.546	-2.167	7.23382	978064.5	35.5604	4.839621	4.8580066	-0.084695
50548	1691.05	271.319	-2.17	7.23842	978064.7	34.6125	4.252833	4.2953474	-0.165033
50558	1692.41	266.04	-2.169	7.23888	978066.1	34.3749	4.605987	4.6825203	0.0085
50564	1689.5	279.573	-2.167	7.23427	978063.2	35.7829	4.499643	4.5226346	-0.210928
50565	1688.87	284.697	-2.166	7.23473	978062.4	36.4742	4.617559	4.6592424	0.132085
50571	1692.76	265.624	-2.169	7.23944	978066.2	34.3791	4.656659	4.743814	0.042807
50591	1688.48	284.159	-2.164	7.23563	978061.8	35.7685	3.97206	4.0065947	-0.086115
50596	1692.61	265.889	-2.167	7.23959	978066	34.174	4.421993	4.5022561	0.060166
50616	1689.08	281.115	-2.164	7.23607	978062.5	35.5268	4.071044	4.0927012	-0.037439
50617	1690.36	276.517	-2.163	7.23654	978063.6	35.1212	4.179938	4.1970648	-0.058372
50623	1688.87	280.358	-2.166	7.2413	978062.1	34.719	3.347922	3.3738689	0.000253
50630	1691.29	271.677	-2.162	7.23699	978064.5	34.5391	4.139442	4.1687249	-0.140796
50636	1688.13	283.093	-2.165	7.24169	978061.4	34.849	3.17188	3.1957296	-0.029402
50656	1691.76	270.007	-2.16	7.23786	978064.9	34.4014	4.188523	4.2321748	-0.009963
50662	1687.3	286.562	-2.163	7.24247	978060.4	34.9524	2.887115	2.9162295	-0.001744
50669	1690.68	275.629	-2.16	7.2383	978063.7	34.9006	4.058636	4.0796429	0.015343
50674	1687.97	284.853	-2.162	7.24221	978061	34.9701	3.09605	3.1225247	0.117835
50682	1689.6	280.109	-2.159	7.23872	978062.5	35.0914	3.748164	3.7632002	-0.034937
50688	1686.42	290.582	-2.162	7.24347	978059.4	35.1329	2.617781	2.6688019	0.093298
50695	1689.07	282.095	-2.158	7.23919	978061.9	35.0954	3.530005	3.5466751	0.004972
50701	1686.15	291.434	-2.161	7.24388	978059	35.0032	2.392785	2.4534919	-0.014182
50714	1686.38	290.826	-2.16	7.24442	978059.2	34.9799	2.43748	2.4997835	0.099789
50720	1688.33	285.505	-2.157	7.23965	978061	35.2823	3.335306	3.3603758	-0.007696
50721	1687.98	286.934	-2.157	7.24009	978060.7	35.4309	3.324017	3.355868	0.023861
50727	1687.14	287.63	-2.159	7.24482	978059.8	34.6322	2.447436	2.4960211	0.043808

50752	1691.21	271.069	-2.157	7.245	978063.8	33.4427	3.111062	3.1583593	0.190862
50753	1690.45	272.838	-2.158	7.24578	978063.1	33.2726	2.742942	2.788646	0.066702
50760	1689.84	279.317	-2.154	7.24146	978062.5	34.8022	3.54762	3.5667019	-0.027523
50766	1690.53	272.477	-2.157	7.24616	978063.2	33.2776	2.788379	2.8378013	0.06591
50773	1685.99	298.873	-2.176	7.2426	978058.5	36.8144	3.371567	3.4375779	0.167971
50779	1680.82	318.364	-2.178	7.24724	978053.3	37.5452	1.921408	2.0109899	-0.235649
50784	1684.32	297.194	-2.181	7.25118	978056.8	34.4197	1.164758	1.2360343	0.061917
50785	1686.17	297.934	-2.175	7.24302	978058.6	36.5717	3.233901	3.2904411	0.089992
50791	1681.47	318.022	-2.178	7.24759	978053.9	38.0411	2.455597	2.5399196	-0.004853
50797	1686.38	296.776	-2.174	7.24345	978058.8	36.4288	3.220606	3.268916	-0.158865
50803	1682.31	312.613	-2.177	7.24822	978054.7	37.1111	2.13085	2.1832822	-0.378006
50809	1688.37	287.812	-2.173	7.24403	978060.8	35.6465	3.441278	3.4942278	-0.195788
50815	1683.41	309.832	-2.176	7.24868	978055.7	37.2934	2.624307	2.6658081	-0.05493
50821	1689.81	282.394	-2.172	7.24449	978062.1	35.3104	3.711521	3.792141	0.070363
50827	1683.5	310.428	-2.175	7.24912	978055.8	37.4926	2.756778	2.7992711	0.027105
50833	1687.79	290.556	-2.172	7.24486	978060.1	35.7897	3.277449	3.3175596	-0.028458
50839	1683.34	311.13	-2.174	7.24951	978055.6	37.5825	2.768103	2.8129127	0.031295
50845	1686.08	298.717	-2.171	7.24531	978058.2	36.4448	3.019446	3.0561985	0.048045
50851	1682.89	313.776	-2.174	7.24994	978055	37.7916	2.681189	2.7395675	0.004962
50857	1685.71	299.984	-2.17	7.2458	978057.9	36.5069	2.939764	2.9773308	0.072125
50863	1682.29	316.466	-2.173	7.25043	978054.5	38.0568	2.645304	2.7246604	0.103159
50869	1686.63	296.643	-2.169	7.24615	978058.7	36.2066	3.013245	3.0604787	-0.085892
50875	1682.49	314.514	-2.172	7.25088	978054.5	37.4517	2.258705	2.3272119	-0.126748
50881	1685.63	301.821	-2.169	7.24674	978057.4	36.5572	2.784547	2.8264842	0.089161
50887	1682.27	316.69	-2.171	7.25134	978054.3	37.965	2.528539	2.6159047	0.17225
50893	1685.54	301.591	-2.168	7.24712	978057.4	36.413	2.666034	2.7076318	0.081042
50899	1682.41	316.659	-2.171	7.25178	978054.2	37.8381	2.405059	2.4955239	0.116516
50905	1684.72	305.176	-2.167	7.24759	978056.6	36.7954	2.647228	2.7094832	0.096226
50911	1682.29	314.871	-2.17	7.2523	978054.2	37.2742	2.041198	2.1206255	-0.085936
50917	1685.32	303.392	-2.166	7.24804	978057	36.5934	2.644931	2.6995243	0.102647
50923	1682.66	314.043	-2.169	7.25274	978054.4	37.1262	1.985965	2.0612718	-0.03808
50929	1685	304.438	-2.165	7.24849	978056.7	36.5903	2.524763	2.5879361	0.097326
50935	1682.92	311.871	-2.168	7.25323	978054.6	36.6985	1.801248	1.8618707	-0.092457
50941	1685.29	303.149	-2.165	7.24891	978056.9	36.3669	2.445591	2.5048071	0.116158
50947	1683.21	309.904	-2.167	7.25368	978054.9	36.3887	1.711537	1.7606291	-0.063864
50953	1684.35	306.844	-2.164	7.24943	978055.9	36.5433	2.208575	2.2949435	-0.100777
50959	1683.54	309.963	-2.167	7.25408	978055.1	36.5714	1.887627	1.9365735	0.203346
50965	1684.16	307.177	-2.163	7.2499	978055.7	36.4577	2.08573	2.1788586	-0.22677
50971	1683.98	304.051	-2.166	7.25458	978055.5	35.1827	1.160542	1.1882826	-0.222828
50977	1684.45	303.778	-2.162	7.25029	978056	35.6678	1.676179	1.7438911	-0.468965
50983	1684.21	302.461	-2.165	7.25525	978055.8	34.9077	1.063293	1.0903546	-0.06041
50989	1685.19	298.163	-2.162	7.25078	978056.7	34.6087	1.2453	1.2834384	-0.481599
50995	1686.03	294.439	-2.164	7.25551	978057.5	34.1477	1.200954	1.2482303	0.082944

51008	1684.79	297.209	-2.164	7.25678	978056.3	33.7455	0.488773	0.5385858	0.037508
51021	1683.03	304.866	-2.164	7.25799	978054.4	34.2252	0.111781	0.146991	-0.010223
51026	1682.9	306.615	-2.181	7.25276	978054.2	34.7002	0.391094	0.4233762	-0.204416
51031	1678.26	322.836	-2.184	7.25669	978049.6	34.9929	-1.13127	-0.966868	-0.071012
51039	1680.95	314.877	-2.181	7.25397	978052.3	35.2909	0.057267	0.1114963	-0.062553
51043	1677.37	329.436	-2.183	7.25707	978048.7	36.114	-0.7487	-0.490674	0.083608
51051	1680.07	319.401	-2.18	7.2544	978051.4	35.7397	-0.0001	0.0848699	-0.152627
51055	1676.45	336.643	-2.182	7.25747	978047.7	37.3603	-0.30888	0.0858878	0.343095
51061	1681.53	315.09	-2.179	7.25336	978052.8	35.877	0.619536	0.6680345	0.037149
51062	1680.33	320.329	-2.179	7.25411	978051.6	36.3041	0.460377	0.5468777	-0.035759
51067	1675.36	338.886	-2.181	7.25806	978046.6	36.9205	-0.99968	-0.541396	-0.063143
51073	1680.69	318.478	-2.178	7.25378	978051.9	35.9816	0.344998	0.4138315	0.009693
51085	1680.37	318.086	-2.177	7.25424	978051.4	35.3499	-0.24287	-0.17477	-0.23127
51091	1676.99	330.951	-2.18	7.25886	978048.1	35.9115	-1.12072	-0.789829	0.308949
51097	1680.52	317.26	-2.176	7.25468	978051.6	35.3277	-0.1726	-0.107964	-0.025453
51103	1675.92	332.832	-2.179	7.25933	978047	35.4138	-1.829	-1.447295	0.003468
51109	1680.68	316.05	-2.176	7.25515	978051.7	34.9884	-0.37645	-0.316758	-0.015719
51115	1675.82	332.785	-2.178	7.25983	978046.8	35.1812	-2.05626	-1.652749	-0.137753
51121	1681.54	310.853	-2.175	7.25565	978052.5	34.2644	-0.51893	-0.482483	-0.029156
51127	1679.28	317.869	-2.177	7.2603	978050.3	34.0559	-1.5125	-1.337096	0.040825
51133	1682.63	306.63	-2.174	7.25607	978053.4	33.8366	-0.47416	-0.447963	0.014681
51139	1681.52	307.764	-2.177	7.26066	978052.3	33.0032	-1.43451	-1.354604	-0.017142
51145	1683.93	299.848	-2.173	7.25649	978054.8	33.1575	-0.3944	-0.364925	-0.035976
51151	1682.32	302.473	-2.176	7.26114	978053.3	32.2667	-1.57894	-1.526098	-0.128483
51157	1686.17	290.876	-2.172	7.25697	978056.8	32.33	-0.21797	-0.144041	-0.023171
51163	1684.18	293.972	-2.175	7.26162	978054.9	31.2599	-1.63454	-1.596669	-0.216146
51175	1685.64	287.136	-2.174	7.26208	978056.4	30.6279	-1.50158	-1.438667	-0.128099
51181	1687.21	286.649	-2.171	7.2579	978057.8	32.0204	-0.0546	0.0688765	0.105271
51187	1685.52	288.079	-2.174	7.26255	978056.1	30.6613	-1.57379	-1.50232	-0.054359
51193	1685.37	294.623	-2.17	7.25839	978056	32.6349	-0.33238	-0.267245	0.096833
51199	1683.77	295.973	-2.173	7.263	978054.4	31.3299	-1.78847	-1.730658	-0.007541
51205	1684.4	298.567	-2.169	7.25886	978055	32.8147	-0.59383	-0.54074	0.097269
51211	1682.71	300.498	-2.172	7.26356	978053.2	31.5965	-2.02812	-1.96263	0.000811
51217	1683.46	302.434	-2.169	7.25929	978054	33.0489	-0.7925	-0.746669	-0.042163
51223	1682.14	303.745	-2.171	7.26397	978052.7	31.9956	-1.99234	-1.921829	0.014916
51229	1682.77	307.563	-2.168	7.25973	978053.3	33.9368	-0.47845	-0.438219	0.106785
51235	1681.08	311.049	-2.17	7.26445	978051.6	33.1817	-1.62358	-1.546932	0.209462
51241	1681.91	311.618	-2.167	7.26021	978052.4	34.2732	-0.59579	-0.554586	-0.010464
51247	1679.52	318.855	-2.17	7.26487	978050	33.9492	-1.7295	-1.640465	0.066719
51253	1681.09	315.808	-2.166	7.26068	978051.6	34.7456	-0.59216	-0.546731	0.054481
51259	1677.5	328.352	-2.169	7.26542	978048	34.8525	-1.88889	-1.764621	-0.011084
51266	1679.87	322.009	-2.166	7.26198	978050.2	35.2599	-0.77178	-0.71163	0.045901
51270	1676.44	334.604	-2.168	7.26514	978046.8	35.6488	-1.79217	-1.644614	-0.010276

A.2 Processed Subenso South Ground Magnetic Data

X_UTM [m]	Y_UTM [m]	READING_1 [nT]	Diurnal_1 [nT]	Diurnal Filter [nT]	Mag levelling [nT]	longitude	latitude
590730.63	801154.325	32021.324	-179.663	-80.200625	-69.76431	-2.1781317	7.2471649
590730.63	801154.415	32040.999	-159.988	-84.616167	-74.27321	-2.1781317	7.2471657
590730.63	801154.505	32060.796	-140.191	-90.370375	-80.12067	-2.1781317	7.2471665
590730.63	801154.595	32074.299	-126.688	-95.053611	-84.89826	-2.1781317	7.2471673
590730.535	801154.963	32087.53	-113.457	-97.114678	-87.05525	-2.1781325	7.2471706
590730.345	801155.608	32101.252	-99.735	-99.735	-89.77197	-2.1781342	7.2471765
590730.575	801155.885	32094.891	-106.096	-92.82835	-82.96166	-2.1781321	7.247179
590731.225	801155.795	32089.211	-111.776	-85.204528	-75.43527	-2.1781263	7.2471782
590732.053	801155.38	32207.879	6.892	6.892	16.262657	-2.1781188	7.2471744
590732.053	801155.335	32239.165	38.178	38.178	47.446441	-2.1781188	7.247174
590731.958	801155.245	32244.565	43.578	43.578	52.743795	-2.1781196	7.2471732
590731.82	801155.385	32230.583	29.596	29.596	38.659099	-2.1781209	7.2471744
590731.64	801155.755	32214.552	13.565	13.565	22.524342	-2.1781225	7.2471778
590731.55	801156.03	32199.035	-1.952	-1.952	6.9019052	-2.1781233	7.2471803
590731.55	801156.21	32186.83	-14.157	-5.64075	3.1073133	-2.1781233	7.2471819
590726.295	801161.038	32174.731	-26.256	-16.040333	-7.398214	-2.1781708	7.2472257
590715.785	801170.513	32176.118	-24.869	-24.869	-16.33387	-2.1782659	7.2473115
590710.875	801175.319	32177.142	-23.845	-23.845	-15.41856	-2.1783103	7.2473551
590711.565	801175.456	32179.541	-21.446	-21.446	-13.12863	-2.178304	7.2473563
590712.255	801175.594	32180.86	-20.127	-20.127	-11.91886	-2.1782978	7.2473576
590712.945	801175.731	32179.901	-21.086	-21.086	-12.98811	-2.1782915	7.2473588
590712.185	801176.258	32178.408	-22.579	-22.579	-14.59308	-2.1782984	7.2473636
590709.975	801177.173	32173.974	-27.013	-27.013	-19.13941	-2.1783184	7.2473719
590708.918	801177.725	32168.726	-32.261	-32.261	-24.49994	-2.178328	7.2473769
590709.013	801177.915	32161.694	-39.293	-39.293	-31.64548	-2.1783271	7.2473786
590708.095	801178.285	32154.2	-46.787	-46.787	-39.25475	-2.1783354	7.247382
590706.165	801178.835	32147.14	-53.847	-53.847	-46.43036	-2.1783529	7.247387
590704.095	801179.245	32141.349	-59.638	-59.638	-52.33721	-2.1783716	7.2473907
590701.885	801179.515	32138.743	-62.244	-62.244	-55.06004	-2.1783916	7.2473932
590700.411	801179.879	32138.455	-62.532	-62.532	-55.46663	-2.178405	7.2473965
590699.674	801180.336	32140.851	-60.136	-60.136	-53.18951	-2.1784116	7.2474007
590698.936	801180.794	32142.009	-58.978	-58.978	-52.15069	-2.1784183	7.2474048
590698.199	801181.251	32144.449	-56.538	-56.538	-49.83082	-2.178425	7.247409
590698.795	801182.128	32145.264	-55.723	-55.723	-49.13771	-2.1784196	7.2474169
590700.725	801183.423	32145.558	-55.429	-55.429	-48.96587	-2.1784021	7.2474286

590702.104	801183.997	32144.325	-56.662	-56.662	-50.32138	-2.1783896	7.2474337
590702.932	801183.851	32138.861	-62.126	-62.126	-55.9088	-2.1783821	7.2474324
590703.76	801183.705	32133.501	-67.486	-67.486	-61.39399	-2.1783746	7.2474311
590704.588	801183.559	32127.582	-73.405	-73.405	-67.43841	-2.1783671	7.2474297
590705.416	801183.413	32125.905	-75.082	-75.082	-69.24123	-2.1783596	7.2474284
590706.244	801183.267	32129.121	-71.866	-71.866	-66.15192	-2.1783521	7.2474271
590707.072	801183.121	32134.236	-66.751	-66.751	-61.16538	-2.1783446	7.2474257
590707.9	801182.975	32148.901	-52.086	-52.086	-46.62904	-2.1783371	7.2474244
590708.728	801182.829	32164.832	-36.155	-36.155	-30.82714	-2.1783296	7.2474231
590709.556	801182.683	32189.222	-11.765	-11.765	-6.567078	-2.1783221	7.2474217
590709.785	801182.933	32212.358	11.371	11.371	16.437221	-2.17832	7.247424
590709.415	801183.578	32235.049	34.062	34.062	38.996355	-2.1783234	7.2474298
590709.09	801184.223	32251.961	50.974	50.974	55.776005	-2.1783263	7.2474357
590708.81	801184.868	32262.364	61.377	61.377	66.045858	-2.1783288	7.2474415
590708.625	801185.605	32267.691	66.704	66.704	71.237961	-2.1783305	7.2474482
590708.535	801186.435	32268.141	67.154	67.154	71.552934	-2.1783313	7.2474557
590708.535	801187.218	32262.093	61.106	61.106	65.369381	-2.1783313	7.2474627
590708.625	801187.953	32251.391	50.404	50.404	54.531073	-2.1783304	7.2474694
590706.69	801193.615	32232.212	31.225	31.225	34.373714	-2.1783479	7.2475206
590706.41	801194.265	32231.043	30.056	30.056	33.06227	-2.1783504	7.2475265
590705.993	801194.955	32231.169	30.182	30.182	33.044147	-2.1783542	7.2475328
590705.438	801195.685	32231.412	30.425	30.425	33.143002	-2.1783592	7.2475394
590705.343	801196.328	32230.538	29.551	29.551	32.124218	-2.17836	7.2475452
590705.708	801196.883	32232.088	31.101	31.101	33.52882	-2.1783567	7.2475502
590705.8	801197.438	32235.327	34.34	34.34	36.620777	-2.1783559	7.2475552
590705.62	801197.993	32239.808	38.821	38.821	40.954748	-2.1783575	7.2475603
590705.483	801198.593	32244.049	43.062	43.062	45.048047	-2.1783587	7.2475657
590705.388	801199.238	32253.207	52.22	52.22	54.057784	-2.1783596	7.2475715
590705.018	801199.65	32264.424	63.437	63.437	65.124914	-2.1783629	7.2475753
590704.373	801199.83	32273.31	72.323	72.323	73.861097	-2.1783688	7.2475769
590703.728	801199.965	32281.26	80.273	80.273	81.660576	-2.1783746	7.2475781
590703.083	801200.055	32284.383	83.396	83.396	84.632546	-2.1783804	7.247579
590702.485	801200.423	32284.718	83.731	83.731	84.814953	-2.1783858	7.2475823
590701.935	801201.068	32281.478	80.491	80.491	81.422452	-2.1783908	7.2475881
590701.52	801201.528	32278.02	77.033	77.033	77.811217	-2.1783946	7.2475923
590701.24	801201.803	32275.624	74.637	74.637	75.26153	-2.1783971	7.2475948
590701.053	801202.125	32274.131	73.144	73.144	73.613328	-2.1783988	7.2475977
590700.958	801202.495	32272.12	71.133	71.133	71.447256	-2.1783996	7.2476011
590700.865	801202.958	32272.125	71.138	71.138	71.296425	-2.1784005	7.2476052
590700.775	801203.513	32274.864	73.877	73.877	73.879198	-2.1784013	7.2476103
590698.378	801207.288	32253.737	52.75	52.75	51.47862	-2.1784229	7.2476444
590698.1	801207.954	32253.942	52.955	52.955	51.521364	-2.1784254	7.2476505
590697.64	801208.181	32253.514	52.527	52.527	50.931356	-2.1784296	7.2476525

590697.18	801208.409	32252.615	51.628	51.628	49.869526	-2.1784338	7.2476546
590695.2	801210.638	32288.263	87.276	87.276	84.696238	-2.1784517	7.2476748
590695.105	801211.145	32305.067	104.08	104.08	101.33401	-2.1784525	7.2476794
590694.915	801211.515	32319.984	118.997	118.997	116.08511	-2.1784542	7.2476827
590694.683	801211.883	32324.404	123.417	123.417	120.33836	-2.1784563	7.2476861
590694.408	801212.248	32312.388	111.401	111.401	108.15553	-2.1784588	7.2476894
590694.18	801212.708	32290.697	89.71	89.71	86.296562	-2.1784609	7.2476935
590694	801213.263	32266.607	65.62	73.330375	69.749338	-2.1784625	7.2476986
590691.605	801215.843	32224.712	23.725	23.725	19.468361	-2.1784841	7.2477219
590690.96	801216.533	32215.089	14.102	14.102	9.6753659	-2.17849	7.2477282
590690.22	801217.358	32207.049	6.062	6.062	1.4654166	-2.1784967	7.2477357
590689.253	801218.138	32200.053	-0.934	-0.934	-5.701504	-2.1785054	7.2477427
590688.058	801218.873	32193.155	-7.832	-7.832	-12.76998	-2.1785162	7.2477494
590687.135	801219.608	32185.377	-15.61	-15.61	-20.71933	-2.1785246	7.2477561
590685.815	801221.951	32150.051	-50.936	-50.936	-56.56032	-2.1785365	7.2477773
590685.585	801222.779	32138.47	-62.517	-62.517	-68.31382	-2.1785386	7.2477848
590685.355	801223.606	32136.105	-64.882	-64.882	-70.85115	-2.1785406	7.2477923
590684.742	801226.333	32202.509	1.522	1.522	-5.139583	-2.1785461	7.2478169
590684.358	801226.885	32229.091	28.104	28.104	21.268483	-2.1785496	7.2478219
590683.713	801227.435	32248.277	47.29	47.29	40.28111	-2.1785554	7.2478269
590683.115	801228.445	32254.694	53.707	53.707	46.523871	-2.1785608	7.2478361
590682.794	801229.295	32257.357	56.37	56.37	49.01295	-2.1785637	7.2478438
590682.701	801229.525	32253.91	52.923	52.923	45.391413	-2.1785646	7.2478458
590682.609	801229.755	32246.347	45.36	45.36	37.654475	-2.1785654	7.2478479
590682.516	801229.985	32239.268	38.281	38.281	30.400679	-2.1785662	7.24785
590682.7	801230.01	32231.271	30.284	30.284	22.229269	-2.1785646	7.2478502
590683.16	801229.83	32223.206	22.219	22.219	13.989339	-2.1785604	7.2478486
590683.065	801229.923	32216.317	15.33	15.33	6.9260454	-2.1785613	7.2478494
590682.415	801230.288	32213.743	12.756	12.756	4.1769037	-2.1785671	7.2478527
590681.998	801230.592	32214.434	13.447	13.447	4.6932177	-2.1785709	7.2478555
590681.815	801230.835	32216.358	15.371	15.371	6.442109	-2.1785726	7.2478577
590681.632	801231.078	32218.564	17.577	17.577	8.4736723	-2.1785742	7.2478599
590681.358	801231.523	32219.532	18.545	18.545	9.2664017	-2.1785767	7.2478639
590680.122	801236.237	32268.835	67.848	67.848	57.346583	-2.1785878	7.2479066
590679.6	801237	32270.347	69.36	69.36	58.683718	-2.1785925	7.2479135
590678.957	801237.827	32265.832	64.845	64.845	53.994516	-2.1785983	7.247921
590678.59	801238.2	32259.872	58.885	58.885	47.860192	-2.1786017	7.2479244
590678.223	801238.573	32259.991	59.004	59.004	47.805644	-2.178605	7.2479278
590677.3	801239.31	32262.88	61.893	61.893	50.520321	-2.1786133	7.2479344
590676.628	801240.32	32265.988	65.001	65.001	53.454728	-2.1786194	7.2479436
590676.763	801241.24	32269.221	68.234	68.234	56.514116	-2.1786182	7.2479519
590676.898	801242.16	32273.316	72.329	72.329	60.436314	-2.1786169	7.2479602
590677.033	801243.08	32276.785	75.798	75.798	63.731762	-2.1786157	7.2479685

590676.825	801243.955	32277.085	76.098	76.098	63.859006	-2.1786176	7.2479765
590676.275	801244.785	32274.678	73.691	73.691	61.279335	-2.1786225	7.247984
590675.77	801245.475	32269.773	68.786	68.786	56.202506	-2.1786271	7.2479902
590675.31	801246.025	32267.269	66.282	72.421	59.664956	-2.1786312	7.2479952
590674.665	801246.53	32269.035	68.048	68.048	55.120269	-2.1786371	7.2479998
590673.835	801246.99	32274.478	73.491	73.491	60.39177	-2.1786446	7.248004
590673.19	801247.635	32282.009	81.022	70.1595139	56.889658	-2.1786504	7.2480098
590672.73	801248.465	32286.012	85.025	67.5018333	54.060661	-2.1786546	7.2480173
590672.293	801249.248	32284.642	83.655	74.96625	61.35469	-2.1786585	7.2480244
590671.878	801249.983	32277.544	76.557	69.9199583	56.138302	-2.1786623	7.2480311
590671.463	801250.718	32268.442	67.455	67.455	53.504152	-2.178666	7.2480377
590671.048	801251.453	32260.051	59.064	74.0306296	59.909932	-2.1786698	7.2480444
590670.655	801252.188	32258.27	57.283	78.7018827	64.412331	-2.1786733	7.248051
590670.285	801252.923	32264.297	63.31	79.9306944	65.472682	-2.1786766	7.2480577
590669.96	801253.568	32277.166	76.179	86.4370448	71.811505	-2.1786796	7.2480635
590669.68	801254.123	32288.704	87.717	87.717	72.923313	-2.1786821	7.2480685
590668.988	801254.675	32296.563	95.576	95.576	80.615223	-2.1786884	7.2480735
590667.883	801255.225	32301.254	100.267	100.267	85.13963	-2.1786984	7.2480785
590667.145	801255.733	32304.586	103.599	103.599	88.306	-2.178705	7.2480831
590666.775	801256.198	32306.025	105.038	105.038	89.578787	-2.1787084	7.2480874
590666.175	801256.75	32304.589	103.602	103.602	87.977695	-2.1787138	7.2480924
590665.345	801257.39	32298.035	97.048	97.048	81.259203	-2.1787213	7.2480982
590663.005	801259.133	32287.781	86.794	86.794	70.352633	-2.1787425	7.248114
590662.815	801259.778	32290.955	89.968	89.968	73.365489	-2.1787442	7.2481198
590662.445	801260.745	32293.714	92.727	92.727	75.962846	-2.1787475	7.2481286
590662.03	801261.573	32297.04	96.053	96.053	79.128445	-2.1787513	7.248136
590661.75	801261.938	32301.439	100.452	100.452	83.367846	-2.1787538	7.2481394
590661.29	801262.168	32310.159	109.172	109.172	91.929289	-2.178758	7.2481414
590660.65	801262.263	32319.365	118.378	118.378	100.97628	-2.1787638	7.2481423
590659.999	801262.383	32327.838	126.851	126.851	109.29157	-2.1787697	7.2481434
590659.337	801262.529	32335.283	134.296	134.296	116.57976	-2.1787757	7.2481447
590658.675	801262.675	32340.99	140.003	140.003	122.13102	-2.1787816	7.2481461
590658.013	801262.821	32343.402	142.415	142.415	124.38687	-2.1787876	7.2481474
590657.351	801262.967	32339.828	138.841	138.841	120.65808	-2.1787936	7.2481487
590656.650	801263.595	32332.115	131.128	131.128	112.79129	-2.1788	7.2481544
590656.218	801264.333	32321.141	120.154	120.154	101.66458	-2.1788039	7.2481611
590656.095	801264.7	32308.197	107.21	95.4325	76.790026	-2.178805	7.2481644
590655.995	801267.6	32203.329	2.342	2.342	-17.05013	-2.1788058	7.2481907
590656.545	801267.88	32203.905	2.918	2.918	-16.62122	-2.1788009	7.2481932
590656.820	801268.08	32204.866	3.879	3.879	-15.80617	-2.1787984	7.248195
590656.820	801268.2	32205.633	4.646	4.646	-15.18538	-2.1787984	7.2481961
590656.820	801268.32	32211.316	10.329	10.329	-9.647063	-2.1787984	7.2481972
590656.683	801268.565	32223.232	22.245	22.245	2.1255273	-2.1787996	7.2481994

590656.408	801268.935	32238.439	37.452	37.452	17.190273	-2.1788021	7.2482027
590656.085	801269.35	32252.608	51.621	51.621	31.216823	-2.178805	7.2482065
590655.715	801269.81	32264.26	63.273	63.273	42.727945	-2.1788083	7.2482107
590655.438	801270.455	32273.248	72.261	72.261	51.57643	-2.1788108	7.2482165
590655.253	801271.285	32276.725	75.738	75.738	54.915091	-2.1788125	7.2482224
590655.113	801271.928	32284.353	83.366	83.366	62.404611	-2.1788138	7.2482298
590655.018	801272.383	32287.662	86.675	86.675	65.576753	-	7.2482339
590654.833	801272.843	32288.303	87.316	87.316	66.082344	-2.1788163	7.2482381
590654.558	801273.308	32288.882	87.895	87.895	66.52713	-2.1788188	7.2482423
590654.238	801273.77	32290.508	89.521	89.521	68.018833	-2.1788217	7.2482465
590653.873	801274.23	32295.125	94.138	94.138	72.503205	-2.178825	7.2482507
590653.55	801274.783	32300.973	99.986	99.986	78.220108	-2.1788279	7.2482557
590653.27	801275.428	32304.731	103.744	103.744	81.848224	-2.1788304	7.2482615
590653.035	801276.028	32301.183	100.196	100.196	78.170317	-2.1788325	7.2482669
590652.845	801276.583	32289.361	88.374	88.374	66.220124	-2.1788342	7.248272
590652.568	801277.088	32270.631	69.644	69.644	47.363542	-2.1788367	7.2482765
590652.203	801277.543	32256.572	55.585	55.585	33.179189	-2.17884	7.2482807
590651.788	801278.048	32243.132	42.145	42.145	19.613874	-2.1788438	7.2482852
590651.323	801278.603	32233.571	32.584	32.584	9.9293164	-2.178848	7.2482903
590650.863	801279.108	32227.208	26.221	26.221	3.4444465	-2.1788521	7.2482948
590650.408	801279.563	32225.885	24.898	24.898	2.0008222	-2.1788563	7.248299
590649.993	801280.023	32227.244	26.257	26.257	3.2392963	-2.17886	7.2483031
590649.618	801280.488	32231.7	30.713	30.713	7.5765699	-2.1788634	7.2483073
590649.155	801281.36	32236.746	35.759	35.759	12.505604	-2.1788676	7.2483152
590648.65	801282.233	32243.975	42.988	42.988	19.6189	-2.1788721	7.2483231
590648.190	801282.698	32251.21	50.223	50.223	26.738356	-2.1788763	7.2483273
590647.913	801283.158	32257.225	56.238	56.238	32.639651	-2.1788788	7.2483315
590647.818	801283.613	32262.079	61.092	61.092	37.381776	-2.1788796	7.2483356
590647.633	801284.163	32265.978	64.991	64.991	41.170177	-2.1788813	7.2483406
590647.358	801284.808	32268.242	67.255	67.255	43.323802	-2.1788838	7.2483464
590646.990	801285.36	32267.138	66.151	66.151	42.111303	-2.1788871	7.2483514
590646.530	801285.82	32264.728	63.741	63.741	39.594702	-2.1788913	7.2483556
590646.115	801286.375	32259.049	58.062	58.062	33.810389	-2.178895	7.2483606
590645.745	801287.025	32253.138	52.151	52.151	27.794363	-2.1788984	7.2483665
590645.468	801287.625	32243.339	42.352	42.352	17.89225	-2.1789009	7.248372
590645.283	801288.175	32234.005	33.018	33.018	8.4570967	-2.1789025	7.2483769
590645.098	801288.603	32223.473	22.486	22.486	-2.174755	-2.1789042	7.2483808
590644.915	801288.91	32209.663	8.676	8.676	-16.08426	-2.1789059	7.2483836
590644.732	801289.217	32200.983	-0.004	-0.004	-24.86181	-2.1789075	7.2483864
590644.455	801289.598	32198.484	-2.503	-2.503	-27.45635	-2.17891	7.2483898
590644.085	801290.053	32202.81	1.823	1.823	-23.22457	-2.1789133	7.2483939
590643.620	801290.745	32211.529	10.542	10.542	-14.59938	-2.1789175	7.2484002
590643.203	801291.578	32230.215	29.228	22.524	-2.708788	-2.1789213	7.2484077

590642.928	801292.313	32246.518	45.531	24.675	-0.647414	-2.1789238	7.2484144
590642.560	801292.91	32254.68	53.693	29.818	4.4072762	-2.1789271	7.2484198
590642.10	801293.37	32253.661	52.674	38.870	13.371228	-2.1789313	7.248424
590641.747	801293.753	32251.459	50.472	50.472	24.886715	-2.1789345	7.2484275
590641.500	801294.06	32253.087	52.1	52.1	26.430897	-2.1789367	7.2484302
590641.253	801294.367	32257.847	56.86	56.86	31.108414	-2.1789389	7.248433
590640.855	801295.165	32264.701	63.714	63.714	37.880476	-2.1789425	7.2484402
590640.440	801296.04	32272.647	71.66	71.66	45.746571	-2.1789463	7.2484482
590640.160	801296.5	32279.529	78.542	78.542	52.55084	-2.1789488	7.2484523
590639.838	801297.05	32285.439	84.452	84.452	58.384454	-2.1789517	7.2484573
590639.473	801297.69	32289.124	88.137	88.137	61.993676	-2.178955	7.2484631
590639.105	801298.195	32291.029	90.042	90.042	63.824958	-2.1789583	7.2484677
590638.735	801298.565	32291.086	90.099	90.099	63.810455	-2.1789617	7.248471
590638.413	801299.028	32288.914	87.927	87.927	61.568308	-2.1789646	7.2484752
590638.138	801299.583	32283.651	82.664	82.664	56.235832	-2.1789671	7.2484802
590637.908	801300.135	32276.365	75.378	75.378	48.88244	-2.1789691	7.2484852
590637.723	801300.685	32266.044	65.057	65.057	38.496302	-2.1789708	7.2484902
590637.538	801301.238	32259.795	58.808	58.808	32.183528	-2.1789725	7.2484952
590637.353	801301.793	32258.46	57.473	57.473	30.785489	-2.1789741	7.2485002
590637.075	801302.393	32262.268	61.281	61.281	34.532554	-2.1789766	7.2485057
590636.705	801303.038	32270.288	69.301	69.301	42.49391	-2.17898	7.2485115
590636.335	801303.59	32284.395	83.408	83.408	56.543636	-2.1789833	7.2485165
590635.965	801304.05	32298.7	97.713	97.713	70.792161	-2.1789867	7.2485207
590635.550	801304.555	32312.976	111.989	111.989	85.013808	-2.1789904	7.2485253
590635.090	801305.105	32322.446	121.459	121.459	94.431777	-2.1789946	7.2485302
590634.628	801305.748	32327.789	126.802	126.802	99.724124	-2.1789988	7.2485361
590634.163	801306.483	32310.523	109.536	109.536	82.40833	-2.179003	7.2485427
590633.793	801307.035	32270.128	69.141	84.4993	57.32401	-2.1790063	7.2485477
590633.518	801307.405	32229.295	28.308	56.4482	29.22758	-2.1790088	7.2485511
590632.868	801309.065	32213.68	12.693	12.693	-14.69387	-2.1790146	7.2485661
590632.730	801309.435	32228.746	27.759	27.759	0.3350465	-2.1790159	7.2485694
590632.550	801309.805	32254.703	53.716	53.716	26.255942	-2.1790175	7.2485728
590632.320	801310.218	32281.856	80.869	80.869	53.375004	-2.1790196	7.2485765
590632.040	801310.673	32317.326	116.339	116.339	88.813457	-2.1790221	7.2485806
590631.763	801311.225	32338.667	137.68	137.68	110.1243	-2.1790246	7.2485856
590631.488	801311.875	32362.563	161.576	161.576	133.99119	-2.1790271	7.2485915
590631.165	801312.338	32381.211	180.224	180.224	152.61225	-2.17903	7.2485957
590630.795	801312.613	32391.732	190.745	190.745	163.10872	-2.1790334	7.2485982
590630.333	801312.978	32394.28	193.293	193.293	165.63359	-2.1790375	7.2486015

Appendix B

B. 1 Used Software

- Geosoft Oasis Montaj version 7.1: data processing and enhancement
- ArcGIS version 10.1: Structural interpretation and map production
- MapInfo 10.5-Discover 11.1: data processing and enhancing
- CorelDraw X5: graphics
- Microsoft Paint: graphics
- Microsoft word 2010: typesetting and layout

